

**University of Alberta**

Temperature-dependent butterfly dynamics

by

Jeanette D. Wheeler

A thesis submitted to the Faculty of Graduate Studies and Research in partial fulfillment of the requirements for the degree of

Master of Science  
in  
Applied Mathematics

Department of Mathematical and Statistical Sciences

©Jeanette D. Wheeler  
Fall 2010  
Edmonton, Alberta

Permission is hereby granted to the University of Alberta Libraries to reproduce single copies of this thesis and to lend or sell such copies for private, scholarly or scientific research purposes only. Where the thesis is converted to, or otherwise made available in digital form, the University of Alberta will advise potential users of the thesis of these terms.

The author reserves all other publication and other rights in association with the copyright in the thesis and, except as herein before provided, neither the thesis nor any substantial portion thereof may be printed or otherwise reproduced in any material form whatsoever without the author's prior written permission.

**Examining Committee**

Mark Lewis, Mathematical and Statistical Sciences

Caroline Bampfylde, Alberta Environment

Jens Roland, Biological Sciences

Hao Wang, Mathematical and Statistical Sciences

For Joe, with love.

# Abstract

Climate change is currently a central problem in ecology, with far-reaching effects on species that may be difficult to quantify. Ectothermic species which rely on environmental cues to complete successive stages of their life history are especially sensitive to temperature changes and so are good indicators of the impacts of climate change on ecosystems. Based on data collected in growth experiments for the alpine butterfly *Parnassius smintheus* (Rocky Mountain Apollo), a novel mathematical model is presented to study developmental rate in larval insects. The movement of an individual through larval instars is treated as a discrete-time four-outcome Markov process, where class transition and death are assigned temperature-dependent probabilities. Transition and mortality probabilities are estimated using maximum likelihood estimation techniques. This adult emergence model is then integrated into a reproductive success model, and multi-year implications of climate change on the population dynamics of *P. smintheus* are explored.

# Acknowledgements

I would like to thank my supervisor, Dr. Mark Lewis, for his support and guidance for the last two years. Similarly, my thesis committee of Dr. Caroline Bampfyld, Dr. Jens Roland, and Dr. Hao Wang have been instrumental in directing my research and helping me to navigate this interdisciplinary field. Thanks also go to Dr. Roland for directing the experimental sections of my research and giving his invaluable expertise in butterfly biology.

The Lewis Research Group has been a source of invaluable discussions and research suggestions, so I would like to thank all of the students, postdocs, and research associates with whom it has been a privilege to work with for two years: Jaime Ashander, Marie Auger-Methe, Andria Dawson, Jon Jacobsen, Yu Jin, Justin Marleau, Hannah McKenzie, Peter Molnar, Jim Muirhead, Mario Pineda-Krch, Alex Potapov, Harshana Rajakaruna, Ulrike Schlaegel, Carly Strasser, and Meike Wittmann. Thanks also to Cecilia Hutchinson for her tireless administrative work.

The Roland Lab has also been instrumental in my understanding of butterfly biology and experimental design, and I would like to thank Amanda Doyle, Kurt Illerbrun, Amy Nixon, and Jennifer Waller for many insightful conversations. My experimental work was a collaborative work with Amanda Doyle, without whom much of my data collection would have been impossible. Her field assistant Sarah McPike was also instrumental in data collection. Thanks also to Jane Cooper, who collected data in my absence.

Dr. Roland also permitted me to use his *P. smintheus* mark-recapture data set, collected with Dr. Steve Matter, for use in model validation. Dr. Matter also allowed me to use his female fecundity experimental data for model parameterization, and answered many questions about *Parnassius* butterfly biology.

I would like to thank my family for their tireless love and support, and my sister Julia Wheeler for helpful comments on experimental design. Finally, I would like to thank Joe Fitzgerald for countless hours of discussion and debate, useful research avenues, and patient manuscript revision.

# Contents

<b>1</b>	<b>Introduction</b>	<b>11</b>
	Bibliography . . . . .	16
<b>2</b>	<b>Experimental temperature-dependent development</b>	<b>17</b>
2.1	Introduction . . . . .	17
2.2	Materials and methods . . . . .	19
2.2.1	Study species . . . . .	19
2.2.2	Experimental design . . . . .	21
2.2.3	Data management and statistical methods . . . . .	23
2.3	Results . . . . .	24
2.3.1	Developmental time in fifth instar . . . . .	24
2.3.2	Body size . . . . .	24
2.4	Discussion . . . . .	25
2.4.1	Time spent in fifth instar . . . . .	25
2.4.2	Body size . . . . .	28
2.4.3	Implications for <i>P. smintheus</i> . . . . .	29
	Bibliography . . . . .	31
<b>3</b>	<b>A multi-outcome Bernoulli process model</b>	<b>32</b>
3.1	Introduction . . . . .	32
3.1.1	A review of temperature-dependent insect developmental models and a motivation for the present study . . . . .	33
3.2	Modelling insect development with constant transitional probabilities	37
3.2.1	Development times for two classes . . . . .	38
3.2.2	Developmental times for multiple classes . . . . .	39
3.2.3	Expectation and variance for developmental times . . . . .	43
3.2.4	Modelling mortality . . . . .	46
3.3	Modelling insect development with varying transitional probabilities .	50
3.4	Parameter estimation . . . . .	51

3.4.1	Constant-valued transition and mortality probabilities . . . . .	51
3.4.2	Variable transition probabilities . . . . .	54
3.5	Model validation . . . . .	55
3.5.1	Converting mark-recapture data to emergence data . . . . .	56
3.5.2	Statistical methods for model validation . . . . .	56
3.6	Results . . . . .	57
3.6.1	Constant-valued transition and mortality probabilities . . . . .	58
3.6.2	Variable transition probabilities . . . . .	58
3.6.3	Validation of variable transition probability model . . . . .	61
3.7	Discussion . . . . .	68
3.7.1	Constant-valued transition and mortality probabilities . . . . .	68
3.7.2	Variable transition probabilities . . . . .	68
3.7.3	Implications for <i>P. smintheus</i> . . . . .	70
	Bibliography . . . . .	74
<b>4</b>	<b>Temperature-dependent reproductive success</b>	<b>75</b>
4.1	Introduction . . . . .	75
4.2	Model formulation and parameterization . . . . .	77
4.2.1	Emergence rate functions . . . . .	78
4.2.2	Error propagation . . . . .	81
4.3	Results . . . . .	83
4.3.1	Gaussian emergence function . . . . .	83
4.3.2	Temperature-dependent emergence function . . . . .	83
4.3.3	Effects of temperature on multi-year population dynamics . . . . .	90
4.4	Discussion . . . . .	94
4.4.1	Comparing results of emergence functions . . . . .	94
4.4.2	Toward quantitative predictions . . . . .	95
4.4.3	Model extensions and future directions . . . . .	96
	Bibliography . . . . .	99
<b>5</b>	<b>General discussion and conclusions</b>	<b>100</b>
	Bibliography . . . . .	105
<b>A</b>	<b>Dunn's test calculation</b>	<b>106</b>
<b>B</b>	<b>Probability distribution for developmental time to adulthood</b>	<b>107</b>
<b>C</b>	<b>Verification of model solutions</b>	<b>109</b>



# List of Figures

2.1	Alpine meadow in Kananaskis, Alberta. . . . .	19
2.2	Projected fractional increase for the 2050s in Alberta relative to 1961-1990 baseline data, for degree days $> 5^{\circ}\text{C}$ (in percent). Predictions were based on the following IPCC GCMs (left to right from top to bottom): NCARPCM A1B, HadCM3 A2(a), CGCM2 B2(3), CCSRNIES A1FI, and HadCM3 B2(b), each with attached prediction summaries for changes to Alberta's climate. The field site is indicated by an X (modified from Barrow and Yu (2005)). . . . .	20
2.3	A fifth instar <i>P. smintheus</i> larva feeding on <i>S. lanceolatum</i> (left) and an adult male nectar feeding on <i>Potentilla fruticosa</i> (right). . . . .	21
2.4	a) Developmental time in fifth instar; b) Weight at pupation; c) Maximum weight. The mean and median of each treatment are indicated by the square and red line, respectively, the edges of the box are the 25th and 75th percentiles, whiskers extend to the most extreme data points not considered outliers, and outliers are denoted by crosses. . . . .	26
2.5	Developmental rate versus temperature: a) Proximity to a lower temperature threshold for development may produce similar developmental rates; b) Developmental rates may decrease at greater than optimal developmental temperatures; c) Expected increase in developmental rate given a normal temperature range. Modified from Taylor (1981). . . . .	27
3.1	Schematic representation of the $r$ instar insect life history where $\mu_i$ is the probability of leaving the $i$ th class in a time step and $d_i$ is the probability of mortality in a time step. Daily outcomes for individuals are as described in Table 3.3. Individuals accumulate in the $r$ th instar (adulthood). . . . .	39

3.2	The negative binomial probability mass function (3.2) with $\mu = 0.1$ , with respect to number of classes $r$ and total developmental time $k$ . These distributions illustrate the probability of reaching adulthood on the $k$ th day, for varying numbers of classes, given transitional success probability $\mu = 0.1$ . . . . .	41
3.3	The probability mass function for total developmental time $k$ given geometric distributions (3.1) for developmental time within each class, for $r$ classes. Parameter values used are $\mu_1 = 0.1$ , $\mu_2 = 0.095$ , $\mu_3 = 0.0925$ , $\mu_4 = 0.0857$ (probability of transition decreases 5% for each successive class from the previous class probability). . . . .	44
3.4	Study site at Jumpingpound Ridge, Kananaskis, where mark-recapture field experiments for adult <i>P. smintheus</i> are carried out. Letters identify meadows, and bars between meadows indicate spatial connection through broken treeline. Used with permission from Matter et al. (2009). 56	56
3.5	Maximum likelihood estimates for cooler (triangle), ambient (diamond) and warmer (square) treatments, with adjusted Wald 95% confidence intervals (3.23) denoted by bars, for $\mu$ and $d$ parameters. . . . .	59
3.6	Predicted adult emergence $\epsilon_n$ in different temperature treatments with associated error (3.24) shaded, having constant transition and mortality probabilities. Later emergence occurs in a) cooler treatment and b) ambient treatment than in c) warmer treatment. . . . .	60
3.7	For each instar, black squares on left denote original maximum likelihood estimates for $a_i$ , with bars denoting associated 95% confidence intervals (3.26), as presented in Table 3.6 for $T_0 = 5$ . On the right, for each instar, the estimates for $a_i$ from 1000 bootstrapping trials are presented, with the mean $a_i$ value denoted by the black square. The means of the bootstrapping trials are hereafter used as the estimates for $a_i$ . . . . .	62
3.8	Linear transitional probability functions, $\mu_i(T) = a_i(T-5)$ , $i = 3, \dots, 6$ , using bootstrapped slope estimates as presented in Figure 3.7. . . . .	63
3.9	Adult emergence probability distributions $\epsilon_n$ (black curves) predicted from the variable transition probability model, with associated error (3.27) shaded in blue. Temperature regimes used as input are those from 2001, 2003 – 2005. . . . .	64

3.10	Adult emergence probability distributions $\epsilon_n$ (black curves) predicted from the variable transition probability model, with associated error (3.27) shaded in blue. Temperature regimes used as input are those from 2006 – 2009. . . . .	65
3.11	Observed versus predicted emergence probability distributions in 2001, 2003-2005. Black curves denote observed emergence (generated from mark-recapture data) and blue curves denote predicted emergence (generated from variable transition probability model with appropriate year’s temperature regime as input). . . . .	66
3.12	Observed versus predicted emergence probability distributions in 2006-2009. Black curves denote observed emergence (generated from mark-recapture data) and blue curves denote predicted emergence (generated from variable transition probability model with appropriate year’s temperature regime as input). . . . .	67
4.1	Sample adult emergence functions $\epsilon(t)$ : a) Gaussian emergence function with $A = 0.1$ , $\sigma = 15$ , and $t_1 = 210$ . b) Temperature-dependent emergence function generated from 2009 temperature data, using parameter values in Table 4.1. . . . .	82
4.2	Reproductive success ratios in year $\tau$ with respect to initial number of eggs, using a Gaussian emergence function. The reproductive success threshold is denoted by the dashed line. a) Varying the total emergence $A$ in the Gaussian emergence function demonstrates an increase in reproductive success with increasing $A$ . Sample reproductive success curves represent guaranteed reproductive failure (blue curve), reproductive success at a given threshold $E_\tau$ (green curve), and guaranteed reproductive success at all but very low initial numbers of eggs (red curve), given $A = 0.06$ , $0.07$ , and $0.08$ , respectively. Other parameter values are fixed at $t_1 = 210$ and $\sigma = 20$ . b) Varying standard deviation $\sigma$ in the Gaussian emergence function demonstrates a decrease in reproductive success with increasing $\sigma$ . Sample reproductive success curves represent guaranteed reproductive failure (red curve), reproductive success at a given threshold $E_\tau$ (green curve), and guaranteed reproductive success except at very low initial egg numbers (blue curve). Other parameter values are fixed at $t_1 = 210$ and $A = 0.08$ . 84	84

4.3	Predicted number of eggs $E_{\tau+1}$ (wide bars) each year given initial $E_{\tau} = 10^4$ , with associated error $\delta E_{\tau+1}$ denoted by bars. Error values are taken from Table 4.2. Parameter values used are as presented in Table 4.1. The reproductive success threshold is denoted by the dashed line.	86
4.4	Effects of daily temperature change (experienced by larvae) on overall adult emergence, using parameter values presented in Table 4.1. a) Adult emergence function $\epsilon(t)$ (green curve) changes when 2009 daily temperature values are decreased and increased by 3°C (blue and red curves, respectively). b) The positive relationship between temperature and total adult emergence. . . . .	87
4.5	Effects on standard deviation of temperature-dependent emergence function, due to varying parameter $d$ and varying input $T$ . a) Positive relationship of temperature and standard deviation of emergence function. b) Within 95% confidence interval for $d$ , a roughly quadratic relationship with standard deviation is observed. . . . .	88
4.6	Effects of varying larval mortality probability $d$ on overall adult emergence, using parameter values presented in Table 4.1. a) Adult emergence function $\epsilon(t)$ (green curve) changes when mortality probabilities are decreased and increased to the extrema of the estimate's 95% confidence interval (red and blue curves, respectively). b) The negative relationship between larval mortality and total adult emergence. . . .	89

4.7	Reproductive success ratios in year $\tau$ with respect to the initial number of eggs, using a temperature-dependent emergence function with 2009 temperature data as input. The reproductive success threshold is denoted by the dashed line. a) Increasing daily temperature input to the temperature-dependent emergence function demonstrates an increase in reproductive success. The reproductive success model predicts reproductive failure in 2009 with the observed temperature regime (blue curve), reproductive failure with a 1.0°C degree increase in daily temperature (green curve), and reproductive success at all but very low initial egg numbers with a 2.0°C degree increase in daily temperature (red curve). b) Decreasing larval mortality probability $d$ increases reproductive success. The reproductive success model predicts reproductive failure in 2009 with maximum likelihood estimate $\hat{d} = 0.01981$ (blue curve). Decreasing $d = 0.01581$ allows reproductive success at a threshold $E_\tau$ (green curve), and $d = 0.01181$ allows guaranteed reproductive success at all but very low initial egg numbers (red curve). . . . .	91
4.8	Fluctuations in captured adult population sizes from 2001–2009, taken from mark-recapture data for new adult captures. The time series exhibits a large amount of variability over a ten year period. . . . .	92
4.9	Simulated change in population size over a three year period where temperature-forcing drives reproductive success. Potential overwinter mortality is neglected. An initial number of eggs in Year 1, $E_1 = 10^4$ produces 0.71 times its initial number, given a “cooler” year (green curve). The population of eggs in Year 2 correspondingly decreases to $E_2 = 7100$ . Another cool year prompts 0.70 times the initial number of eggs to give $E_3 = 4970$ for Year 3. If Year 3 is “warmer” (red curve), the reproductive success threshold (denoted by the dashed line) is surpassed and 1.18 times the initial number of eggs is produced, giving $E_4 = 5865$ for the start of Year 4, denoted by the star. . . . .	93
D.1	Predicted adult emergence under varying start dates, 2001, 2003-2005.	114
D.2	Predicted adult emergence under varying start dates, 2006-2009. . . . .	115

# List of Tables

2.1	Ambient experimental temperatures corresponding to historical weather data for given weeks. . . . .	23
3.1	Potential paths taken to adulthood ( $r = 4$ ) in 5 days, denoted by number of days spent in each class. . . . .	42
3.2	Potential paths taken to adulthood ( $r = 4$ ) in $k$ days, denoted by the number of days spent in each class. . . . .	42
3.3	Potential outcomes in each time step in the constant transition probability model with constant mortality. Probabilities associated with each outcome for the $i$ th instar are presented. . . . .	46
3.4	Number and proportion of dispersal events each year recorded in <i>P. smintheus</i> adult mark-recapture experiments, with respect to number of individuals and number of captures. . . . .	57
3.5	Maximum likelihood estimates with associated 95% confidence intervals for constant transitional and mortality treatments, in each of the three temperature treatments. . . . .	58
3.6	Maximum likelihood estimates for $a_i$ with associated 95% confidence intervals, when transitional probabilities $\mu_i(T) = a_i(T - T_0)$ change due to varying developmental lower threshold temperatures $T_0$ . . . . .	61
3.7	Results of Wilcoxon signed-rank test, with critical values taken from Zar (2010). Predicted model emergence is not significantly different from observed emergence in all years. . . . .	62
3.8	Results of linear regression of observed on predicted emergence, with critical values taken from Zar (2010). Predicted model emergence is not significantly different from observed emergence in 2001 – 2008, and is significantly different in 2009. . . . .	63

4.1	Summary of parameters for adult emergence model (3.9)-(3.12) and reproductive success model (4.1). Transitional success probability functions are expressed $a_i(T - 5)$ due to prior fixing of $T_0 = 5^\circ\text{C}$ as the lower temperature threshold for development. . . . .	79
4.2	Error in total number of eggs produced in year $\tau$ , $\delta E_{\tau+1}$ , as contributed by each parameter, for $\tau = 2001, 2003, \dots 2009$ , given initial number of eggs $E_\tau = 10^4$ . Parameter values $x$ and associated error $\delta x$ are as presented in Table 4.1. Larval mortality probability $d$ and fecundity rate $\beta$ contribute the most error each year to the total error, denoted in bold in the table. . . . .	85
A.1	Results of Dunn's test for significance of differences between fifth instar developmental times in the temperature treatments, with critical values taken from Zar (2010). . . . .	106

# Chapter 1

## Introduction

Since the late twentieth century, climate change has been attributed as a major driver of changes to ecological systems worldwide. Understanding the effects of climate change at individual, population, community, and ecosystem levels has since become a primary area of research in ecology (Parmesan, 2006). Changes to climatic variables can affect species in empirically detectable ways. For instance, at an individual level, temperature changes can influence developmental rate, body size, and egg production in ectotherms (Taylor, 1981; Atkinson, 1994; Gibbs et al., 2010). At a population level, temperature changes can impact timing of life history events (Post et al., 2001), and at a community level, the shift in time of such life history events (such as egg hatching, adult emergence, and flowering) can remove or alter the temporal overlap of previously interacting species (most common in predator-prey and insect-host plant interactions) (Visser and Both, 2005).

Impacts of climate change have long been studied through indicator species like insects (reviewed in (Parmesan, 2006)). Insects, and butterflies in particular, are especially sensitive to climatic changes due to their reliance on environmental cues such as temperature and photoperiod to complete stages of their life history (Taylor, 1981). Butterflies make excellent study species when considering climatic effects, as data sets for certain species extend back as far as 100 years (Parmesan et al., 1999), so that the influences of long-term climatic shifts may be studied. Further, many species may be reared experimentally to determine temperature effects on larval growth or body size (see Taylor, 1981; Atkinson, 1994). These effects are often understood in a “normal” temperature range, but potential climatic changes predicted by global climate models may challenge this understanding of temperature-dependent dynamics. Further, these perturbations may present threats to species persistence through multiple mechanisms: habitat fragmentation and range shifts (Hill et al., 1999; Parmesan et al., 1999), and changing phenology, which may impact a popula-

tion by way of trophic mismatches (Thomson et al., 2010; Schweiger et al., 2008; Hoyer and Forchhammer, 2008; Both et al., 2009), temporal overlap with new predators or parasites (Thomson et al., 2010), and density-regulated activities such as successfully attacking resources (Berryman et al., 1985) and mate-finding (Calabrese and Fagan, 2004; Calabrese et al., 2008). The adaptability of species to rapid climatic shifts may ensure their survival, and mathematical modelling provides a tool which may allow the prediction of such persistence. By studying the effects of temperature on larval growth on a small population sample, for instance, a mathematical model may be parameterized by which predictions for a vast array of climatic scenarios may be made. It is at this interface of biology and mathematics in which the present study is conducted.

In this study, the effects of temperature on development time, phenology, and adult reproductive success are considered for the alpine butterfly *Parnassius smintheus* (Rocky Mountain Apollo). Found in isolated populations in alpine meadows surrounded by the treeline in the Rocky Mountains of Western Canada and the United States, this species is under the potential threat of climate change due to its geographical isolation. As an alpine species, if climate warming shifts the temperatures in these habitats outside the species' thermal tolerance range, extinction of populations may occur due to their inability to migrate to new suitable habitats (Parmesan, 2006). The following research questions are addressed in this study: How does temperature affect development time and final larval body size in *P. smintheus* larvae? Secondly, how does a changing temperature regime impact adult emergence in *P. smintheus*? Finally, does temperature as experienced by larvae affect adult reproductive success in *P. smintheus*?

In this work, influences of temperature on developmental time and resultant effects on phenology and adult reproductive success of *P. smintheus* are studied. In Chapter 2, an experiment to determine direct effects of temperature on developmental time in *P. smintheus* larvae is detailed. Larvae were collected from a field site in Kananaskis, Alberta and reared in temperature-controlled growth chambers. The thermal regime for an ambient temperature treatment was determined from historical weather data with constant day and night time temperatures which changed weekly to simulate temperatures experienced by larvae in the wild. Two other treatments reared larvae in warmer and cooler thermal regimes by increasing and decreasing the ambient treatment by 2°C respectively. Larval weights and successful transitions were recorded daily, as well as temperature on a given day. Significant differences in development time or body size would motivate further exploration of temperature impacts on *P. smintheus*, through the use of mathematical models. In fact, the experimental

data is used to parameterize the models presented in Chapters 3 and 4.

A significant experimental result for temperature on developmental time would illustrate the potential utility for a mathematical model that predicts the direct effects of temperature on larval development and subsequent adult emergence. Due to the small number of treatments and the variable temperature regimes, a cumulative developmental model where the temperature profile of previous days influences the present development (such as a degree-day model) would not be very useful for predicting effects outside the experimental regimes. The data may be used, however, to parameterize a model which treats temperature-dependent development as non-cumulative (that is, only the temperature in a given time step impacts its development in that time step). These considerations prompt a novel method of predicting temperature-dependent insect development presented in Chapter 3. Survival and transition through successive larval instars are modelled as Bernoulli processes with temperature-dependent transition probabilities. The model is exactly solved in the simple case in which transition and mortality probabilities are constants (i. e., comparing developmental times in “cooler”, “ambient”, and “warmer” scenarios with different transition and mortality probabilities as estimated from the experimental data sets). The case in which transitional probabilities are modelled as temperature-dependent functions is considered numerically. In both constant and varying probability cases, the probabilities are estimated by maximum likelihood methods. Due to the memoryless nature of the Bernoulli process underlying the developmental model, the experimental data for a given day (temperature and transitional success/failure) may be considered as independent of any other day, allowing the parameterization of the model for a large range of temperatures. The resultant model takes as input a seasonal temperature regime under which the larvae develop and predicts adult emergence distributions in time. These emergence distributions are then validated using mark-recapture data for *P. smintheus* adults.

Changes to phenology, as previously discussed, may adversely affect a population through changing temporal overlap with host plants and predators (Thomson et al., 2010; Schweiger et al., 2008; Hoyer and Forchhammer, 2008; Both et al., 2009), and through density-regulated activities such as attacking resources (Berryman et al., 1985) and finding mates (Calabrese and Fagan, 2004; Calabrese et al., 2008). In Chapter 4, this final point is considered. A model is constructed to predict direct effects of temperature (as experienced by larvae) on adult reproductive success in *P. smintheus*. A system of coupled non-linear ordinary differential equations, this model tracks the size of male, unmated female, and mated female populations within a season, as well as the number of eggs produced. This model incorporates the temperature-dependent

larval development model of Chapter 3, and the adult emergence function from that model acts as input to the male and unmated female populations. Direct effects of temperature (as experienced by larvae) on adult reproductive success have not previously been modelled, since such a model framework requires an appropriately parameterized adult emergence function such as that derived in Chapter 3, which itself relies on the temperature-dependent transitional success data from the experiment detailed in Chapter 2. The reproductive success model may be used to predict the number of eggs produced in a given breeding season. The presence of some initial number of eggs in the system, which produces the population, allows the iteration of the model through multiple seasons. Changing temperature regimes produce different adult emergence functions, so the model may be used to determine qualitative behaviour of the population in a changing climate. Quantitative predictions of reproductive success (using mark-recapture data for validation) are impossible due to accumulated error in the model parameters, as well as unknown overwinter mortality in eggs, an area of future study. However, a potential explanation is presented for observed yearly fluctuations in population size, which may be temperature driven, as higher adult emergence in warmer years prompts reproductive success which is not achieved in cooler years.

In this study, effects of temperature on larval *P. smintheus* are considered both experimentally and from a modelling perspective, with implications for reproductive success in adults. It presents a first attempt at understanding the effects of a warming climate on the population dynamics of this alpine butterfly.

# Bibliography

- Atkinson, D. (1994). Temperature and organism size – A biological law for ectotherms? *Advances in Ecological Research* 25, 1–58.
- Berryman, A. A., B. Dennis, K. F. Raffa, and N. C. Stenseth (1985). Evolution of optimal group attack, with particular reference to bark beetles (Coleoptera: Scolytidae). *Ecology* 66(3), 898–903.
- Both, C., M. van Asch, R. B. Bijlsma, A. B. van den Burg, and M. E. Visser (2009). Climate change and unequal phenological changes across four trophic levels: Constraints or adaptations? *Journal of Animal Ecology* 78, 73–83.
- Calabrese, J. M. and W. F. Fagan (2004). Lost in time, lonely, and single: Reproductive asynchrony and the Allee effect. *The American Naturalist* 164(1), 25–37.
- Calabrese, J. M., L. Ries, S. F. Matter, D. M. Debinski, J. N. Auckland, J. Roland, and W. F. Fagan (2008). Reproductive asynchrony in natural butterfly populations and its consequences for female matelessness. *Journal of Animal Ecology* 77, 146–156.
- Gibbs, M., H. V. Dyck, and B. Karlsson (2010). Reproductive plasticity, ovarian dynamics and maternal effects in response to temperature and flight in *Pararge aegeria*. *Journal of Insect Physiology* 56(9), 1275–1283.
- Hill, J. K., C. D. Thomas, and B. Huntley (1999). Climate and habitat variability determine 20th century changes in a butterfly’s range margin. *Proceedings of the Royal Society of London* 266, 1197–1206.
- Hoye, T. T. and M. C. Forchhammer (2008). Phenology of high-arctic arthropods: Effects of climate on spatial, seasonal, and inter-annual variation. *Advances in Ecological Research* 40, 299–324.
- Parmesan, C. (2006). Ecological and evolutionary responses to recent climate change. *Annual Review of Ecology, Evolution and Systematics* 37, 637–669.
- Parmesan, C., N. Ryrholm, C. Stefanescu, J. Hill, C. Thomas, H. Descimon, B. Huntley, L. Kaila, J. Kullberg, T. Tammaru, W. J. Tennent, J. A. Thomas, and M. Warren (1999). Poleward shifts in geographical ranges of butterfly species associated with regional warming. *Nature* 399(6736), 579–583.
- Post, E., S. A. Levin, Y. Iwasa, and N. C. Stenseth (2001). Reproductive asynchrony increases with environmental disturbance. *Evolution* 55, 830–834.
- Schweiger, O., J. Settele, O. Kudrna, S. Klotz, and I. Kühn (2008). Climate change can cause spatial mismatch of trophically interacting species. *Ecology* 89, 3472–3479.
- Taylor, F. (1981). Ecology and evolution of physiological time in insects. *The American Naturalist* 117, 1–23.

Thomson, L. J., S. Macfadyen, and A. A. Hoffmann (2010). Predicting the effects of climate change on natural enemies of agricultural pests. *Biological Control* 52, 296–306.

Visser, M. E. and C. Both (2005). Shifts in phenology due to global climate change: The need for a yardstick. *Proceedings of the Royal Society B* 272, 2561–2569.

## Chapter 2

# Experimental test of temperature-dependent development in larval *Parnassius smintheus* (Lepidoptera: Papilionidae)

### 2.1 Introduction

Climate change is currently a central problem in ecology, with far-reaching effects on species that may be difficult to quantify (Parmesan, 2006). Ectothermic species such as insects, which rely on environmental cues to complete successive stages of their life history, are especially sensitive to temperature changes and so are good indicators of the impacts of climate change on ecosystems.

In insects, temperature affects individual physiology and spatial distributions of populations: within the lifetime of a single organism, a change in temperature may influence developmental rate, body size, and mortality (Atkinson, 1994). Over multiple generations, consequences of a changing temperature regime may include range expansion or contraction (Parmesan et al., 1999; Hill et al., 1999), changing voltinism patterns (Powell and Logan, 2005; Bryant et al., 1997) and speciation (Scriber and Ording, 2005).

Ecological theories of body size dependence on temperature also consider both physiological and spatial perspectives. The temperature-size rule posits that the final size of an organism decreases as environmental temperature increases. Multiple measures have been used to describe “size”, especially in insects, where weight, length, wingspan, and head size are common. Strong correlation between such measures allow such a breadth to the definition, and the temperature-size rule is consistently

seen in ectotherms, where more than 83.5% of species studied exhibit this pattern (Atkinson, 1994). Bergmann's rule presents a similar idea for the geographic range of a species, where individuals are expected to have larger body masses at increasing latitudes, towards the northern edge of their range (associated with cooler temperatures) (Bergmann, 1847). When considering optimum temperatures for development, Taylor has suggested that insects in more northerly latitudes adapt for lower optimum temperatures, with sharp developmental declines at temperatures away from this optimum, while in southern latitudes insect development becomes more seasonally-dependent (Taylor, 1981).

As species evolve under past environmental conditions, perturbations to their environment may make species unsuited to new environmental conditions (Fred and Brommer, 2010). The ability of the present generation to adapt to environmental perturbations, however, may indicate the potential for long-term survival of the species. This provides a motivation for studying the effects of temperature on growth in many species, especially those encountering warming climate conditions. Insects are ideal ectotherms for studying physiological responses to environmental pressures, due to relatively short generations, high fecundity, and ease of capture for use in field and laboratory experiments. Understanding the relationship between temperature and development in insect species is crucial for predicting their survival under changing climatic regimes. This relationship is increasingly relevant for species in geographically isolated habitats such as mountaintops (Parmesan, 2006). Changing climatic regimes may not provide an escape outlet for such alpine species; should they be unable to adapt to new environmental conditions, they have no new habitats into which they may expand, and must go extinct.

The study species *Parnassius smintheus* (Rocky Mountain Apollo) is one such alpine species that may be threatened by climate change. A butterfly commonly found in the alpine meadows of the Rocky Mountain foothills in Western Canada and the United States, *P. smintheus* is a pollinator of many alpine plants. Figure 2.1 illustrates the alpine meadow habitat of *P. smintheus*. The Albertan habitat of this parnassian is under potential threat from climate change, with some global climate models (GCMs) predicting that mean spring and summer temperatures in Alberta may rise by 3°C in the next 40 years. Days of mean temperature greater than 5°C (a lower threshold for insect development) are predicted to increase in excess of 20% with respect to 1961-1990 (Barrow and Yu, 2005). Figure 2.2 indicates the projections of five GCMs for the increase per year in number of degree days > 5°C.

Potential effects of climate change for *P. smintheus* include changes to phenology or timing of life history events, caused by direct effects of temperature on develop-



Figure 2.1: Alpine meadow in Kananaskis, Alberta.

mental time in larvae. The objectives of the present study are to determine effects of temperature on developmental rates of *P. smintheus* larvae, which were collected from the wild and reared under three temperature regimes: an ambient regime reflecting the temperatures recorded near the field site, a cooler regime shifted  $2^{\circ}\text{C}$  below the ambient regime, and a warmer regime shifted  $2^{\circ}\text{C}$  above the ambient regime. The hypotheses under consideration are as follows: growth rates increase in the higher temperature regimes and body size (both maximum weight and weight at pupation) decrease with temperature according to the temperature-size rule.

## 2.2 Materials and methods

### 2.2.1 Study species

*Parnassius smintheus* is an alpine butterfly with a geographic range stretching throughout mountainous areas of Western Canada and the United States. It is a common butterfly in the Rocky Mountain foothills of Alberta (Roland et al., 2000) and larvae are specialists, feeding on the leaves and occasionally flowers of *Sedum lanceolatum*. Egg hatching is triggered by snowmelt, and five larval instars occur prior to pupation. In Alberta, adults are seen to emerge in early to mid-July, with males emerging first (Calabrese et al., 2008).

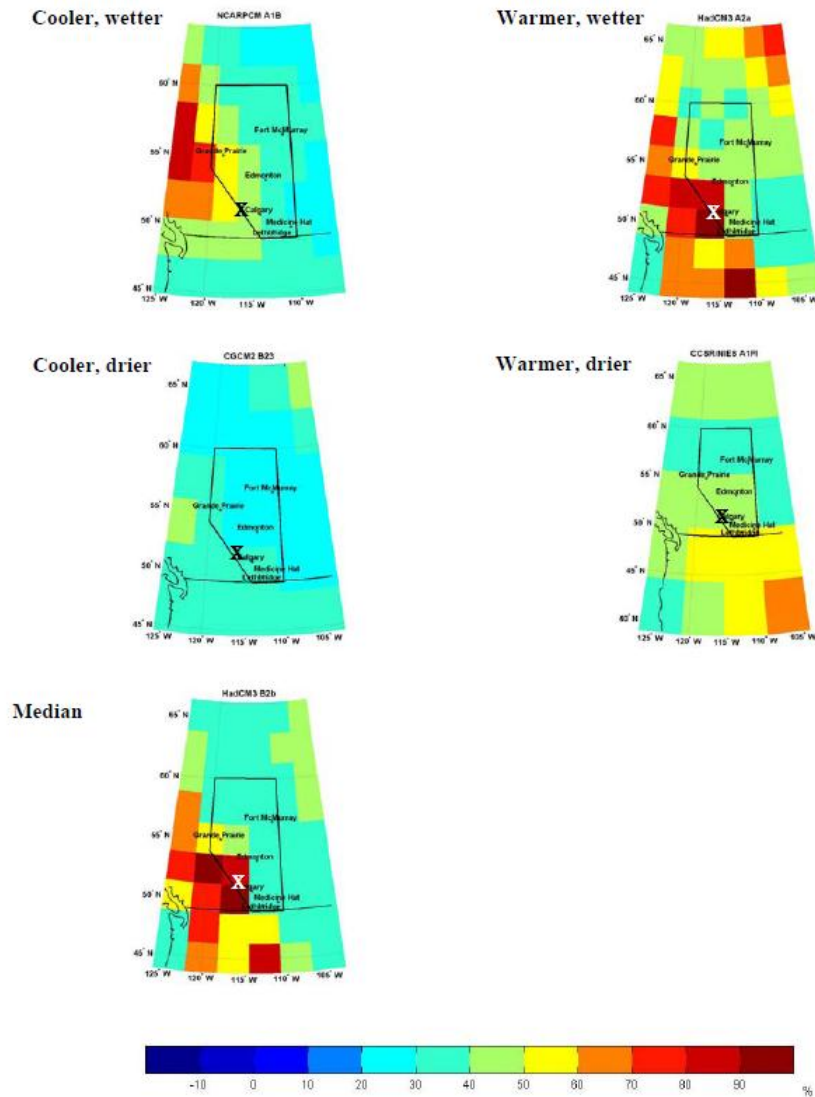


Figure 2.2: Projected fractional increase for the 2050s in Alberta relative to 1961-1990 baseline data, for degree days  $> 5^{\circ}\text{C}$  (in percent). Predictions were based on the following IPCC GCMs (left to right from top to bottom): NCARPCM A1B, HadCM3 A2(a), CGCM2 B2(3), CCSRNIES A1FI, and HadCM3 B2(b), each with attached prediction summaries for changes to Alberta's climate. The field site is indicated by an X (modified from Barrow and Yu (2005)).



Figure 2.3: A fifth instar *P. smintheus* larva feeding on *S. lanceolatum* (left) and an adult male nectar feeding on *Potentilla fruticosa* (right).

### 2.2.2 Experimental design

An experiment was developed to test hypotheses regarding thermal effects on growth rates and body size, and also to collect data for the partial parameterization of the temperature-dependent larval development model presented in Chapter 3. This experiment was designed in collaboration with Amanda Doyle (Department of Biological Sciences, University of Alberta). Ninety three *P. smintheus* caterpillars ranging from third to fifth instar were collected from field sites at Lusk and Jumpingpound Ridges (51°57' N, 114°54' W), both in Kananaskis, Alberta. A sufficient supply of *S. lanceolatum* was also collected to serve as a food source for the caterpillars.

Caterpillars were divided into three groups and placed in individual plastic cups containing soil from a Lusk meadow and a *S. lanceolatum* plant. See Figure 2.3 for the relative size of a fifth instar caterpillar to the cup. Caterpillars were then placed in temperature-regulated growth chambers: an ambient chamber, a chamber 2°C warmer than the ambient and a chamber 2°C cooler than the ambient. Sample sizes in the ambient, warmer, and cooler chambers are denoted  $n_a = 15$ ,  $n_{+2} = 15$ , and  $n_{-2} = 63$ , respectively. Sample size in the cooler chamber was larger than the others due to geographic proximity to the field site and because other experiments were conducted concurrently on a portion of this sample which did not significantly affect

growth rates (pers. comm., Doyle). The extra *S. lanceolatum* was divided between the growth chambers, so that the plants were kept in the same temperature-controlled environment as the caterpillars. Host plant quality has been seen to influence growth rates and final size in several insect species (see (Atkinson, 1994) for review), and thus *S. lanceolatum* was kept in alpine meadow soil and well-watered for the duration of the experiment. Further, experiments comparing larval growth in lab and field settings have detected no significant difference in development of larvae reared on transplanted versus non-transplanted *S. lanceolatum* plants (pers. comm., Doyle), so it may be concluded that transplanting does not induce any significant defenses in the host plant in the time period of the experiment.

Chambers were programmed with 16/8 hour diurnal cycles having constant temperature and humidity in the day and night periods, changed weekly according to the procedure described below. Photoperiod was held constant across all treatments, as changes in daylight length have been shown to induce developmental response in several species of butterfly (Gotthard, 2008). Historical weather data for Nakiska Ridgetop, Kananaskis (50° 56.550' N, 115° 11.417' W), having a comparable elevation to the field sites, as well as a geographic proximity, determined the weekly temperature profile for the ambient chamber (Environment Canada, 2010). Each week, an averaging procedure was applied to the data corresponding to the same week over a ten year period (1999-2008), given as follows:

1. To account for differences between air and ground temperature, 5°C was added to the maximum daytime temperature (weather station is located approximately 1 m above the ground). This offset was recorded in May 2009 at Kananaskis.
2. Of these new maximum temperature values, the mean was calculated from seventy data points (seven data points per week over a ten year period).
3. A mean minimum temperature was calculated similarly, though without the offset of the air-to-ground temperature difference (see growth chamber limitations below).

The mean maximum and minimum temperatures were then used as the daytime and night time temperatures, respectively, in the ambient chamber. The other two chambers had their day and night temperatures adjusted accordingly from those of the ambient chamber. Technical considerations in the growth chambers required a low temperature threshold to be set at 5°C, which was the substituted night temperature in the event of a lower mean temperature, for all the chambers. Because 5°C is an approximate lower threshold for larval development in many insect species (Taylor,

1981), this technical limitation was deemed permissible. Humidity in all growth chambers was maintained at 80% during the day and 65% at night, as high humidity was required for larval survival, as low humidity results in desiccation (pers. comm., Matter) but low night time temperatures prevented higher humidity (as chambers would develop frost). Following this procedure for obtaining temperature regimes, the ambient temperature regime for each week is recorded in Table 2.1.

Week	Day Temperature	Night Temperature
June 19 – 25	14.5° C	2.3° C
June 26–July 2	17.1° C	5.1° C
July 3 – 9	17.3° C	4.3° C
July 10 – 16	19.9° C	6.2° C
July 17 – 23	20.0° C	6.9° C
July 24 – 30	19.8° C	6.3° C
July 31–Aug 6	18.0° C	4.6° C
Aug 7 – 13	17.3° C	4.6° C
Aug 14 – 20	19.2° C	6.1° C
Aug 21 – 27	19.2° C	6.1° C

Table 2.1: Ambient experimental temperatures corresponding to historical weather data for given weeks.

At 6 pm daily, caterpillars were removed from their growth chambers and their weights were recorded. Mortality and moultings (indicative of an instar transition) which had occurred in the previous twenty four hours were also recorded. *S. lanceolatum* in each individual cup was watered and replaced as necessary, so that a sufficient food source was always present. Caterpillars did not move between cups.

### 2.2.3 Data management and statistical methods

Each day both weight and instar were recorded for each living caterpillar; from this data, both maximum weight and weight at pupation, as well as number of days from fifth instar onset to pupation were documented. Both pupal and maximum weight were documented as the larvae were observed to lose weight prior to pupation, so pupal weight might not demonstrate the temperature-size rule.

Given the disparity in the (relatively small) sample sizes, all statistical tests are non-parametric. In the ambient and warmer treatments, time spent in fifth instar was documented only for individuals which were captured prior to fifth instar onset (the date of fifth instar onset was known). However, the cooler treatment, when subjected to this restriction, had too small a sample size, so individuals collected from the field in fifth instar were included in the group (though dates of transition to fifth instar were unknown). Any statistical estimates of time spent in fifth instar in the cooler treatment are thus decreased.

The Kruskal-Wallis Rank Sum Test is used to determine the significance of differences between temperature treatments in both developmental time to pupation, pupation weight, and maximum weight. The null hypotheses state that the developmental time (or pupal weight or maximum weight, depending on the case) are the same in the different treatments, and the alternate hypotheses state that these times (or weights) are different. Dunn’s test for non-parametric multiple comparisons (with standard error modified to account for tied ranks) (Zar, 2010) is applied to isolate significant differences between treatments. Using Dunn’s test for each measure as required, the null hypotheses state that the development time (or pupal weight or maximum weight) are the same between two specific treatments, while the alternate hypotheses state that these times (or weights) are different in the specified treatments.

## 2.3 Results

### 2.3.1 Developmental time in fifth instar

Thirty-eight larvae survived to pupation ( $np_a = 6$ ,  $np_{+2} = 9$  and  $np_{-2} = 23$ ), and a significant difference existed between the treatments (Kruskal-Wallis Rank Sum test,  $p = 0.00111$ ,  $df = 2$ ). The developmental times to pupation were significantly different between the ambient and the warmer treatment (Dunn’s test,  $Q_{\text{obs}} = 2.638$ ) and between the colder treatment and the warmer treatment ( $Q_{\text{obs}} = 3.591$ ). The difference between the ambient and the colder treatment was not significant ( $Q_{\text{obs}} = 0.0473$ ). See Appendix A for details of the Dunn’s test calculation. The distributions of waiting times across the different treatments are presented in Figure 2.4a. The null hypothesis was thus rejected for the warmer treatment, in that the developmental time was significantly shorter than in the cooler and ambient treatments. The null hypothesis was not rejected when comparing the ambient and cooler treatments, in that the difference between developmental times was non-significant.

### 2.3.2 Body size

Of the thirty-eight larvae surviving to pupation, no significant difference existed between the weights at pupation (Kruskal-Wallis Rank Sum test,  $p = 0.1862$ ,  $df = 2$ ). The null hypothesis, that body size does not change across temperature treatments, was not rejected. However, recalling that the anticipated result from the temperature-size rule was that body size would decrease in increasing temperatures, the opposite result was seen. The mean weights ( $m$ ) at pupation ( $m_{-2} = 0.3845$  g,  $m_a = 0.4192$  g, and  $m_{+2} = 0.4279$  g) increased as the temperature regimes warmed, contrary to

the temperature-size rule. The distributions of body weight at pupation across the different treatments are presented in Figure 2.4b.

Differences between maximum body weight across the three treatments were also non-significant (Kruskal Wallance Rank Sum test,  $p = 0.4747$ ,  $df = 2$ ), not rejecting the null hypothesis that body size does not change with temperature. The opposite pattern as that expected from the temperature-size rule was present in the mean maximum weights ( $\bar{m}$ ): they increased with increasing temperature ( $\bar{m}_{-2} = 0.4949$  g,  $\bar{m}_a = 0.5067$  g,  $\bar{m}_{+2} = 0.5225$  g). See Figure 2.4c for the distribution of maximum body weight across the different temperature treatments.

## 2.4 Discussion

The developmental time spent in the fifth instar is significantly longer in both the ambient and cooler treatments than in the warmer treatment, though no significant difference in developmental time was observed between the ambient and cooler treatments. Larval body size, measured by both weight at pupation and maximum larval weight, does not differ significantly between the temperature treatments, and in fact mean weights increase with temperature.

### 2.4.1 Time spent in fifth instar

Developmental times are significantly shorter in the warmer temperature treatment, which satisfies the first hypothesis linking increasing temperatures to faster growth. The developmental times in the cooler and ambient developmental times are interesting because no significant difference is detected between them. Unless the experimental temperatures fall near a threshold for development (Figure 2.5a) or the optimal developmental temperature (Figure 2.5b), one would expect developmental rates to increase as temperature increases (Figure 2.5c) (Taylor, 1981). Given that field temperatures for *P. smintheus* larvae demonstrably fall outside the experimental thermal range (Environment Canada, 2010), the former case is unlikely from an evolutionary perspective. Since developmental rates are higher in the warmer treatment, the temperatures associated with the cooler and ambient treatments are unlikely to be near an optimum growth temperature, ruling out the latter case.

It is possible, however, that the cooler treatment is sufficiently near a lower developmental threshold that mortality reduces the variability in development times, due to death of individuals having longer developmental times (Sharpe et al., 1977). That is, the statistical analysis only considers the developmental times of larvae that survive to pupation, and if lower temperatures prompt longer developmental times,

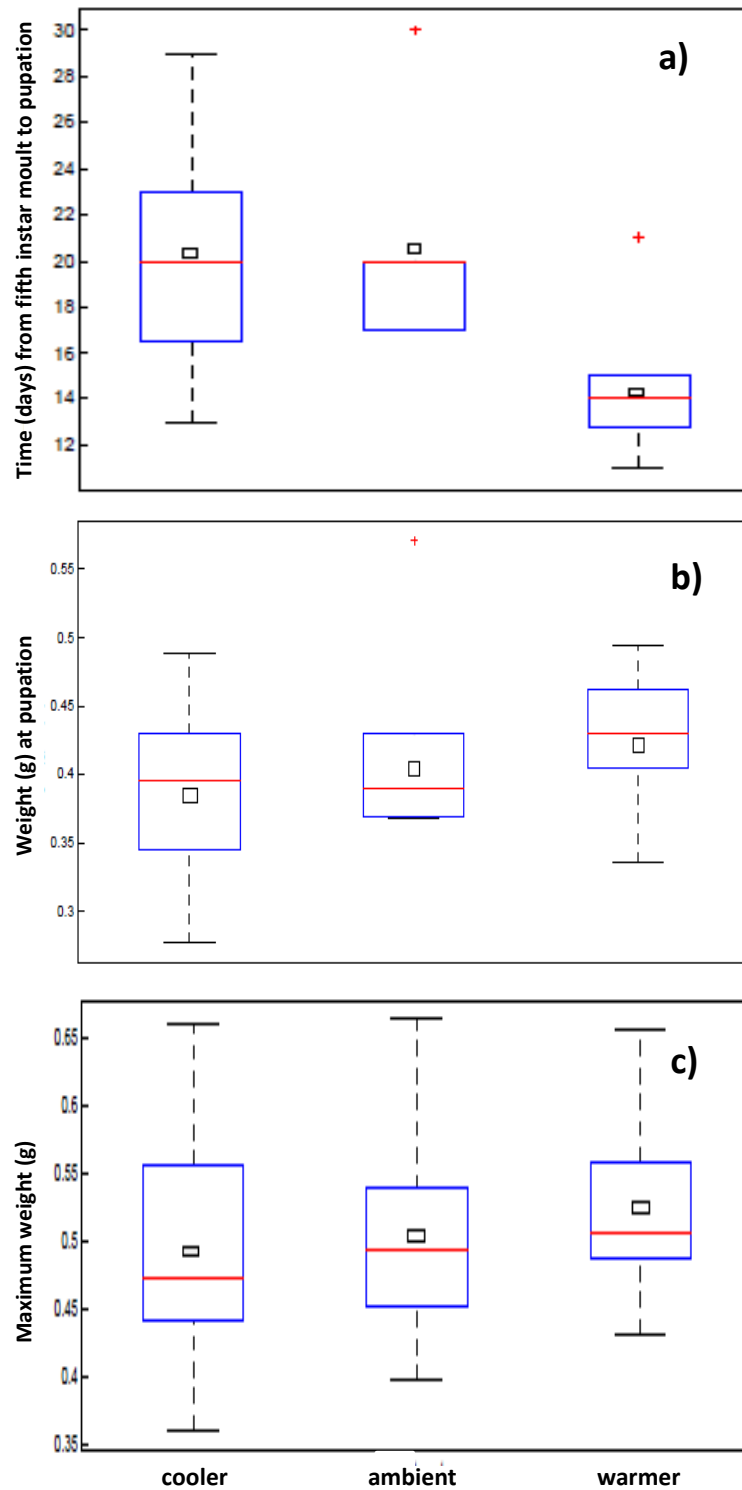


Figure 2.4: a) Developmental time in fifth instar; b) Weight at pupation; c) Maximum weight. The mean and median of each treatment are indicated by the square and red line, respectively, the edges of the box are the 25th and 75th percentiles, whiskers extend to the most extreme data points not considered outliers, and outliers are denoted by crosses.

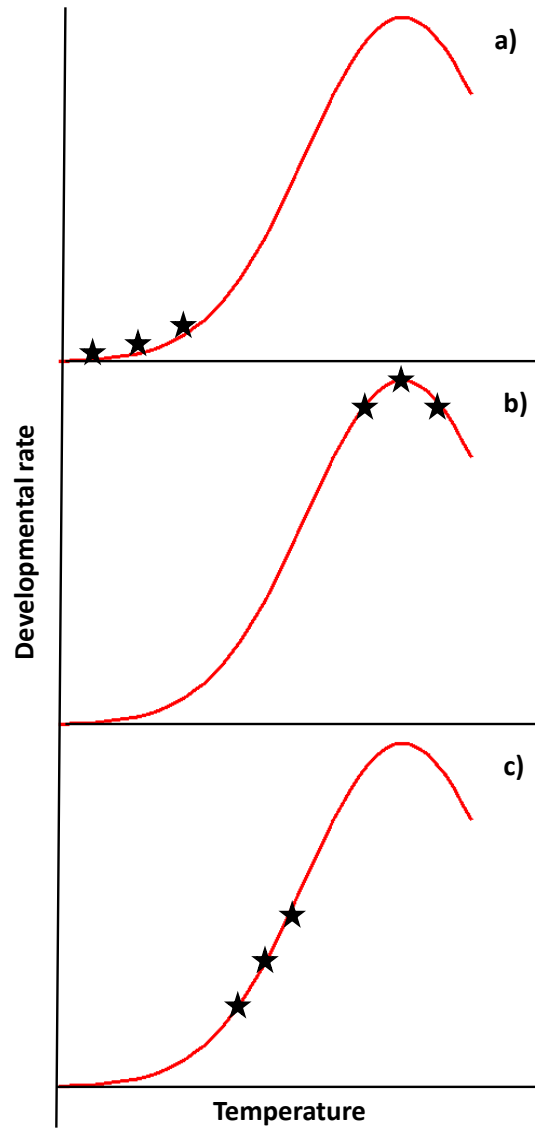


Figure 2.5: Developmental rate versus temperature: a) Proximity to a lower temperature threshold for development may produce similar developmental rates; b) Developmental rates may decrease at greater than optimal developmental temperatures; c) Expected increase in developmental rate given a normal temperature range. Modified from Taylor (1981).

slow-developing larvae have the most opportunity to die. Such individuals are thus excluded from the analysis and thus the developmental time is skewed towards a shorter than expected time. This idea is supported by a comparison of development time variability and mortality in the ambient and cooler treatments: mortality is higher in the cooler treatment and development time variability is higher in the ambient treatment. A decrease in variability may be prompted by the lack of longer developmental times (induced by greater mortality). Thus it is possible that the developmental times in the ambient and cooler treatments are non-significantly different because the cooler temperatures prompt a higher mortality in longer-developing individuals.

#### 2.4.2 Body size

Patterns expected by the temperature-size rule, as documented in multiple butterfly species (Atkinson, 1994), are absent in this experiment. No significant differences are detected between temperature treatments. This is potentially an artefact of the small sample size, but when considering both the mean weight at pupation and mean maximum weight, an increase is present in increasing temperature treatments, which actively contradicts the temperature-size rule. Further experimental work, with larger sample sizes, is thus needed to determine if body size in *P. smintheus* larvae is independent of temperature or if perhaps *P. smintheus* is an exception to the temperature-size rule. Such exceptions have previously been experimentally demonstrated in Lepidoptera for *Pseudaletia unipuncta* (Guppy, 1969). Occasionally, reversals to the temperature-size rule have been documented in species subjected to extreme environmental conditions: *Manduca sexta* larvae, which under expected environmental conditions follow the temperature-size rule, may reverse this growth behaviour when subjected to combined lower temperatures and sub-optimal host plant quality (Diamond and Kingsolver, 2010). Given the present experimental design, however, it is unlikely that a poor food source significantly influenced body size in the *P. smintheus* larvae, as *S. lanceolatum* is the primary food source for *P. smintheus* larvae and it was refreshed regularly.

It should also be noted that measures of body size used in this analysis are both absolute. Only weight at pupation and maximum weight are considered, neither of which account for body weight at the beginning of the experiment. No measures were undertaken in this analysis to consider relative growth, because the individuals were of different ages and instars at the start of the experiment. The data could not be normalized to consider relative body size, which might have influenced the results.

### 2.4.3 Implications for *P. smintheus*

Further study is needed to understand how changes to developmental time in *P. smintheus* affect interactions with other species. Vegetation generally responds more slowly to climatic changes than insects (Singer and Parmesan, 2010), and potential temporal asynchronies in *P. smintheus* with its host plants have not been studied. For instance, little is known about the effects of warming temperatures on *S. lanceolatum*, the primary host plant for *P. smintheus* larvae. Should *S. lanceolatum* development also increase, and flowering occur earlier, its nutritional value as a host plant would decrease. If temperature change has no effect on flowering, then early emergence of *P. smintheus* adults might no longer synchronize with flower emergence, and nectar resources for adults (essential for reproduction, Matter et al. (2009)) would decrease. Furthermore, a significant enough temperature increase, while still within the thermal tolerance for *P. smintheus*, might force host and nectar flowers out of the shared habitat. Even a change to host plant density or spatial heterogeneity might influence larval survivorship, as is the case in *Parnassius apollo* (Fred and Brommer, 2010). This experiment and subsequent statistical analysis of developmental data for *P. smintheus* have indicated some effects of temperature on development in larvae. One may now consider how to predict temperature-dependent changes in *P. smintheus* larval development, and what effects such phenological changes may have to the population dynamics of the species. These questions are addressed in Chapters 3 and 4.

# Bibliography

- Atkinson, D. (1994). Temperature and organism size – A biological law for ectotherms? *Advances in Ecological Research* 25, 1–58.
- Barrow, E. and G. Yu (2005). Climate scenarios for Alberta: A report prepared for the Prairie Adaptation Research Council in co-operation with Alberta Environment. Technical report, Prairie Adaptation Research Council and Alberta Environment.
- Bergmann, C. (1847). Über die Verhältnisse der Wärmeökonomie der Thiere zu ihrer Grösse. *Göttinger Studien* 3(1), 595–708.
- Bryant, S. R., C. D. Thomas, and J. S. Bale (1997). Nettle-feeding nymphalid butterflies: Temperature, development, and distribution. *Ecological Entomology* 22, 390–398.
- Calabrese, J. M., L. Ries, S. F. Matter, D. M. Debinski, J. N. Auckland, J. Roland, and W. F. Fagan (2008). Reproductive asynchrony in natural butterfly populations and its consequences for female matelessness. *Journal of Animal Ecology* 77, 146–156.
- Diamond, S. E. and J. G. Kingsolver (2010). Environmental dependence of thermal reaction norms: Host plant quality can reverse the temperature-size rule. *The American Naturalist* 175(1), 1–10.
- Environment Canada (2010). National climate data and information archive. [www.climate.weatheroffice.ec.gc.ca](http://www.climate.weatheroffice.ec.gc.ca), accessed May 2009 - January 2010.
- Fred, M. S. and J. E. Brommer (2010). Olfaction and vision in host plant location by *Parnassius apollo* larvae: Consequences for survival and dynamics. *Animal Behaviour* 79, 313–320.
- Gotthard, K. (2008). Adaptive growth decisions in butterflies. *BioScience* 58(3), 222–230.
- Guppy, J. C. (1969). Some effects of temperature on the immature stages of the armyworm *Pseudaletia unipuncta* (Lepidoptera: Noctuidae), under controlled conditions. *Canadian Entomologist* 101, 1320–1327.
- Hill, J. K., C. D. Thomas, and B. Huntley (1999). Climate and habitat variability determine 20th century changes in a butterfly’s range margin. *Proceedings of the Royal Society of London* 266, 1197–1206.
- Matter, S. F., M. Ezzeddine, E. Duermit, J. Mashburn, R. Hamilton, T. Lucas, and J. Roland (2009). Interactions between habitat quality and connectivity affect immigration but not abundance or population growth of the butterfly *Parnassius smintheus*. *Oikos* 118, 1461–1470.
- Parmesan, C. (2006). Ecological and evolutionary responses to recent climate change. *Annual Review of Ecology, Evolution and Systematics* 37, 637–669.

- Parmesan, C., N. Ryrholm, C. Stefanescu, J. Hill, C. Thomas, H. Descimon, B. Huntley, L. Kaila, J. Kullberg, T. Tammaru, W. J. Tennent, J. A. Thomas, and M. Warren (1999). Poleward shifts in geographical ranges of butterfly species associated with regional warming. *Nature* 399(6736), 579–583.
- Powell, J. and J. Logan (2005). Insect seasonality: Circle map analysis of temperature-driven life cycles. *Theoretical Population Biology* 67(3), 161–179.
- Roland, J., N. Keyghobadi, and S. Fownes (2000). Alpine *Parnassius* butterfly dispersal: Effects of landscape and population size. *Ecology* 81(6), 1642–1653.
- Scriber, J. M. and G. J. Ording (2005). Ecological speciation without host plant specialization; possible origins of a recently described cryptic *Papilio* species. *Entomologia Experimentalis et Applicata* 115, 247–263.
- Sharpe, P. J. H., G. L. Curry, D. W. DeMichele, and C. L. Cole (1977). Distribution model of organism development times. *Journal of Theoretical Biology* 66, 21–38.
- Singer, M. C. and C. Parmesan (2010). Phenological asynchrony between herbivorous insects and their hosts: Signal of climate change or pre-existing adaptive strategy? *Philosophical Transactions of the Royal Society B* 365(1555), 3161–3176.
- Taylor, F. (1981). Ecology and evolution of physiological time in insects. *The American Naturalist* 117, 1–23.
- Zar, J. H. (2010). *Biostatistical Analysis* (5th ed.). Prentice Hall.

## Chapter 3

# A multi-outcome Bernoulli process model to predict development time in insect larvae

### 3.1 Introduction

Temperature-dependent developmental rates in insects have long been a question of scientific interest, and the advent of anthropogenic climate change offers a new motivation for such study. Phenology, or the study of climatic effects on the timing of life history events, becomes particularly relevant under changing climatic conditions. The ability to accurately model the changes to life history events in insects (larval moultings and adult emergence, for instance) is relevant from a conservation perspective. Appropriate emergence times in larval instars may, for instance, allow individuals to avoid predators and parasites which they would otherwise encounter (Visser and Both, 2005; Thomson et al., 2010). Further, temperature-dependent timing can control adult emergence, which can affect mating success (Calabrese and Fagan, 2004; Calabrese et al., 2008) or ability to attack resources (Berryman et al., 1985).

Perhaps most significantly, individual development time must coincide with resource availability, a consideration especially important for specialist herbivores and pollinators (Yurk and Powell, 2009). In the worst-case scenario, a host plant or other necessary resource cannot persist within a changing temperature regime, which results in habitat fragmentation for the insect species under consideration (Stork et al., 2009; Schweiger et al., 2008). Habitat fragmentation and contraction is especially dangerous for species that are geographically isolated or have barriers to dispersal, such as mountainous species (Parmesan, 2006). Resources need not be absent from a habitat, however, to make them unavailable. Trophic mismatches can occur when the seasonal temporal overlap of a resource and its consumer are influenced by cli-

matic changes (documented in Lepidoptera *Epiphyas postvittana*, *Boloria titania*, the *Nymphalidae* family, and *Operophtera brumata* and *Tortrix viridana* in (Thomson et al., 2010; Schweiger et al., 2008; Hoye and Forchhammer, 2008; Both et al., 2009), respectively). Thus, understanding how climate drives developmental rate change in insects is important for species conservation.

### **3.1.1 A review of temperature-dependent insect developmental models and a motivation for the present study**

The study of temperature-dependent dynamics in insects is an old one, with experimental work conducted as early as the 1800s (Uvarov, 1931). Prior to the 1970s, much of the modelling work conducted for temperature-dependent dynamics in insects focused on degree-day models, which assume a linear relationship between temperature and developmental rate, where development is measured in terms of time accumulated above a lower threshold temperature. Degree-day models were commonly used as they were computationally tractable and adequately predictive within the usual range of temperatures insects might encounter in the field (Worner, 1992). With the advent of more powerful computing resources, researchers began to re-evaluate these linear models and their deficiencies; linear degree-day models do not perform well for extreme temperature ranges for organisms, nor under variable conditions (Stinner et al., 1974). Further, they do not capture behaviours, such as diapause or hibernation, which occur in insects during periods of environmental stress (Tanigoshi and Logan, 1979). Studying non-linear effects becomes especially important in the face of climatic change, where temperature regimes may become more variable or shift into entirely new ranges.

Early non-linear developmental models were pioneered in the 1970s as computational resources improved, using various techniques to introduce skewed non-linear development times, and to capture effects of varying temperatures. Two major frameworks exist in the literature for modelling temperature-dependent insect development, consisting of developmental rate models to predict larval growth rates or development times, and distribution models to predict completed development times.

Stinner et al. (1974) were among the first to address non-linear dynamics in growth rates for insect modelling, proposing a sigmoid curve to represent insect growth rates at different temperatures. They published the paper with a FORTRAN code to demonstrate the tractability of the non-linear problem. Logan et al. (1976) captured the non-linear dynamics of a temperature-dependent growth rate by formulating it as a boundary layer problem, with low and high temperature growth rates modelled as outer and inner solutions, respectively. They considered the question of

variable temperature input by assuming additive effects of temperature on development, so the model allowed for variable temperatures in simulation by dividing a variable temperature regime into short intervals of constant temperature. This model later was modified by Lactin et al. (1995) to better simulate development near the lower temperature developmental threshold. While Stinner et al. (1974) and Logan et al. (1976) were more concerned with phenomenological approaches to temperature-dependent insect growth rates, Sharpe and DeMichele (1977) were among the first to consider a mechanistic approach. In their model, development is considered proportional to the temperature-dependent reaction rate of control enzymes. Later modified by Schoolfield et al. (1981) to improve parameter estimation techniques, this biophysical model is presently known as the Sharpe-Schoolfield equation. It was modified by van der Have and de Jong (1996) who developed it further to consider both growth (body size) and differentiation (rate of movement between developmental stages) as independent temperature-driven processes.

From the perspective of climate change studies, this separation of body size from differentiation rate is an important consideration in insect growth, as perturbations caused by climate change may affect the environmental cues that insects use in development. Under increasing temperature regimes, insects may complete development faster at the expense of body size (Atkinson, 1994; van der Have and de Jong, 1996), and environmental perturbations may in fact increase variability in developmental times (Iwasa and Levin, 1995). It is therefore crucial to understand how a varying temperature regime impacts developmental time (which may or may not influence body size) in larval insects. With these considerations in mind, the mechanistic model presented in this chapter will consider direct effects of temperature on developmental time.

As the present objective of this study is to mechanistically consider direct effects of temperature on larval development time, a model that considers this developmental time independently of growth rate is most appropriate. This satisfies the first of the major framework types presented in the literature, the temperature-dependent developmental rate model. The second framework that is often discussed is, as previously mentioned, the distribution model which considers completed development times from a probabilistic perspective. Such a framework is useful for studying effects of larval environmental conditions on adult dynamics. Variability in developmental times may, as previously suggested, impact density-dependent adult activities such as mate-finding (Calabrese and Fagan, 2004; Calabrese et al., 2008) or resource-attacking (Berryman et al., 1985). The importance of developmental variability was first considered by Stinner et al. (1975) using fitted phenomenological cumulative developmental distri-

butions , and was later modelled by Sharpe et al. (1977) using inverted normal and quadratic probability distributions, and by Wagner et al. (1984) using cumulative Weibull distributions.

As environmental conditions (such as temperature) experienced by larvae may be important to adult population dynamics, the model presented in this chapter will also predict a cumulative development distribution, or an adult emergence distribution. This will allow further consideration of how variability in developmental times may impact population dynamics.

A review of the literature has, up until this point, motivated a mechanistic temperature-dependent developmental time model which predicts an adult emergence distribution. The final consideration which must be addressed in the present model is the difference between constant and variable temperature input. In most of the models discussed above, temperature is considered as a constant, or, when varied, is discretized into small intervals of constant temperature. Worner (1992) suggested that this method is inherently flawed when considering cumulative development. When cumulative development is summed from discrete intervals of developmental rates, and these developmental rates change non-linearly according to a non-constant temperature regime, a rate summation or Kauffmann error results, giving very different results for constant and non-constant temperature regimes. Worner tested the boundary layer model of Logan et al. (1976) and the mechanistic control enzyme model of Sharpe and DeMichele (1977) under constant and variable temperature regimes and found large differences in their predictions, especially apparent when developmental rates were strongly non-linear or diurnal amplitudes (differences between constant day and night time temperatures) were large.

The contention in the literature between constant and variable temperature regime developmental models, as well as the available data for parameterization motivates here a different kind of model. The experimental design of Chapter 2 resulted in a data set which gives transitions and mortality for three different variable temperature regimes. Because the rearing temperatures were not constant, developmental rate curves such as the ones proposed in Bentz et al. (1991) (which incorporate the previously mentioned developmental rate model of Logan et al. (1976) and the developmental distribution models of Stinner et al. (1975) and Wagner et al. (1984)) are not appropriate for the present data set. A degree-day model formulation would permit the prediction of cumulative effects of temperature on development for the three experimental temperature treatments, but might not be quantitatively useful given temperature regimes outside the experimental range. Therefore, a model which ignores cumulative effects of temperature on growth is proposed.

To consider direct and non-cumulative effects of temperature on developmental times and in adult emergence, a Bernoulli process model is proposed, where temperature-dependent transition between larval instars and mortality are modelled as memoryless Bernoulli outcomes. That is, in a given time step, the transition and mortality probabilities are independent of those of the previous time steps, though maturation to adulthood is conditional on having successfully transitioned through all the larval classes. A probabilistic framework also allows for a measure of uncertainty in transitional success and emergence, unlike many of the deterministic models discussed above. Further, previous modelling efforts consider various mechanisms by which temperature influences developmental rates and emergence times, but larval mortality is largely ignored; for many univoltine species, long development times (associated with lower temperatures) are indicative of lower individual fitness and higher juvenile mortality (Atkinson, 1994). A change in developmental time may also change temporal overlaps with predator or host-plant species which may influence juvenile mortality. The model presented in the following section thus considers larval survival as a prerequisite to adult emergence.

The objectives of the present study are to determine direct effects of temperature on larval development in *Parnassius smintheus* from the perspective of developmental time and adult emergence. To this end, a model is designed (for a general insect species) which presents the probability distribution of an individual insect being alive in a given instar (class) at a given time step. The model is a discrete-time pure-birth Markov process, where each time step allows for one of two outcomes in the no-mortality model (transition or non-transition) and four outcomes in the mortality model (transition and survival, transition and death, non-transition and survival, or non-transition and death). The transitional probabilities are considered as both constants and temperature-dependent functions, while the mortality probabilities are considered solely as constants, due to negligible effects of small temperature changes on mortality. These probabilities act as the parameters in the distributions under consideration. These models for general temperature-dependent larval insect development are then parameterized specifically for *P. smintheus*.

The model is derived from multi-outcome Bernoulli distributions, where first the constant transition and mortality probability two-class and multi-class model are derived with no mortality (Sections 3.2.1 and 3.2.2). The derivation of the distribution of larval development time (through an arbitrary number of larval classes) is demonstrated, and the expectation and variance of this distribution are computed (Section 3.2.3). The model is then derived with mortality as a system of non-homogeneous linear difference equations (master equations) in Section 3.2.4. Time evolution in the

system is governed by this set of discrete-time master equations, the solution of which generates the time-dependent probability that an individual larva resides in a given larval class on a given day. From here, probability distributions for adult emergence are derived for the constant transition and mortality probability model. In Section 3.3, the varying transitional probability model is formulated.

The transition and mortality probabilities are then estimated using maximum likelihood methods from data for *P. smintheus* collected in the experiment detailed in Chapter 2, for both the constant and varying probability cases (Sections 3.4.1 and 3.4.2). In the constant transitional probability case, these constants correspond to three different scenarios for spring and early summer temperatures: one which reflects the present-day ambient temperature regime for the elevation of the field site from which the *P. smintheus* larvae were obtained, one which shifts this regime 2°C higher than ambient, and one which shifts this regime 2°C lower. In the varying transitional probability case, linear functions of temperature-dependent transitional success are set from experimental data with slopes estimated by bootstrapped maximum likelihood estimates.

Section 3.5 presents methods by which mark-recapture data for adult *P. smintheus* is analysed for model validation, and describes the statistical tests used to determine model validity.

Results of the two models are presented in Section 3.6, and are discussed in Section 3.7 along with a discussion of climate change impacts on mortality and emergence times in *P. smintheus*.

Temperature regimes under which larvae develop influence instar developmental times and adult emergence times in both the constant and varying transition probability models. Under parameterization of *P. smintheus* transition and mortality data, the constant transition probability model predicts earlier emergence in the warmer treatment, with higher mortality in the colder treatment. The varying transition probability model is statistically indistinguishable from observed adult emergence, though the model performs better in cooler years. More data for parameterization would allow a more biologically accurate transitional success probability function for prediction of adult emergence from temperature regimes experienced by larvae.

## **3.2 Modelling insect development with constant transitional probabilities**

Suppose there exist multiple populations of larval insects, where each population develops under a different temperature regime. Consider the transition of an individual

in the population from one instar/larval class to the next as a Bernoulli stochastic process. The following assumptions must hold:

- the process is memoryless, that is, the development of an individual in one time interval is independent of its development in any other time interval
- the probability of transitioning (movement between classes) is constant (for a given temperature regime)

Supposing first a simple two class life history for the insect, the development of a population under a given temperature regime may be considered. The probability that individuals leave the first class for the second, for all individuals within the population, is denoted  $\mu(T(t))$ , where  $T(t)$  represents a thermal regime (in this case, a diurnal cycle). A thermal regime is defined as temperature as a function of time over the course of a season. In the simplest case, transitional probability is a constant function of temperature, so for a given regime  $T(t)$ , suppose  $\mu$  to be constant.

### 3.2.1 Development times for two classes

Let  $X_n$  be a Bernoulli random variable in a distribution with mean  $\mu(T(n))$ , and  $X_0 = 0$ . This random variable, having possible values of 0 and 1, denotes the failure or success (respectively) of an individual to leave the first class for the second with probability  $\mu(T(n))$  in the  $n$ th time step. Note that this process does not consider mortality for the population.

Of interest is the developmental time of the individual, or the amount of time it spends in the first class. This time is the number of steps  $k$  before the first occurrence of  $X_k = 1$ , or success in leaving the class. The developmental time for the individual insect governed by  $X_n$  is denoted by  $Y$ . So the developmental time  $Y = k$  is equivalent to the occurrence of the events

$$X_0 = 0, X_1 = 0, \dots, X_{k-1} = 0, X_k = 1.$$

The random variable which represents the number of failures before the first success in a sequence of Bernoulli trials is governed by a geometric distribution having a mean equal to that of the Bernoulli distribution (Larson and Schubert, 1979). The random variable  $Y$  therefore has a geometric distribution with mean  $\mu(T(n))$ , so that the probability of a development time of duration  $k$ , where  $k \in \mathbb{Z}^+$ , has probability mass function (pmf)

$$P(Y = k) = (1 - \mu(T(n)))^{k-1} \mu(T(n)). \quad (3.1)$$

A difference equation model can be formulated which considers the probability of an individual's remaining in the first class at time  $n + \Delta n$ , given that it is in the first class at time step  $n$ . Let  $p_n = P(Y > n)$ , so that  $p_n$  denotes the probability of an individual's presence in the first class at time  $n$ . The probability of leaving the class in the time step  $n + \Delta n$ , given that the development time already exceeds  $n$ , is

$$P(Y = n + \Delta n | Y > n) = \mu(T(n))\Delta n.$$

Then

$$\begin{aligned} P(Y > n) &= P(Y = n + \Delta n) + P(Y > n + \Delta n) \\ &= P(Y = n + \Delta n | Y > n) P(Y > n) + P(Y > n + \Delta n) \\ &= P(Y > n) \mu(T(n)) \Delta n + P(Y > n + \Delta n) \end{aligned}$$

which gives the difference equation

$$p_{n+\Delta n} = (1 - \mu(T(n))\Delta n)p_n.$$

Supposing  $\Delta n = 1$  day, the above equation can be rewritten as

$$p_{n+1} = (1 - \mu(T(n)))p_n.$$

### 3.2.2 Developmental times for multiple classes

Suppose there are now  $r$  classes in the life history, where the  $r$ th class is adulthood. A schematic representation of the life history of the insect having  $r - 1$  larval instars prior to adulthood is given in Figure 3.1. The transition probability from class  $i$  to class  $i + 1$  at the  $n$ th time step is  $\mu_i(T(n))$  and the death rate in class  $i$  is  $d_i(T(n))$ .

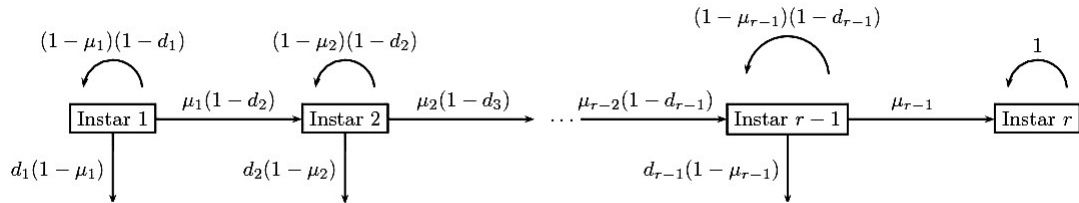


Figure 3.1: Schematic representation of the  $r$  instar insect life history where  $\mu_i$  is the probability of leaving the  $i$ th class in a time step and  $d_i$  is the probability of mortality in a time step. Daily outcomes for individuals are as described in Table 3.3. Individuals accumulate in the  $r$ th instar (adulthood).

In the simplest case, there is no larval mortality in any class ( $d_i = 0$ ,  $i = 1, 2, \dots, r - 1$ ), and the probability that the larvae mature between any two classes

is identical and constant ( $\mu_1(T(n)) = \mu_2(T(n)) = \dots = \mu_{r-1}(T(n)) = \mu$ ). Hereafter the functional dependence of  $\mu_i(T(n))$  is suppressed for brevity, and it is denoted  $\mu_i$ , for all  $i = 1, 2, \dots, r - 1$ .

Given an unchanging constant probability of movement from class to class, denoted  $\mu$ , the number of time steps required for  $r - 1$  successes (a successful transition to adulthood) has a negative binomial distribution (Larson and Schubert, 1979). If the developmental time to adulthood is  $k$  time steps,  $k - 1$  steps must be spent in the larval classes, followed by a successful transition on the  $k$ th step. Let the random variable  $Y_i$  denote the number of time steps spent in the  $i$ th class. That is, the event  $\sum_{j=1}^{r-1} Y_j = k - 1$  is equivalent to  $\sum_{j=1}^{k-1} X_j = r - 2$  and  $X_k = 1$  (since an individual starts in the first class and moves forward to the  $r$ th class in  $r - 1$  developmental events). So the probability that the developmental time to adulthood is  $k$  has pmf

$$P\left(\sum_{j=1}^{r-1} Y_j = k - 1\right) = \binom{k-2}{r-2} \mu^{r-1} (1-\mu)^{k-r}. \quad (3.2)$$

where  $k \geq r$ . See Figure 3.2 for sample pmfs.

A more complicated case occurs when  $\mu_1 \neq \mu_2 \neq \dots \neq \mu_{r-1}$ . Neglecting mortality once more, a model giving probabilities of an individual's being in each class at time step  $n + 1$  can be expressed as follows:

$$\begin{aligned} p_{n+1}^1 &= (1 - \mu_1)p_n^1 \\ p_{n+1}^2 &= \mu_1 p_n^1 + (1 - \mu_2)p_n^2 \\ &\vdots \\ p_{n+1}^{r-1} &= \mu_{r-2} p_n^{r-2} + (1 - \mu_{r-1})p_n^{r-1} \\ p_{n+1}^r &= \mu_{r-1} p_n^{r-1} + p_n^r \end{aligned}$$

where  $p_n^i = P(\sum_{j=1}^{i-1} Y_j < n \cap Y_i > n - \sum_{j=1}^{i-1} Y_j)$ . That is,  $p_n^i$  is the probability that the insect is still in the  $i$ th class, where the individual has entered the  $i$ th class by the  $n$ th time step ( $\sum_{j=1}^{i-1} Y_j < n$ ) and has not yet transitioned to the  $(i + 1)$ th class ( $Y_i > n - \sum_{j=1}^{i-1} Y_j$ ).

The probability distribution for the value of the developmental time through  $r - 1$  classes,  $P(\sum_{j=1}^{r-1} Y_j = k - 1)$ , can also be derived. Here  $r$  is the adult class. Before deriving the general formula for the developmental time distribution given arbitrary  $r$  and  $k$ , consider first a simple illustrative example. Choose  $r - 1 = 3$  and  $k = 5$ , a four stage life history where an individual takes five days to mature. Then the 5th step moves into the fourth and final class, and one step must be spent moving into each larval class, so the steps can be distributed as illustrated in Table 3.1.

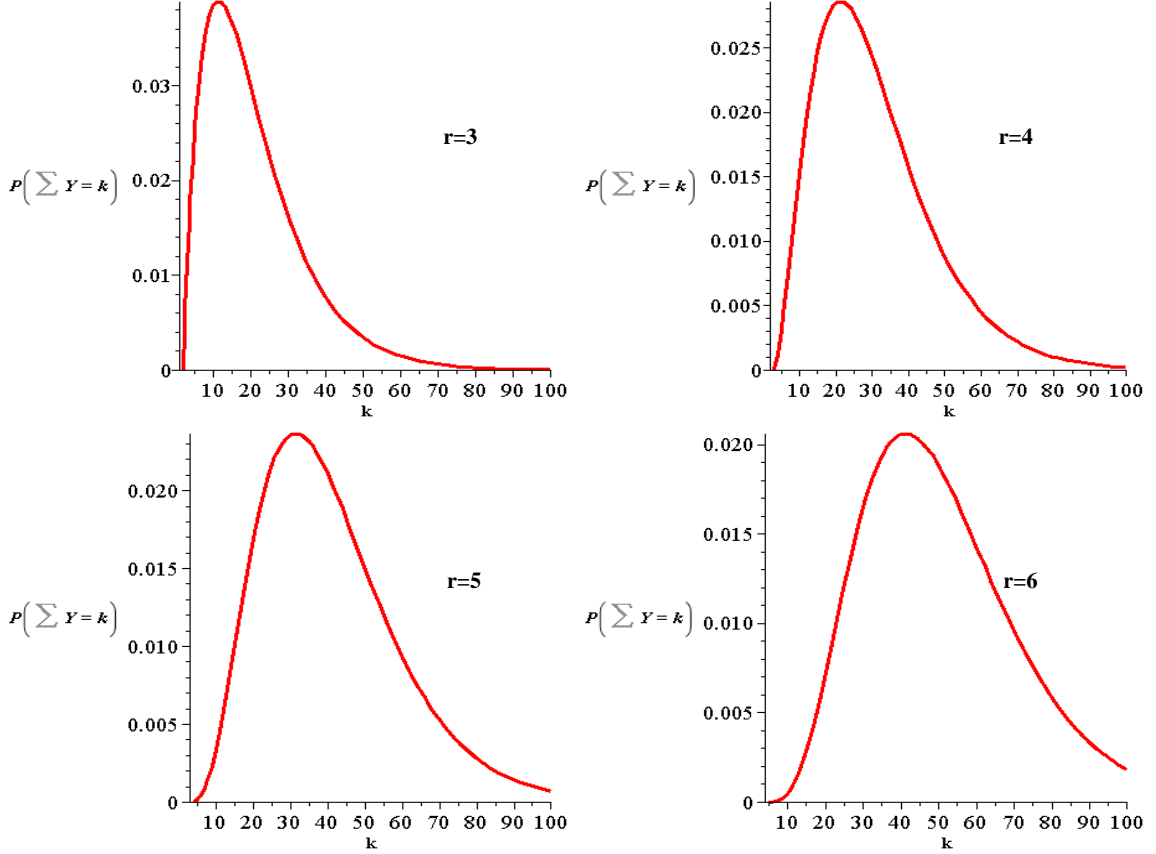


Figure 3.2: The negative binomial probability mass function (3.2) with  $\mu = 0.1$ , with respect to number of classes  $r$  and total developmental time  $k$ . These distributions illustrate the probability of reaching adulthood on the  $k$ th day, for varying numbers of classes, given transitional success probability  $\mu = 0.1$ .

The probability distribution can thus be directly computed:

$$P\left(\sum_{j=1}^3 Y_j = 4\right) = P(Y_1 = 2 \cap Y_2 = 1 \cap Y_3 = 1) + P(Y_1 = 1 \cap Y_2 = 2 \cap Y_3 = 1) + P(Y_1 = 1 \cap Y_2 = 1 \cap Y_3 = 2)$$

gives the sum of probabilities of all possible paths the insect can take to adulthood in five time steps. Since the random variables  $Y_i$  are independent with a geometric distribution,

$$\begin{aligned} P\left(\sum_{j=1}^3 Y_j = 4\right) &= P(Y_1 = 2)P(Y_2 = 1)P(Y_3 = 1) + P(Y_1 = 1)P(Y_2 = 2)P(Y_3 = 1) \\ &\quad + P(Y_1 = 1)P(Y_2 = 1)P(Y_3 = 2) \\ &= (1 - \mu_1)\mu_1\mu_2\mu_3 + \mu_1(1 - \mu_2)\mu_2\mu_3 + \mu_1\mu_2(1 - \mu_3)\mu_3. \end{aligned}$$

This example can be extended by allowing the development time  $k$  to be arbitrary. Now an insect matures on the  $k$ th time step, and has  $k - 1$  time steps to spend in the first three classes. Table 3.2 illustrates how these steps can be distributed. Using geometric distribution probability mass functions and the given table, the first terms in the series for  $P(\sum_{j=1}^3 Y_j = k - 1)$  may be expressed. The coefficient  $\mu_1\mu_2\mu_3$  in front of the series arises from the condition that each class must be exited

Class 1	Class 2	Class 3
2	1	1
1	2	1
1	1	2

Table 3.1: Potential paths taken to adulthood ( $r = 4$ ) in 5 days, denoted by number of days spent in each class.

Class 1	Class 2	Class 3
$k - 3$	1	1
$k - 4$	2	1
$k - 4$	1	2
$k - 5$	3	1
$k - 5$	2	2
$k - 5$	1	3
$\vdots$	$\vdots$	$\vdots$

Table 3.2: Potential paths taken to adulthood ( $r = 4$ ) in  $k$  days, denoted by the number of days spent in each class.

since adulthood is reached in a finite number of time steps  $k$  (and because an individual spends one time step moving into each class). The first three terms of the series are the paths illustrated in the first three rows of Table 3.2:

$$P\left(\sum_{j=1}^3 Y_j = k - 1\right) = \mu_1 \mu_2 \mu_3 [(1 - \mu_1)^{k-4} + (1 - \mu_1)^{k-5} (1 - \mu_2) + (1 - \mu_1)^{k-5} (1 - \mu_3) + \dots].$$

Consider now the general case with  $k$  time steps in  $r$  classes. If the individual reaches adulthood ( $r$ th class) in the  $k$ th time step, and at least one time step must be spent transitioning through the  $r - 1$  larval classes, then  $k - (r - 1)$  steps remain to be distributed between the larval classes (where transitional success does not occur). The number of possible paths to adulthood through the classes is then given by

$$\binom{k - (r - 1) + (r - 1) - 1}{k - (r - 1)} = \binom{k - 1}{k - (r - 1)}$$

(Nelson, 1995). One may see from the previous examples that the terms in the probability distribution must have exponents that sum to the total number of steps spent in the first  $r - 1$  classes. Supposing that the number of steps an insect spends in the first class without transitioning is initially fixed at  $k - (r - 1)$  and iterating downward, one may find all possible paths through the intermediate  $r - 2$  classes that take the remaining time steps not used in the first class. Let  $m_i$  denote the iterate for number of time steps spent in the  $i$ th class, except for  $m_1$ , where  $k - (r - 1) - m_1$  denotes the number of time steps spent in the first class. For notational brevity, let  $M_1 = k - (r - 1) - m_1$ . One may thus express the probability mass function for development times for different numbers of classes. When  $r = 2$ , the probability mass function is the geometric pmf:

$$P(Y_1 = k - 1) = \mu_1 (1 - \mu_1)^{k-1}.$$

When  $r = 3$ ,

$$P\left(\sum_{j=1}^2 Y_j = k - 1\right) = \mu_1 \mu_2 \sum_{m_1=0}^{k-2} (1 - \mu_1)^{k-2-m_1} (1 - \mu_2)^{m_1}.$$

For  $r > 3$ ,

$$P\left(\sum_{j=1}^{r-1} Y_j = k-1\right) = \mu_1 \mu_2 \cdots \mu_{r-1} \sum_{M_1+m_2+\cdots+m_{r-1}=k-(r-1)} (1-\mu_1)^{M_1} \cdot (1-\mu_2)^{m_2} \cdots (1-\mu_{r-1})^{m_{r-1}} \quad (3.3)$$

or equivalently,

$$\begin{aligned} P\left(\sum_{j=1}^{r-1} Y_j = k-1\right) &= \mu_1 \mu_2 \cdots \mu_{r-1} \sum_{m_1=0}^{k-(r-1)} (1-\mu_1)^{k-(r-1)-m_1} \sum_{m_2=0}^{m_1} (1-\mu_2)^{m_2} \\ &\cdot \sum_{m_3=0}^{m_1-m_2} (1-\mu_3)^{m_3} \cdots \sum_{m_{r-3}=0}^{m_1-m_2-\cdots-m_{r-4}} (1-\mu_{r-3})^{m_{r-3}} \\ &\cdot \sum_{m_{r-2}=0}^{m_1-m_2-\cdots-m_{r-3}} (1-\mu_{r-2})^{m_{r-2}} (1-\mu_{r-1})^{m_1-m_2-\cdots-m_{r-2}}. \end{aligned} \quad (3.4)$$

Summing over all possible values of  $k$  using repeated applications of the geometric summation formula gives

$$\sum_{k=r-1}^{\infty} P\left(\sum_{j=1}^{r-1} Y_j = k-1\right) = 1 \quad (3.5)$$

as required for a probability distribution. See Figure 3.3 for some examples of this probability mass function given varying total development times and a varying number of classes. In Appendix B, a sample calculation is carried out for summation (3.5) with  $r = 4$ .

### 3.2.3 Expectation and variance for developmental times

Having derived the development time distribution (3.4), the expectation and variance of the distribution may be calculated directly or by the use of generating functions.

First the expectation may be calculated using the standard method for discrete probability distributions:

$$\begin{aligned} E\left(\sum_{j=1}^{r-1} Y_j\right) &\equiv \sum_{k=r-1}^{\infty} k \cdot P\left(\sum_{j=1}^{r-1} Y_j = k-1\right) \\ &= \frac{1}{\prod_{i=1}^{r-1} \mu_i} \left( \sum_{1 \leq j_1 < j_2 < \cdots < j_{r-2} \leq r-1} \mu_{j_1} \mu_{j_2} \cdots \mu_{j_{r-2}} \right) \end{aligned}$$

where the rightmost sum denotes the sum of the set of all  $(r-2)$  element combinations of the  $(r-1)$  larval classes. The expectation may then be simplified to give

$$E\left(\sum_{j=1}^{r-1} Y_j\right) = \sum_{i=1}^{r-1} \frac{1}{\mu_i}. \quad (3.6)$$

For instance, when  $r = 4$ , the expectation of total development time is

$$E\left(\sum_{j=1}^3 Y_j\right) = \frac{1}{\mu_1 \mu_2 \mu_3} (\mu_1 \mu_2 + \mu_1 \mu_3 + \mu_2 \mu_3) = \frac{1}{\mu_1} + \frac{1}{\mu_2} + \frac{1}{\mu_3}.$$

One may consider (3.6) for the special cases  $\mu_i = 0$  and  $\mu_i = 1$ ,  $i = 1, \dots, r-1$ . When  $\mu_i = 0$  for any  $i$ , the expected developmental time to adulthood is infinite, because individuals become trapped

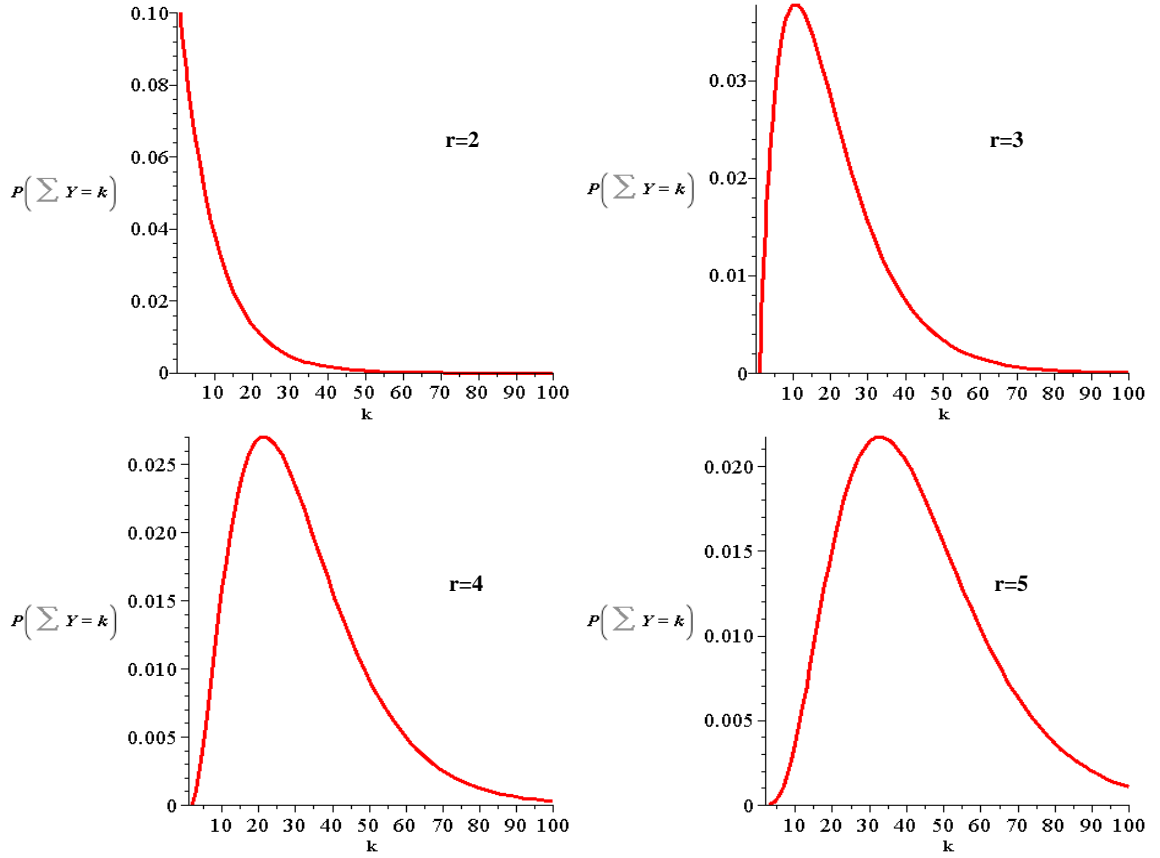


Figure 3.3: The probability mass function for total developmental time  $k$  given geometric distributions (3.1) for developmental time within each class, for  $r$  classes. Parameter values used are  $\mu_1 = 0.1$ ,  $\mu_2 = 0.095$ ,  $\mu_3 = 0.0925$ ,  $\mu_4 = 0.0857$  (probability of transition decreases 5% for each successive class from the previous class probability).

in the  $i$ th class. If  $\mu_i = 1$  for all  $i$ , the expected developmental time to adulthood is  $r - 1$  time steps, as individuals pass through each instar with probability 1 on each time step.

The variance of the distribution,  $E\left(\left(\sum_{j=1}^{r-1} Y_j\right)^2\right) - E\left(\sum_{j=1}^{r-1} Y_j\right)^2$ , may also be calculated, using standard computational techniques:

$$\begin{aligned}
\text{Var}\left(\sum_{j=1}^{r-1} Y_j\right) &\equiv E\left(\left(\sum_{j=1}^{r-1} Y_j\right)^2\right) - E\left(\sum_{j=1}^{r-1} Y_j\right)^2 \\
&= \sum_{k=r-1}^{\infty} k^2 \cdot P\left(\sum_{j=1}^{r-1} Y_j = k - 1\right) - \left(\sum_{k=r-1}^{\infty} k \cdot P\left(\sum_{j=1}^{r-1} Y_j = k - 1\right)\right)^2 \\
&= \frac{-1}{\prod_{i=1}^{r-1} \mu_i^2} \left( \prod_{i=1}^{r-1} \mu_i \sum_{1 \leq j_1 < j_2 < \dots < j_{r-2} \leq r-1} \mu_{j_1} \mu_{j_2} \dots \mu_{j_{r-2}} \right. \\
&\quad \left. - \sum_{1 \leq j_1 < j_2 < \dots < j_{r-2} \leq r-1} \mu_{j_1}^2 \mu_{j_2}^2 \dots \mu_{j_{r-2}}^2 \right) \\
&= \sum_{i=1}^{r-1} \left( \frac{1}{\mu_i^2} - \frac{1}{\mu_i} \right). \tag{3.7}
\end{aligned}$$

So for instance, when  $r = 4$ ,

$$\begin{aligned}
\text{Var}\left(\sum_{j=1}^3 Y_j\right) &= \frac{-1}{\mu_1^2 \mu_2^2 \mu_3^2} (\mu_1 \mu_2^2 \mu_3^2 + \mu_1^2 \mu_2 \mu_3^2 + \mu_1^2 \mu_2^2 \mu_3 - \mu_1^2 \mu_2^2 - \mu_1^2 \mu_3^2 - \mu_2^2 \mu_3^2) \\
&= \left( \frac{1}{\mu_1^2} - \frac{1}{\mu_1} \right) + \left( \frac{1}{\mu_2^2} - \frac{1}{\mu_2} \right) + \left( \frac{1}{\mu_3^2} - \frac{1}{\mu_3} \right).
\end{aligned}$$

As with the expectation, the variance (3.7) may be considered in the special cases  $\mu_i = 0$  and  $\mu_i = 1$ ,  $i = 1, \dots, r - 1$ . When  $\mu_i = 0$  for any  $i$ , the variance is infinite, as adulthood is not reached in finite time. If  $\mu_i = 1$  for all  $i$ , the variance in developmental times is 0, as each individual reaches adulthood in  $r - 1$  steps with probability 1.

One may also calculate the expectation and variance of the total development time distribution using the method of generating functions. Recall that each larval class  $i$  independently follows a geometric distribution with probability  $\mu_i$  of leaving the class. The developmental time in each class  $Y_i$  then has an associated polynomial generating function, where the coefficient of each term gives the probability that the developmental time in the class is equal to the power of said term. For a class  $i$ ,

$$\begin{aligned}
0 \cdot 1 + \mu_i \cdot s + \mu_i(1 - \mu_i) \cdot s^2 + \mu_i(1 - \mu_i)^2 \cdot s^3 + \dots &= \mu_i \sum_{j=1}^{\infty} (1 - \mu_i)^{j-1} s^j \\
&= \mu_i s \sum_{j=0}^{\infty} (s(1 - \mu_i))^j \\
&= \frac{\mu_i s}{1 - s(1 - \mu_i)} \\
&\equiv g_i(s)
\end{aligned}$$

gives the generating function for  $Y_i$ . The total developmental time to adulthood  $\sum_{j=1}^{r-1} Y_j$  then has a generating function that is the product of the generating functions for the developmental time in

each individual class, since the random variables are independent. A generating function

$$\begin{aligned} G(s) &= g_1(s)g_2(s)\cdots g_{r-1}(s) \\ &= \frac{\mu_1\mu_2\cdots\mu_{r-1}s^{r-1}}{(1-s(1-\mu_1))(1-s(1-\mu_2))\cdots(1-s(1-\mu_{r-1}))} \end{aligned}$$

may be defined for the total development time. This function agrees with that derived by Flajolet and Sedgewick (2009) for a pure-birth type random walk. Further similarities of this model to a pure birth type process are discussed in Section 3.2.4. As usual, the expectation and variance of the total development time distribution can be derived from this generating function:

$$E\left(\sum_{j=1}^{r-1} Y_j\right) = \left.\frac{dG}{ds}\right|_{s=1}$$

and

$$\text{Var}\left(\sum_{j=1}^{r-1} Y_j\right) = \left.\frac{d^2G}{ds^2}\right|_{s=1} + \left.\frac{dG}{ds}\right|_{s=1} - \left(\left.\frac{dG}{ds}\right|_{s=1}\right)^2$$

(Feller, 1970).

The method of generating functions gives the same expectation and variance as the direct method, when the above formulae are used.

### 3.2.4 Modelling mortality

In this section, mortality is included in the constant transition probability model. The difference equations governing the probability of an individual's presence in a given instar on a given time step are rewritten to incorporate mortality, and the similarities of the model equations to discrete-time pure birth processes are presented, to indicate that the solution to the system of difference equations is a novel result. The equations are then solved and the solutions presented, and a probability function governing mortality prior to adulthood is derived. The section concludes with the derivation of the function governing adult emergence.

The addition of mortality to the model requires the consideration of additional events which may occur in a time step. Without mortality, an individual takes one of two actions in each time step: it remains in class  $i$  or it transitions to class  $i + 1$  with probabilities  $1 - \mu_i$  and  $\mu_i$ , respectively. With mortality, one must consider the following possibilities in each time step: an insect in class  $i$  may remain in class  $i$  and survive, it may remain in class  $i$  and die, it may transition to class  $i + 1$  and survive, or it may transition to class  $i + 1$  and die. The associated probabilities of the four events are given in Table 3.3 for class  $i$ .

Event	Probability of occurrence
no transition and survival	$(1 - \mu_i)(1 - d_i)$
no transition and death	$(1 - \mu_i)d_i$
transition and survival	$\mu_i(1 - d_{i+1})$
transition and death	$\mu_i d_{i+1}$

Table 3.3: Potential outcomes in each time step in the constant transition probability model with constant mortality. Probabilities associated with each outcome for the  $i$ th instar are presented.

The  $r$  class model must now be modified to account for the probability of death in each class in each time step, as well as the probability of survival. The probability of surviving in the  $i$ th class in the  $n$ th time step is denoted by  $p_n^i$  and the probability of dying in the  $i$ th class in the  $n$ th time

step is denoted by  $q_n^i$ . The model can be expressed as follows:

$$\begin{aligned}
p_{n+1}^1 &= [(1 - \mu_1)(1 - d_1)] p_n^1 \\
q_{n+1}^1 &= [(1 - \mu_1)d_1] p_n^1 \\
p_{n+1}^2 &= [(1 - \mu_2)(1 - d_2)] p_n^2 + [\mu_1(1 - d_2)] p_n^1 \\
q_{n+1}^2 &= [(1 - \mu_2)d_2] p_n^2 + [\mu_1 d_2] p_n^1 \\
&\vdots \\
p_{n+1}^i &= [(1 - \mu_i)(1 - d_i)] p_n^i + [\mu_{i-1}(1 - d_i)] p_n^{i-1} \\
q_{n+1}^i &= [(1 - \mu_i)d_i] p_n^i + [\mu_{i-1}d_i] p_n^{i-1} \\
&\vdots \\
p_{n+1}^r &= p_n^r + \mu_{r-1} p_n^{r-1} \\
q_{n+1}^r &= 0
\end{aligned} \tag{3.8}$$

which accounts for all possible survival and death events in each time step. The model assumes no mortality once an individual reaches the adult class, simply because no further development occurs, so individuals accumulate in this class.

### Discrete-time pure birth processes

This model treats daily transitional success and mortality as a Bernoulli process which only permits movement between adjacent states, and thus defines a *discrete-time birth-death process*, but as an individual may only move from the  $i$ th instar to the  $(i + 1)$ th instar and not the  $(i - 1)$ th instar (i. e., the process is transient), it is a *discrete-time pure birth process*. See Tornambè (1995) for the normal formulation of this process. Pure birth processes are normally used to model the size of a population with no mortality, where the population size may increase by one in each time step (Lawler, 2006); the instars of the above model are analogous to the population size in the usual formulation of the pure birth process. To avoid confusion with standard terminology, the difference between a birth-death process and a pure birth process with mortality (like that in the model above) should be mentioned. A birth-death process is one where movement is permitted between all adjacent states, so the process could increment by one unit in the positive or negative direction, or remain in its present state (Tornambè, 1995). In the pure birth process with mortality, the process may only remain in its present state, increment forward, or terminate (representing the individual's non-transition, transition, and death, respectively).

The model given above differs from the standard presentation of the discrete-time pure birth process in two ways. The standard formulation of the pure birth process has an infinite state space (giving the potential for an infinite population size) which does not occur when the states considered are larval instars; as seen above, the state space for the model is  $\{1, 2, \dots, r\}$  with a finite upper bound  $r$ . The usual formulation of the pure birth process also does not consider terminating the system as a potential outcome (mortality), as the usual system is driven by a two-outcome Bernoulli process (to transition or not to transition). Mathematically, this is manifested in the coefficients of the model equation having only the components  $\mu_i$ ,  $i = 1, 2, \dots, r - 1$ :

$$p_{n+1}^i = (1 - \mu_i)p_n^i + \mu_{i-1}p_n^{i-1}$$

as opposed to the above formulation (3.8), where the coefficients are expressed in terms of  $\mu_i$  and  $d_i$ . These deviations from the usual formulation lead to a different analysis of the system, as will be discussed in the next section.

### Solutions to model equations

The model (3.8) as presented above contains equations to determine probabilities of being alive or dead in a given instar in a given time step. One may also consider strictly the probabilities of being

alive, given as follows:

$$p_{n+1}^1 = [(1 - \mu_1)(1 - d_1)] p_n^1 \quad (3.9)$$

$$p_{n+1}^2 = [(1 - \mu_2)(1 - d_2)] p_n^2 + [\mu_1(1 - d_2)] p_n^1 \quad (3.10)$$

⋮

$$p_{n+1}^i = [(1 - \mu_i)(1 - d_i)] p_n^i + [\mu_{i-1}(1 - d_i)] p_n^{i-1} \quad (3.11)$$

⋮

$$p_{n+1}^r = p_n^r + \mu_{r-1} p_n^{r-1}. \quad (3.12)$$

The system has a set of initial conditions which supposes that all individuals begin their lives in the first instar, so  $p_0^1 = 1$  and  $p_0^i = 0$  for all  $i = 2, \dots, r$ .

If  $\mu_i$  and  $d_i$  are treated as constants, then the coupled linear system of difference equations (3.9)-(3.12) may be solved as follows. Equation (3.9) is homogeneous and linear and is solved by iteration to obtain

$$p_n^1 = ((1 - \mu_1)(1 - d_1))^n.$$

This solution is substituted into the second instar equation (3.10), giving it the non-homogeneous linear form

$$p_{n+1}^2 = (1 - \mu_2)(1 - d_2)p_n^2 + \mu_2(1 - d_2)[(1 - \mu_1)(1 - d_1)]^n.$$

It can be shown by induction that the unique solution to this linear non-homogeneous difference equation (with initial condition  $p_0^2 = 0$ ) has the following form (Elaydi, 2005):

$$\mu_2(1 - d_2) \sum_{k=0}^{n-1} [(1 - \mu_2)(1 - d_2)]^{n-k-1} [(1 - d_1)(1 - \mu_1)]^k.$$

One may substitute the solution to the second instar equation into the third instar equation to obtain another linear non-homogeneous difference equation, and subsequent substitutions generate all solutions. Algebraic manipulations give the solutions in a compact form for the first instar equation, all intermediate instar equations, and the final instar equation, respectively:

$$p_n^1 = ((1 - \mu_1)(1 - d_1))^n \quad (3.13)$$

$$p_n^i = \prod_{k=2}^i [\mu_{k-1}(1 - d_k)] \sum_{j=1}^i \left\{ \frac{[(1 - \mu_j)(1 - d_j)]^n}{\prod_{\substack{k \neq j \\ 1 \leq k \leq i}} [(1 - \mu_j)(1 - d_j) - (1 - \mu_k)(1 - d_k)]} \right\}$$

$$p_n^r = \frac{1}{1 - d_1} \prod_{k=1}^{r-1} [\mu_k(1 - d_k)] \left( \sum_{j=1}^{r-1} \left\{ \frac{[(1 - \mu_j)(1 - d_j)]^n}{(-\mu_j - d_j + \mu_j d_j) \prod_{\substack{k \neq j \\ 1 \leq k \leq r-1}} [(1 - \mu_j)(1 - d_j) - (1 - \mu_k)(1 - d_k)]} \right\} \right) + \frac{(-1)^{r-1}}{\prod_{k=1}^{r-1} (-\mu_k - d_k + \mu_k d_k)}$$

where  $i = 2, \dots, r - 1$ .

One may verify that these solutions hold, by direct substitution for the first and last instar solutions and by induction for the intermediate instar solution. See Appendix C for the proof. These solutions are not defined when  $(1 - \mu_j)(1 - d_j) = (1 - \mu_k)(1 - d_k)$  for  $j \neq k \in [1, r - 1]$ ,

recalling the initial assumption in the no-mortality case that  $\mu_1 \neq \mu_2 \neq \dots \neq \mu_{r-1}$ . The second denominator term in  $p_n^r$ ,  $(-\mu_j - d_j + \mu_j d_j)$ , does not affect the solutions because

$$(-\mu_j - d_j + \mu_j d_j) = 0 \implies \mu_j = \frac{d_j}{d_j - 1}$$

which implies  $\mu_j < 0$  if  $0 < d_j < 1$ ,  $\mu_j = \infty$  if  $d_j = 1$ , and  $\mu_j = 0$  if  $d_j = 0$ . In the first two cases,  $\mu_j$  would violate the constraints of probability and in the latter case, a solution could not be reached in finite time.

The method of solution presented here is apparently novel because of differences in the formulation of the birth-death process from the usual. Flajolet and Sedgewick (2009) presented the solution for the intermediate instar equation assuming an infinite state space and no mortality, while Tor-nambè (1995) found the intermediate instar solution in an infinite state space assuming no mortality and equal transition probabilities. Bocharov and D'Apice (2004) gave the intermediate solution to a infinite state space birth-death process. Coolen-Schrijner and van Doorn (2006) proved the existence and uniqueness of a quasi-stationary distribution for a discrete-time birth-death process with mortality, and derived the distribution. Their derivation was analogous to solving the system of difference equations (3.9)-(3.12), though their results relied on infinite state spaces, as well as non-zero probabilities of leftward transition, so their results do not hold for a finite state-space pure birth process with mortality. The probability distributions (3.13) presented in the solutions of (3.9)-(3.12) are therefore not a special case of their result. Lawler (2006) solved the system assuming a finite state space for the continuous-time analogue, though the system of solutions to a finite state space discrete-time pure birth process is apparently novel.

### Probability mass functions for developmental time random variables

Consider a probability distribution for development time to adulthood, given a probability  $d_i$  of dying in class  $i$  in each time step. Recall that in the absence of mortality, the development time in each class  $Y_i$  is independently governed by a geometric distribution:

$$P(Y_i = k) = (1 - \mu_i)^{k-1} \mu_i.$$

A model with mortality included also requires that the individual survives in each time step. Define a development time of  $k$  time steps to be the successful survival in a class for  $k-1$  time steps, followed by a successful transition to the next class on the  $k$ th time step. A successful transition requires that the individual survives to the end of this time step. The new pseudo-geometric distribution (generated by a four-outcome Bernoulli process) for each class is

$$P(Y_i = k) = [(1 - \mu_i)(1 - d_i)]^{k-1} \mu_i(1 - d_{i+1}).$$

One may derive the probability mass function for the total developmental time with mortality by taking the original result (3.3)

$$P\left(\sum_{j=1}^{r-1} Y_j = k-1\right) = \mu_1 \mu_2 \dots \mu_{r-1} \sum_{M_1 + m_2 + \dots + m_{r-1} = k - (r-1)} (1 - \mu_1)^{M_1} (1 - \mu_2)^{m_2} \dots (1 - \mu_{r-1})^{m_{r-1}}$$

and substituting each  $(1 - \mu_i)$  and  $\mu_i$  term with  $(1 - \mu_i)(1 - d_i)$  and  $\mu_i(1 - d_{i+1})$ , respectively, for all  $i = 1, 2, \dots, r-1$ . The modified probability mass function  $P\left(\sum_{j=1}^{r-1} Y_j = k-1\right)$  then becomes

$$\begin{aligned} P\left(\sum_{j=1}^{r-1} Y_j = k-1\right) &= \prod_{j=1}^{r-1} \mu_j(1 - d_{j+1}) \sum_{M_1 + m_2 + \dots + m_{r-1} = k - (r-1)} [(1 - \mu_1)(1 - d_1)]^{M_1} \\ &\cdot [(1 - \mu_2)(1 - d_2)]^{m_2} \dots [(1 - \mu_{r-1})(1 - d_{r-1})]^{m_{r-1}}. \end{aligned} \quad (3.14)$$

This probability mass function, when summed over all possible development times, will be less than 1, since it only accounts for the individual's development time should the individual survive to

adulthood. A second probability mass function is thus necessary to capture all the possible outcomes of the individual's growth, a function governing the probability of an individual's mortality in any time step prior to  $k$ . To derive this function one must use the set of probabilities (3.13) generated by solving the model equations. The model solutions are necessary because both the instar in which the individual dies and the time step in which the death occurs are required in the derivation (whereas in (3.14), only the last time step is significant, since the individual must have survived in all previous time steps). In the pmf governing the development time until death, there is no such condition, as death ends the Bernoulli process on which the individual's development is based. If adulthood transition occurs to class  $r$  at time step  $k$ , then

$$P(\text{death occurs prior to adulthood transition}) \equiv P(Z_k^r)$$

is computed as follows:

$$\begin{aligned} P(Z_k^r) &= P(\text{death from first class in time step } k) + P(\text{death from second class in time step } k) \\ &+ \dots + P(\text{death from penultimate class in time step } k) \\ &= ((1 - \mu_1)d_1 + \mu_1 d_2)p_{k-1}^1 + \dots + ((1 - \mu_{r-1})d_{r-1} + \mu_{r-1}d_r)p_{k-1}^{r-1} \end{aligned}$$

where each model solution  $p_k^i$  has a coefficient made up of the sum of two terms, which yield the probabilities of a non-transition and death and a transition and death, respectively, from the  $i$ th class in the  $k$ th time step. Using computer algebra, it can be shown that summing over all possible development times to adulthood for both the probability mass functions derived (the probability of transitioning to adulthood in the  $k$ th time step and the probability of dying before the  $k$ th time step) yields a value of 1:

$$\sum_{k=1}^{\infty} \left[ P\left(\sum_{j=1}^{r-1} Y_j = k - 1\right) + P(Z_k) \right] = 1.$$

### Adult emergence probability functions

From the model solutions (3.13), an adult emergence distribution  $\epsilon_n$  (the probability that an individual emerges as an adult on day  $n$ ) may be expressed by

$$\begin{aligned} \epsilon_n &\equiv \mu_{r-1} p_{n-1}^{r-1} \\ &= \mu_{r-1} \prod_{k=2}^{r-1} [\mu_{k-1}(1 - d_k)] \sum_{j=1}^{r-1} \left\{ \frac{[(1 - \mu_j)(1 - d_j)]^{n-1}}{\prod_{\substack{k \neq j \\ 1 \leq k \leq r-1}} [(1 - \mu_j)(1 - d_j) - (1 - \mu_k)(1 - d_k)]} \right\}. \end{aligned} \tag{3.15}$$

That is, the adult emergence probability on day  $n$  assumes the individual is alive in the  $(r - 1)$ th class on the  $(n - 1)$ th day and successfully transitions (multiplying by  $\mu_{r-1}$ ) on day  $n$ .

The adult emergence probability function  $\epsilon_n$  using experimental temperature regimes will be considered in the results.

## 3.3 Modelling insect development with varying transitional probabilities

In the case of non-constant transitional probabilities  $\mu_i$ ,  $i = 1, \dots, r - 1$ , the analytic solutions (3.13) no longer hold because the difference equations from which they originated are no longer autonomous. Now  $\mu_i = \mu_i(T_n)$  is temperature-dependent, where  $T_n$  denotes daytime temperature on day  $n$ . The transitional probability may change in each time step according to some temperature-dependent functional form, to be discussed in the next section. The input to the model is therefore

a set of daytime temperatures  $\{T_n\}$  in which the temperature is constant within a time step  $n$ . The master equations (3.9)-(3.12) may be rewritten accordingly:

$$p_{n+1}^1 = [(1 - \mu_1(T_n))(1 - d_1)] p_n^1 \quad (3.16)$$

$$p_{n+1}^2 = [(1 - \mu_2(T_n))(1 - d_2)] p_n^2 + [\mu_1(T_n)(1 - d_2)] p_n^1 \quad (3.17)$$

$\vdots$

$$p_{n+1}^i = [(1 - \mu_i(T_n))(1 - d_i)] p_n^i + [\mu_{i-1}(T_n)(1 - d_i)] p_n^{i-1} \quad (3.18)$$

$\vdots$

$$p_{n+1}^r = p_n^r + \mu_{r-1}(T_n) p_n^{r-1}. \quad (3.19)$$

Mortality in the model is assumed to be constant and independent of temperature, as no relationship between mortality and temperature is observed (as will be discussed further in Section 3.4.2).

Solutions to this system are generated numerically, where the master equations (3.16)-(3.19) are computed in each time step and iterated forward in time accordingly. The adult emergence function  $\epsilon_n$ , similar to in the constant probability case, is expressed as

$$\epsilon_n \equiv \mu_{r-1}(T_n) p_{n-1}^{r-1}.$$

## 3.4 Parameter estimation

The model may now be parametrized using developmental data for *P. smintheus*, the collection details of which were discussed in Chapter 2. The movement of an individual caterpillar through the larval classes is independent of the trajectories of all other individuals, and this transitional success/failure data for each individual will be used for multiple parameter estimates. Both the constant and variable probability cases will be discussed in the following subsections. Because larvae reared in the experiment were collected from the field in the third instar or later, estimates are made for first and second instar parameters based on third instar parameter values.

### 3.4.1 Constant-valued transition and mortality probabilities

Supposing the transition and mortality probabilities to be constants, the simplest way to compare differences in temperature-dependent development is to compare predicted adult emergence for the three different temperature treatments in which the experiment was conducted (Chapter 2).

The treatments are thus considered individually, and constant temperature-dependent transition and mortality probabilities are estimated for each instar according to the following maximum likelihood method. Consider the movement through larval instars of a given caterpillar in the course of the experiment. The probability that larva  $j$  takes its precise trajectory can be expressed generally as

$$P(\mathbf{x}^j | \boldsymbol{\mu}, \mathbf{d}) = \mu_3^{x_3^j} (1 - \mu_3)^{x_2^j} \mu_4^{x_4^j} (1 - \mu_4)^{x_1^j} \mu_5^{x_5^j} (1 - \mu_5)^{x_6^j} \mu_6^{x_6^j} (1 - \mu_6)^{x_8^j} \cdot d_3^{x_9^j} (1 - d_3)^{x_{10}^j} d_4^{x_{11}^j} (1 - d_4)^{x_{12}^j} d_5^{x_{13}^j} (1 - d_5)^{x_{14}^j} d_6^{x_{15}^j} (1 - d_6)^{x_{16}^j} \quad (3.20)$$

where  $x_i^j \in \mathbb{Z}^+$  and  $x_i^j \in \{0, 1\}$  for  $i = 1, 3, 5, 7$  denote the number of successful transitions from the third, fourth, fifth, and sixth/pupating instars, respectively. Similarly,  $x_i^j$  for  $i = 2, 4, 6, 8$  denote the number of non-successful transitions in these instars. Mortality occurring in the third, fourth, fifth, and sixth instars is denoted by  $x_i^j \in \{0, 1\}$  for  $i = 9, 11, 13, 15$  and survival in these instars is denoted by  $x_i^j$  for  $i = 10, 12, 14, 16$ . The vector  $\mathbf{x}^j$  therefore contains all the information for the duration of the experiment about transition and mortality for individual  $j$ .

For instance, suppose individual  $j$  begins the experiment in the third instar, transitions to the fourth instar after seven days, transitions to the fifth instar after fifteen more days, pupates after a

further eighteen days, and emerges as an adult after twenty more days have passed. The probability of that precise trajectory, is

$$P(\mathbf{x}^j | \boldsymbol{\mu}, \mathbf{d}) = \mu_3^1 (1 - \mu_3)^7 \mu_4^1 (1 - \mu_4)^{15} \mu_5^1 (1 - \mu_5)^{18} \mu_6^1 (1 - \mu_6)^{20} \\ \cdot d_3^0 (1 - d_3)^7 d_4^0 (1 - d_4)^{15} d_5^0 (1 - d_5)^{18} d_6^0 (1 - d_6)^{20}$$

which gives

$$\mathbf{x}^j = [1, 7, 1, 15, 1, 18, 1, 20, 0, 7, 0, 15, 0, 18, 0, 20].$$

In a simpler example, if individual  $j$  begins the experiment in the fourth instar and dies after three days, then the probability of this trajectory is

$$P(\mathbf{x}^j | \boldsymbol{\mu}, \mathbf{d}) = (1 - \mu_4)^3 (1 - d_4)^3 (1 - \mu_4) d_4 \\ = (1 - \mu_4)^4 (1 - d_4)^3 d_4$$

so

$$\mathbf{x}^j = [0, 0, 0, 4, 0, 0, 0, 0, 0, 0, 1, 3, 0, 0, 0, 0].$$

Given an experiment with  $n$  individuals, the experimental trajectories of each individual, being independent and having identical distribution (3.20), may be multiplied together to give a likelihood function

$$L(\mathbf{x}^1, \dots, \mathbf{x}^n | \boldsymbol{\mu}, \mathbf{d}) = \prod_{j=1}^n P(\mathbf{x}^j | \boldsymbol{\mu}, \mathbf{d}) \\ = \mu_3^{\sum_{j=1}^n x_1^j} (1 - \mu_3)^{\sum_{j=1}^n x_2^j} \dots d_6^{\sum_{j=1}^n x_{15}^j} (1 - d_6)^{\sum_{j=1}^n x_{16}^j}.$$

The likelihood function may be separated into independent functions of each parameter, denoted by

$$L_{\mu_i} \equiv \mu_i^{\sum_{j=1}^n x_a^j} (1 - \mu_i)^{\sum_{j=1}^n x_b^j} \quad (3.21)$$

and

$$L_{d_i} \equiv d_i^{\sum_{j=1}^n x_a^j} (1 - d_i)^{\sum_{j=1}^n x_b^j}$$

and  $a$  and  $b$  are the associated indices of  $i$ . Maximizing each of these functions individually thus maximizes the entire likelihood function.

Supposing that  $\sum_{j=1}^n x_a^j > 0$  and  $\sum_{j=1}^n x_b^j > 0$ , the maximum likelihood estimate for  $\mu_i$  may be found as follows:

$$L_{\mu_i} = \mu_i^{\sum_{j=1}^n x_a^j} (1 - \mu_i)^{\sum_{j=1}^n x_b^j} \\ \frac{dL_{\mu_i}}{d\mu_i} = \left( \sum_{j=1}^n x_a^j \right) \mu_i^{(\sum_{j=1}^n x_a^j) - 1} (1 - \mu_i)^{\sum_{j=1}^n x_b^j} - \mu_i^{\sum_{j=1}^n x_a^j} \left( \sum_{j=1}^n x_b^j \right) (1 - \mu_i)^{(\sum_{j=1}^n x_b^j) - 1}.$$

For notational convenience, let  $y_k \equiv \sum_{j=1}^n x_k^j$ . Then setting the derivative equal to zero and solving for  $\mu_i$ ,

$$0 = y_a \mu_i^{y_a - 1} (1 - \mu_i)^{y_b} - \mu_i^{y_a} y_b (1 - \mu_i)^{y_b - 1} \\ \mu_i = \frac{y_a}{y_a + y_b}.$$

The second derivative test, after simplification, yields

$$\frac{d^2 L_{\mu_i}}{d\mu_i^2} = -\frac{(y_a + y_b)^3}{y_a y_b} \left( \frac{y_a}{y_a + y_b} \right)^{y_a} \left( \frac{y_b}{y_a + y_b} \right)^{y_b}$$

which is strictly negative when  $\sum_{j=1}^n x_a^j > 0$  and  $\sum_{j=1}^n x_b^j > 0$ . The maximum likelihood estimate for  $\mu_i$ , the value which maximizes  $L_{\mu_i}$ , is

$$\hat{\mu}_i = \frac{\sum_{j=1}^n x_a^j}{\sum_{j=1}^n x_a^j + \sum_{j=1}^n x_b^j}. \quad (3.22)$$

If both  $\sum_{j=1}^n x_a^j = 0$  and  $\sum_{j=1}^n x_b^j = 0$ , then no data exists for the transitions in this instar so no estimate can be made. If  $\sum_{j=1}^n x_a^j = 0$  and  $\sum_{j=1}^n x_b^j > 0$  (no successful transitions), then  $L_{\mu_i}$  is maximized at the left boundary of  $\mu_i$ , so  $\hat{\mu}_i = 0$ . If  $\sum_{j=1}^n x_a^j > 0$  and  $\sum_{j=1}^n x_b^j = 0$  (no failed transitions), then  $L_{\mu_i}$  is maximized at the right boundary of  $\mu_i$ , so  $\hat{\mu}_i = 1$ .

An identical method follows for maximizing  $L_{d_i}$ .

### Confidence intervals and error propagation

The function  $L_{\mu_i}$  as previously defined is equal to the product of a random sample of size  $y_a + y_b$  taken from a Bernoulli distribution with probability of success  $\mu_i$ , with  $y_a$  successes (successful transitions). In other words, take a random sample  $X_1, X_2, \dots, X_{y_a + y_b}$  from a distribution  $\text{bin}(1, \mu_i)$ . From this perspective, the maximum likelihood estimate (3.22) is the sample proportion of successes. Because  $\hat{\mu}_i$  and  $\hat{d}_i$  are binomial proportions of successes, adjusted Wald confidence intervals may be used to compute  $(1 - \alpha)\%$  confidence intervals for transition and mortality probabilities (Zar, 2010). Let

$$\tilde{X} = \sum_{j=1}^n (x_a^j) + \frac{1}{2} Z_{\frac{\alpha}{2}}^2$$

and

$$\tilde{n} = \sum_{j=1}^n x_a^j + \sum_{j=1}^n x_b^j + Z_{\frac{\alpha}{2}}^2$$

where  $Z_{\frac{\alpha}{2}}$  is the normal deviate of critical value  $\alpha$ . Let  $\tilde{\mu}_i = \frac{\tilde{X}}{\tilde{n}}$ ; the adjusted Wald confidence interval for  $\hat{\mu}_i$  is then

$$(\hat{\mu}_i^{\text{LB}}, \hat{\mu}_i^{\text{UB}}) = \left( \tilde{\mu}_i - Z_{\frac{\alpha}{2}} \sqrt{\frac{\tilde{\mu}_i(1 - \tilde{\mu}_i)}{\tilde{n}}}, \tilde{\mu}_i + Z_{\frac{\alpha}{2}} \sqrt{\frac{\tilde{\mu}_i(1 - \tilde{\mu}_i)}{\tilde{n}}} \right). \quad (3.23)$$

Here  $\hat{\mu}_i^{\text{LB}}$  and  $\hat{\mu}_i^{\text{UB}}$  denotes the lower and upper bounds, respectively, on the  $(1 - \alpha)\%$  confidence interval for  $\hat{\mu}_i$ . A similar confidence interval holds for  $\hat{d}_i$ .

Each parameter estimate contributes error to the adult emergence distribution  $\epsilon_n$ , as such a distribution may be considered a function of these parameters. Since *P. smintheus* has six instars prior to adulthood ( $r = 7$ ), and mortality for adults upon emergence is assumed to be non-existent ( $d_7 = 0$ ), the adult emergence function (3.15) can be expressed as

$$\epsilon_n = \mu_6 \prod_{k=2}^6 [\mu_{k-1}(1 - d_k)] \sum_{j=1}^6 \left\{ \frac{[(1 - \mu_j)(1 - d_j)]^{n-1}}{\prod_{\substack{k \neq j \\ 1 \leq k \leq 6}} [(1 - \mu_j)(1 - d_j) - (1 - \mu_k)(1 - d_k)]} \right\}.$$

This distribution may be denoted  $\epsilon(n, \boldsymbol{\mu}, \mathbf{d})$  to emphasize the dependence of the distribution on the model parameters. The  $(1 - \alpha)\%$  confidence interval for  $\hat{\mu}_i$  (3.23) as expressed above is non-symmetric about  $\hat{\mu}_i$ , so denote the upper and lower errors of the estimate as  $\delta\mu_i^{\text{UB}} = |\hat{\mu}_i - \hat{\mu}_i^{\text{UB}}|$  and  $\delta\mu_i^{\text{LB}} = |\hat{\mu}_i - \hat{\mu}_i^{\text{LB}}|$ , respectively. Similar errors, denoted  $\delta d_i^{\text{UB}}$  and  $\delta d_i^{\text{LB}}$ , can be determined for  $\hat{d}_i$ .

Following the method of Taylor (1997), the errors  $\delta\mu_i^{\text{UB/LB}}$  and  $\delta d_i^{\text{UB/LB}}$  propagate through the model to give the following errors for the adult emergence distribution:

$$\delta\epsilon^{\text{UB/LB}} = \sqrt{\sum_{i=1}^6 \left( \frac{\partial\epsilon^{\text{UB/LB}}}{\partial\mu_i} \delta\mu_i^{\text{UB/LB}} \right)^2 + \sum_{i=1}^6 \left( \frac{\partial\epsilon^{\text{UB/LB}}}{\partial d_i} \delta d_i^{\text{UB/LB}} \right)^2}. \quad (3.24)$$

### 3.4.2 Variable transition probabilities

Supposing transitional probabilities to be temperature-dependent functions, the experimental transitional success/failure data may be used to fit function parameters for  $\mu_i(T)$ . Instead of separating treatments into cool/ambient/warm as in the previous section, the experimental data is pooled together and considered with respect to daytime temperature. The function (3.20) is again used to calculate the probability of individual  $j$  demonstrating an observed experimental trajectory, but now each transitional probability  $\mu_i$  is a temperature-dependent function instead of constant. From the experimental data, both daytime temperature and transitional success/failure is recorded, so on day  $n$ , successful and failed transitions appear as  $(T_n, 1)$  and  $(T_n, 0)$  respectively.

A linear functional form

$$\mu_i(T) = a_i(T - T_0)$$

is assumed because the experimental data is constrained to a temperature range of 12.5–22 °C, which neglects lower temperatures at which development occurs. Polynomial fits to this data, supposing  $T$ -intercept is uncontrolled, would intercept zero near 12.5 °C, rendering it less useful for numerical simulations with temperature regimes falling outside the experimental range. Thus  $T_0$ , the lower thermal bound at which development may occur, must be fixed, and because the introduction of higher order polynomials would require further constraints on parameter values, the linear fit is deemed the most straightforward for use. Acceptable values for  $T_0$  are presented in the results.

The transitional success probability on day  $n$  is expressed as

$$\mu_i = a_i(T_n - T_0)$$

and the transitional failure probability is

$$1 - \mu_i = 1 - (a_i(T_n - T_0)),$$

where the binomial experimental data  $(T_n, 1)$  and  $(T_n, 0)$  may now be used for parameter estimation. The slope  $a_i$  for the linear transitional probability function is the sole unknown parameter, and is estimated using linear regression on the binomial data. A likelihood function for each instar similar to (3.21) is constructed using the method detailed in the previous subsection with the new functional form for  $\mu_i$ . The likelihood function may be written in terms of the unknown parameter  $a_i$  and maximized according to the procedure detailed in the previous section. Due to a more complicated likelihood function than that expressed in the constant transitional probability case, the maximum likelihood estimate for  $a_i$  is determined numerically.

A disadvantage to this method is that it produces seemingly low estimates when sample sizes at lower temperatures are larger than those at higher temperatures. Such a dataset was generated from the experiment, as the colder temperatures (early in the experiment in the coldest treatment) had the most individuals, owing to a larger sample population in the colder treatment. This disadvantage may be overcome by generating a maximum likelihood estimate for  $a_i$  using bootstrapped data (randomly selecting the same number of individuals from the cold treatment as from the other treatments). The mean of the slope is then taken from 1000 trials as the parameter value, as demonstrated in the results section.

As no strong relationship between temperature and mortality probability appears in the experimental data, a constant mortality probability  $\hat{d}$  is applied across all instars, set to be the mean of constants  $\hat{d}_i$ ,  $i = 3, \dots, 6$  as estimated in the previous section:

$$\hat{d} = \frac{1}{12} \left( \sum_{i=3}^6 \hat{d}_i^c + \sum_{i=3}^6 \hat{d}_i^a + \sum_{i=3}^6 \hat{d}_i^w \right) \quad (3.25)$$

where  $\hat{d}_i^c$ ,  $\hat{d}_i^a$ , and  $\hat{d}_i^w$  denote the mortality probabilities in the  $i$ th instar in the colder, ambient and warmer treatments, respectively. The input to the larval development model is a time series of daytime temperatures, which changes transitional success on a day by day basis. These temperature time series are taken from Environment Canada (2010) for Nakiska Ridgetop (near the study site at Kananaskis).

### Confidence intervals and sources of error

A Wald test is used to determine  $(1 - \alpha)\%$  confidence intervals for  $\hat{a}_i$ ,  $i = 3, \dots, 6$  (Zar, 2010). The width of the confidence interval is  $Z_{\frac{\alpha}{2}} SE_{\hat{a}_i}$ , where  $SE_{\hat{a}_i}$  is the standard error of the estimate  $\hat{a}_i$ . Since  $\hat{a}_i$  is the slope of a linear regression to the data,

$$SE_{\hat{a}_i} = \sqrt{\frac{1}{\sum_{n=1}^m x_n^2} \left( \frac{\sum_{n=1}^m (y_n - \hat{y}_n)}{m - 2} \right)},$$

where  $m$  is the sample size,  $(x_n, y_n)$  is daytime temperature and associated success/failure data on day  $n$ , and  $\hat{y}_n$  is the predicted transitional success where

$$\hat{y}_n = \mu_i(x_n) = \hat{a}_i(x_n - T_0)$$

(Zar, 2010). The confidence interval for  $\hat{a}_i$  is therefore

$$\left( \hat{a}_i - Z_{\frac{\alpha}{2}} \sqrt{\frac{1}{\sum_{n=1}^m x_n^2} \left( \frac{\sum_{n=1}^m (y_n - \hat{y}_n)}{m - 2} \right)}, \hat{a}_i + Z_{\frac{\alpha}{2}} \sqrt{\frac{1}{\sum_{n=1}^m x_n^2} \left( \frac{\sum_{n=1}^m (y_n - \hat{y}_n)}{m - 2} \right)} \right). \quad (3.26)$$

For the bootstrapped data, 95% confidence intervals for  $\hat{a}_i$  are computed directly by determining a range of values centered at the newly estimated slope in which 95% of the bootstrapped estimates fall.

Error in adult emergence is computed similarly to that in the constant transition probability model, as shown in (3.24). The adult emergence distribution  $\epsilon_n$ , however, does not have an analytic solution in the variable transition probability case, so the derivatives in (3.27) are numerically approximated using forward difference schemes. The error  $\delta a_i$  is the distance between  $\hat{a}_i$  and the edge of the confidence interval. The variable transition probability analogue to (3.24) is then

$$\delta \epsilon^{\text{UB/LB}} = \sqrt{\sum_{i=1}^6 \left( \frac{\partial \epsilon^{\text{UB/LB}}}{\partial a_i} \delta a_i \right)^2 + \left( \frac{\partial \epsilon^{\text{UB/LB}}}{\partial d} \delta d^{\text{UB/LB}} \right)^2}. \quad (3.27)$$

Because the constant mortality probability  $\hat{d}$  is set as the mean of  $\hat{d}_i$  (3.25) as previously estimated for the constant transition probability model, the associated error is computed from the previous errors  $(\delta d_i^{\text{UB/LB}})^2$ , summed in quadrature (Taylor, 1997), and then divided by 12:

$$\delta d^{\text{UB/LB}} = \frac{1}{12} \sqrt{\sum_{i=3}^6 (\delta d_i^{\text{c,UB/LB}})^2 + \sum_{i=3}^6 (\delta d_i^{\text{a,UB/LB}})^2 + \sum_{i=3}^6 (\delta d_i^{\text{w,UB/LB}})^2}.$$

Here  $\delta d_i^{\text{c,UB/LB}}$  denotes upper and lower bound error in the  $i$ th instar of the colder treatment, while  $\delta d_i^{\text{a,UB/LB}}$  and  $\delta d_i^{\text{w,UB/LB}}$  denote the same in the ambient and warmer treatments, respectively.

There are two potential sources of error in the larval development model, as parameterized by these linear temperature-dependent transition probability functions, which will be considered in the results. The thermal lower bound for development,  $T_0$ , is fixed prior to simulation, and while an approximate range of  $T_0$  can be considered for *P. smintheus*, it is necessary to determine if the estimate  $\hat{a}_i$  changes significantly as  $T_0$  is varied. Another source of error in the model, since it is generated numerically, is where to fix the model start date, associated with egg hatching.

## 3.5 Model validation

The larval development model gives an adult emergence distribution as output in both the constant and variable transition probability cases, and in the latter case, the model may be validated using mark-recapture data for *P. smintheus* populations in Kananaskis, Alberta (Roland et al., 2000; Matter and Roland, 2002; Matter et al., 2003, 2004; Roland and Matter, 2007; Matter et al., 2009). In this section, the method by which mark-recapture data is converted into emergence data is explained, as are the statistical methods by which observed and predicted emergences are compared.

### 3.5.1 Converting mark-recapture data to emergence data

In the mark-recapture data, each capture records the following pertinent information about the individual: date, meadow, new or recapture, identification code, and wing condition. To convert this to emergence data, only new captures are considered, then divided into meadows of origin (see Figure 3.4 for a map of the study site identifying the 17 meadows by letter). For model validation, spatially connected meadows are grouped together, giving populations in Meadows F; G,g,H; I,J,K; L,M; O; P,Q; R; S; Y; Z. In a given year, the meadow with the largest number of sampling days is used for validation.

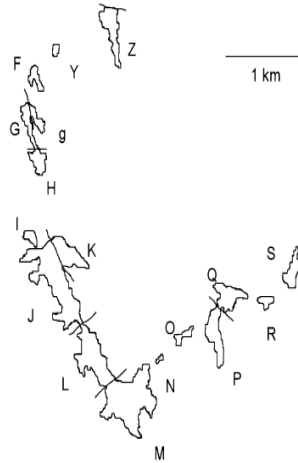


Figure 3.4: Study site at Jumpingpound Ridge, Kananaskis, where mark-recapture field experiments for adult *P. smintheus* are carried out. Letters identify meadows, and bars between meadows indicate spatial connection through broken treeline. Used with permission from Matter et al. (2009).

This data then gives the number of new emergences first observed on a given day, which may be transformed into a probability of emergence on that day by normalizing the frequency data by total number of butterflies having emerged in the meadow. Wing condition data indicates that most butterflies were observed when “new” (as opposed to “old” or “tattered”). Large temporal gaps between sampling days are still problematic, however, as butterflies which emerge after one sampling day may die before the next sampling day. While death of unobserved butterflies may not be quantified from the mark-recapture data, dispersal events (movement of an individual out of one meadow into a spatially unconnected meadow) are rare. Matter *et al.* documented 24 dispersal events in 839 individuals (1136 captures) in 1995 and 27 dispersal events in 759 individuals (873 captures) in 1996 (Matter et al., 2004), or 2.8% and 3.8% of the population migrating, respectively. Table 3.4 documents the number of dispersal events in other years for which mark-recapture experiments were conducted. It can thus be concluded that migration is likely a negligible source of error to observed adult emergence.

### 3.5.2 Statistical methods for model validation

Observed versus predicted emergence on a given day are compared using both a Wilcoxon signed-rank test (Zar, 2010) and linear regression of observed emergence on predicted emergence (Haefner, 2005). The Wilcoxon signed rank test is a non-parametric test used to detect differences between two datasets, where observations from each set are compared pairwise. In this context, emergence as predicted by the model and observed emergence are compared, for each sampling day. Because sampling does not occur every day, the model predictions are aggregated to sampling days in this

Year	# individuals captured	# captures	# migration events	% migrated
2001	1099	2208	15	1.4%
2003	92	176	3	3.3%
2004	380	979	9	2.3%
2005	839	1869	27	3.2%
2006	1443	2356	25	1.7%
2007	1709	2600	15	0.9%
2008	1939	3329	30	1.5%
2009	951	2348	34	3.7%

Table 3.4: Number and proportion of dispersal events each year recorded in *P. smintheus* adult mark-recapture experiments, with respect to number of individuals and number of captures.

analysis. That is, if sampling occurs on day 1 and day 4, the analysis compares the predicted and observed emergence on day 1, but compares the observed emergence on day 4 with the sum of the predicted emergence of days 2, 3, and 4. The null hypothesis states that observed and predicted emergence on a given day are the same, while the alternative hypothesis states that they differ. The differences between the emergences on each sample day are ranked according to absolute size, and the sign of the difference is assigned to the rank. The positive and negative ranks (denoted  $T_+$  and  $T_-$  in the results) are compared to a critical value  $T_{\text{crit}}$  which varies according to significance level and sample size (Zar, 2010). If either  $T_+ < T_{\text{crit}}$  or  $T_- < T_{\text{crit}}$ , then the null hypothesis is rejected and one may conclude that the model does not predict the observed emergence.

The linear regression analysis determines model validity by regressing observations on predicted values. The null hypothesis states that the slope ( $b$ ) and  $x$ -intercept ( $a$ ) of the regression line are 1 and 0, respectively, while the alternative hypothesis states that these values are not 1 and 0. This approach involves comparing a test statistic  $F$

$$F = \frac{na^2 + 2a(b-1) + \sum_{i=1}^n x_i + (b-1)^2 \sum_{i=1}^n x_i^2}{2s_{\text{RMSE}}}$$

against a critical value  $F_{\text{crit}}$ , from an  $F$  distribution with 2 and  $n-2$  degrees of freedom, where  $n$  is the number of paired samples, and  $x_i$  is the model-predicted value on day  $i$ . The term  $s_{\text{RMSE}}$  is the residual mean square error where

$$s_{\text{RMSE}} = \frac{\sum_{i=1}^n (y_i - \hat{y}_i)^2}{n-2}$$

and  $y_i$  is the observed value on day  $i$  and  $\hat{y}_i = a + bx_i$ . Similar to the Wilcoxon signed-rank test, the model predictions are aggregated to sample days.

For both these tests, a non-rejected null hypothesis is desired, so that the observed and predicted emergence distributions are indistinguishable statistically.

### 3.6 Results

In this section, maximum likelihood estimates are first generated for the constant transition and mortality probability case, with associated confidence intervals. Adult emergence is then predicted by the model using these parameter values, with uncertainty as propagated through the model.

The variable transitional probability case is then considered, beginning with error pertaining to thermal lower bound for development. Appropriate maximum likelihood estimates and confidence intervals are then generated for the slopes of transitional probability functions. The validity of these estimates is then tested by bootstrapping the data, and new estimates for the slopes are generated as necessary from the bootstrapping procedure. Finally, the error associated with varying start dates for the model is considered.

This variable transitional probability model is then validated using emergence data for *P. smintheus* by way of Wilcoxon signed-rank tests and linear regression analysis.

### 3.6.1 Constant-valued transition and mortality probabilities

Maximum likelihood estimates and associated 95% confidence intervals are presented in Table 3.5. Because the estimates are calculated from binomial data which has no error, estimates are reported to five decimal places (where appropriate) for brevity.

Parameter	Colder		Ambient		Warmer	
	Estimate	CI	Estimate	CI	Estimate	CI
$\mu_3$	0.06173	(-0.06262, 0.22577)	0.14285	(0.04135, 0.35482)	0.10	(-0.00394, 0.42597)
$\mu_4$	0.06710	(0.04967, 0.08995)	0.05556	(0.03025, 0.09778)	0.09677	(0.05489, 0.16289)
$\mu_5$	0.02216	(0.01464, 0.03320)	0.02206	(0.00901, 0.04842)	0.04663	(0.02350, 0.08747)
$\mu_6$	0.02200	(0.01184, 0.03945)	0.03101	(0.00948, 0.07966)	0.01923	(0.00401, 0.05756)
$d_3$	0.0	(-0.00955, 0.05767)	0.0	(-0.03083, 0.20672)	0.11111	(-0.00182, 0.45672)
$d_4$	0.01391	(0.00657, 0.02771)	0.01579	(0.00324, 0.04753)	0.00885	(-0.00331, 0.05331)
$d_5$	0.02746	(0.01904, 0.03931)	0.01805	(0.00651, 0.04276)	0.02041	(0.00612, 0.05314)
$d_6$	0.02148	(0.01156, 0.03853)	0.01527	(0.00072, 0.05744)	0.03704	(0.01530, 0.08022)

Table 3.5: Maximum likelihood estimates with associated 95% confidence intervals for constant transitional and mortality treatments, in each of the three temperature treatments.

These parameter estimations and confidence intervals are presented graphically in Figure 3.5, to demonstrate overlap in confidence intervals.

Because no experimental data exists for first and second instars, transitional and mortality probabilities in each treatment are fixed as follows:

$$\begin{aligned}\hat{\mu}_1 &= 1.1\hat{\mu}_3 \\ \hat{\mu}_2 &= 1.05\hat{\mu}_3 \\ \hat{d}_1 &= 1.1\hat{d}_3 \\ \hat{d}_2 &= 1.05\hat{d}_3,\end{aligned}$$

recalling the condition of the solutions that  $(1 - \mu_j)(1 - d_j) \neq (1 - \mu_k)(1 - d_k)$  for  $j \neq k$ . These estimates are substituted into (3.13) to generate adult emergence predictions in each treatment (Figure 3.6).

Emergence occurs first in the warmer treatment, with peak emergence occurring 53 days after hatching, with probability 0.01292 (Figure 3.6c). Total probability of emergence in this treatment is 0.07934. Next is the ambient treatment, with peak emergence at day 76 and probability 0.01920 (Figure 3.6b), having total emergence probability 0.1727. The final emergence distribution is the cooler treatment, which peaks at day 78 with probability 0.01410 (Figure 3.6a), with total emergence probability 0.1260.

### 3.6.2 Variable transition probabilities

One source of error in the model is the requirement that  $T_0$  must be fixed prior to maximum likelihood estimation of slopes ( $\hat{a}_i$ ) for transitional probability functions. A range of biologically reasonable  $T_0$  values are fixed, from 3 – 6°C (Taylor, 1981), and  $\hat{a}_i$  are calculated along with associated 95% confidence intervals, to determine the range of freedom available for fixing  $T_0$ , presented in Table 3.6. Because slopes  $\hat{a}_i$  are estimated from binomial data without error, estimates are reported to six decimal places for brevity.

For the remainder of the results,  $T_0 = 5$  is fixed.

The validity of the maximum likelihood estimates for  $a_i$  is tested by bootstrapping the data to determine the number of trials which estimate  $a_i$  outside its 95% confidence interval. In 1000 trials, the estimated  $\hat{a}_3$  value falls outside the acceptable range in 4.3% of cases, while  $\hat{a}_4$  falls outside in 3.1% of cases,  $\hat{a}_5$  falls outside in 90.6% of cases, and  $\hat{a}_6$  falls outside in 53.3% of cases. New parameter values, which will be used in the remainder of the results, are generated from the mean of the bootstrapped estimates, to be

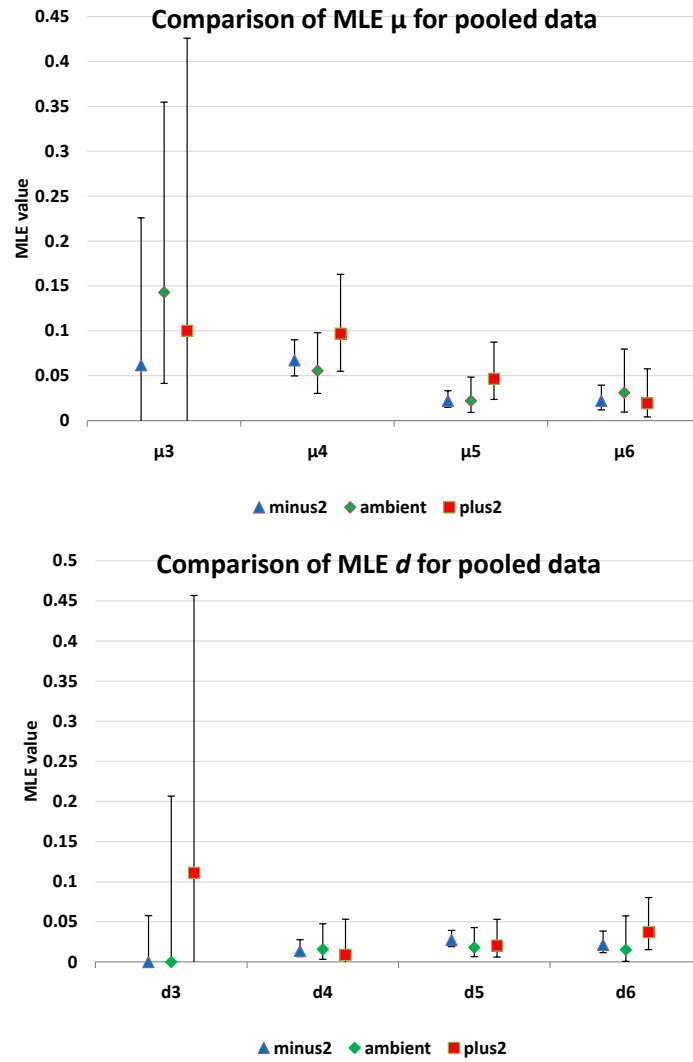


Figure 3.5: Maximum likelihood estimates for cooler (triangle), ambient (diamond) and warmer (square) treatments, with adjusted Wald 95% confidence intervals (3.23) denoted by bars, for  $\mu$  and  $d$  parameters.

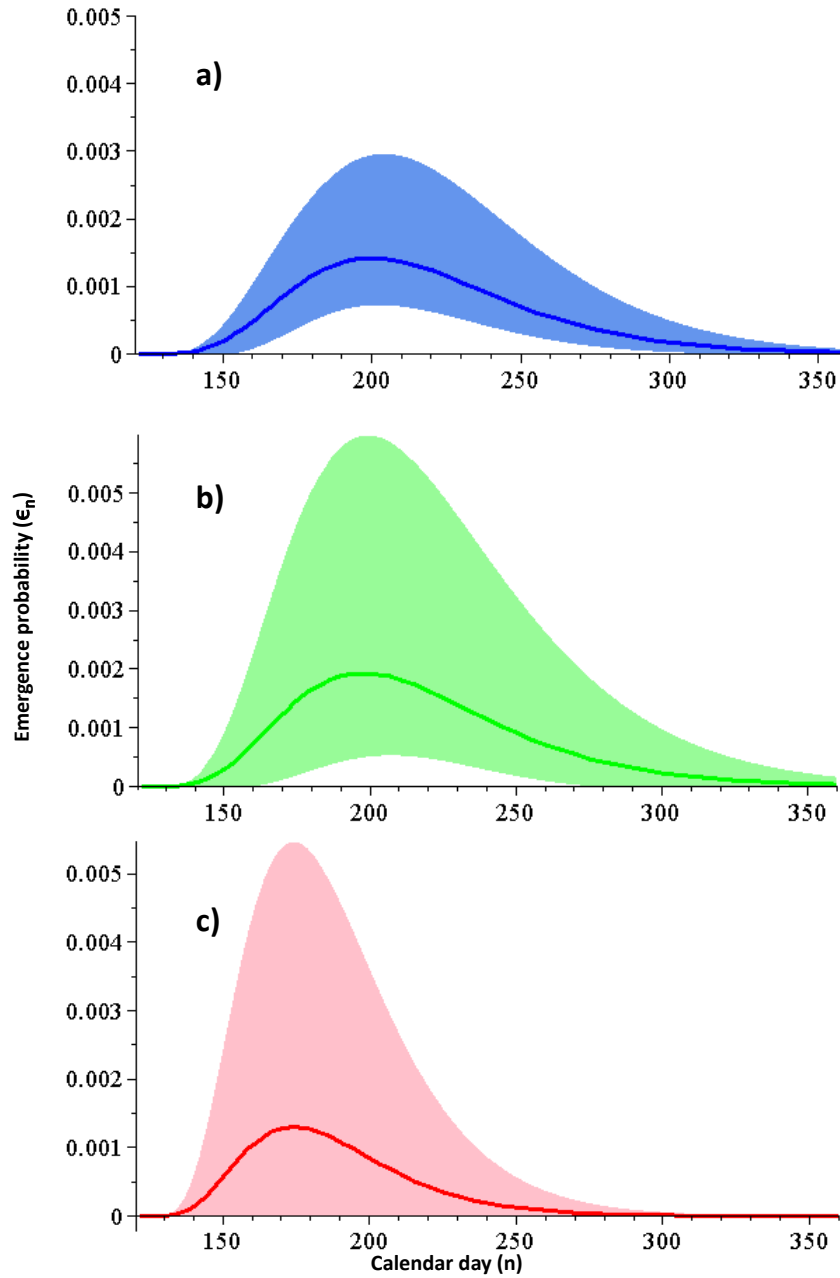


Figure 3.6: Predicted adult emergence  $\epsilon_n$  in different temperature treatments with associated error (3.24) shaded, having constant transition and mortality probabilities. Later emergence occurs in a) cooler treatment and b) ambient treatment than in c) warmer treatment.

Slope	$T_0 = 3$		$T_0 = 4$	
	Estimate	CI	Estimate	CI
$a_3$	0.009876	(0.005387, 0.014366)	0.010860	(0.006375, 0.015346)
$a_4$	0.006199	(0.005035, 0.007363)	0.006758	(0.005594, 0.007922)
$a_5$	0.001720	(0.001282, 0.002158)	0.001854	(0.001416, 0.002292)
$a_6$	0.001496	(0.000956, 0.002036)	0.001600	(0.001060, 0.002140)
Slope	$T_0 = 5$		$T_0 = 6$	
	Estimate	CI	Estimate	CI
$a_3$	0.012060	(0.007581, 0.016543)	0.013560	(0.009085, 0.018037)
$a_4$	0.007428	(0.006265, 0.008592)	0.008245	(0.007082, 0.009409)
$a_5$	0.002010	(0.001573, 0.002448)	0.002196	(0.001759, 0.002634)
$a_6$	0.001720	(0.001180, 0.002261)	0.001860	(0.001319, 0.002400)

Table 3.6: Maximum likelihood estimates for  $a_i$  with associated 95% confidence intervals, when transitional probabilities  $\mu_i(T) = a_i(T - T_0)$  change due to varying developmental lower threshold temperatures  $T_0$ .

$$\begin{aligned}
\hat{a}_3 &= 0.012341 (0.008303, 0.016379) \\
\hat{a}_4 &= 0.007337 (0.006270, 0.008404) \\
\hat{a}_5 &= 0.002837 (0.002314, 0.003361) \\
\hat{a}_6 &= 0.002273 (0.001934, 0.002613).
\end{aligned}$$

Figure 3.7 graphically illustrates the results of the bootstrapping method, and Figure 3.8 illustrates the final transitional probability functions. The constant mortality probability is fixed at  $d = 0.019807$  (0.009127, 0.054254) for each instar, being the mean of the maximum likelihood estimates  $\hat{d}_i$  calculated in the previous section.

The model is quite robust to a changing start date within a two month range of May 1st (calendar day 121 or 122). All numerical simulations are hereafter fixed with a May 1st start date. See Appendix D for figures of adult emergence under varying start dates.

The predicted emergence in each year with associated error is presented in Figures 3.9 and 3.10.

### 3.6.3 Validation of variable transition probability model

The observed emergence of *P. smintheus* adults is first compared graphically to predicted model output in Figures 3.11 and 3.12. The meadows used for comparison were those having the largest number of sampling days in a given year. Within a sampling period, model emergence is aggregated to sampling days for comparative purposes, that is, model predictions between sampling days are summed to the next sampling day to compare against observations. While Figures 3.11 and 3.12 represent discrete data, the data is presented continuously for purposes of clarity.

The results of the Wilcoxon signed-rank tests and linear regression of observed on predicted emergence are presented in Tables 3.7 and 3.8, respectively. Values are compared for both the Wilcoxon signed-rank test and the linear regression only if they occur on sampling days within the observed sampling period. Recall that for both tests, the null hypothesis  $H_0$  states that the observed and predicted emergence distributions are statistically indistinguishable.

The Wilcoxon signed-rank test does not reject the model as a predictor of the observed emergence distribution in any year (save 2005 when the sample size is too small to conduct the test). The linear regression analysis fails to reject the model in 2001 – 2008, and does reject the model in 2009.

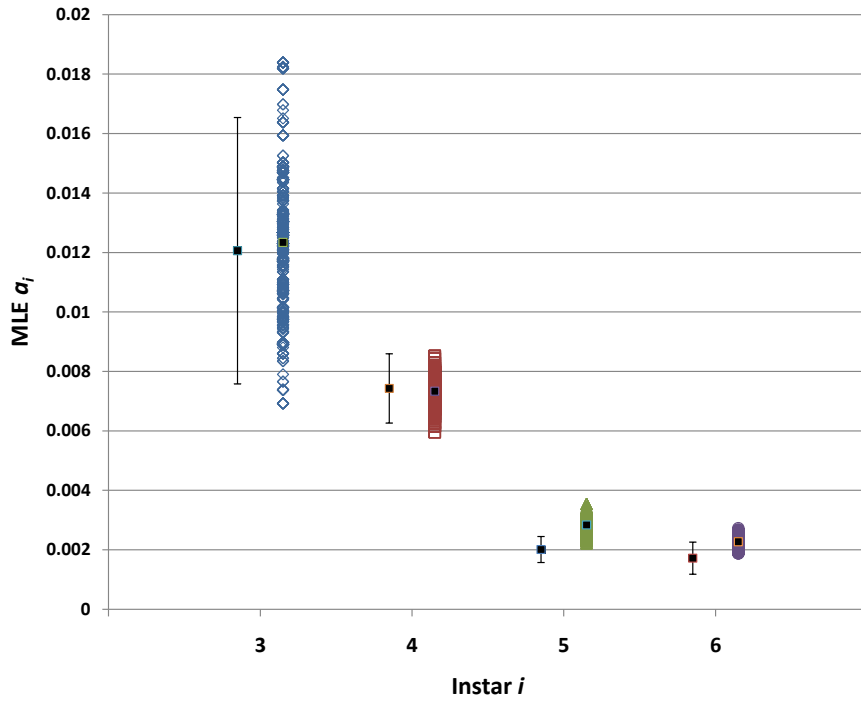


Figure 3.7: For each instar, black squares on left denote original maximum likelihood estimates for  $a_i$ , with bars denoting associated 95% confidence intervals (3.26), as presented in Table 3.6 for  $T_0 = 5$ . On the right, for each instar, the estimates for  $a_i$  from 1000 bootstrapping trials are presented, with the mean  $a_i$  value denoted by the black square. The means of the bootstrapping trials are hereafter used as the estimates for  $a_i$ .

Year	# observations	$T_+, T_-$	$T_{\text{crit}}$	Conclusion
2001	7	7, 21	2	Do not reject $H_0$
2003	6	7, 14	0	Do not reject $H_0$
2004	7	6, 22	2	Do not reject $H_0$
2005	5	—	—	Sample too small
2006	11	23, 43	11	Do not reject $H_0$
2007	20	72, 138	52	Do not reject $H_0$
2008	18	69, 102	40	Do not reject $H_0$
2009	17	57, 96	34	Do not reject $H_0$

Table 3.7: Results of Wilcoxon signed-rank test, with critical values taken from Zar (2010). Predicted model emergence is not significantly different from observed emergence in all years.

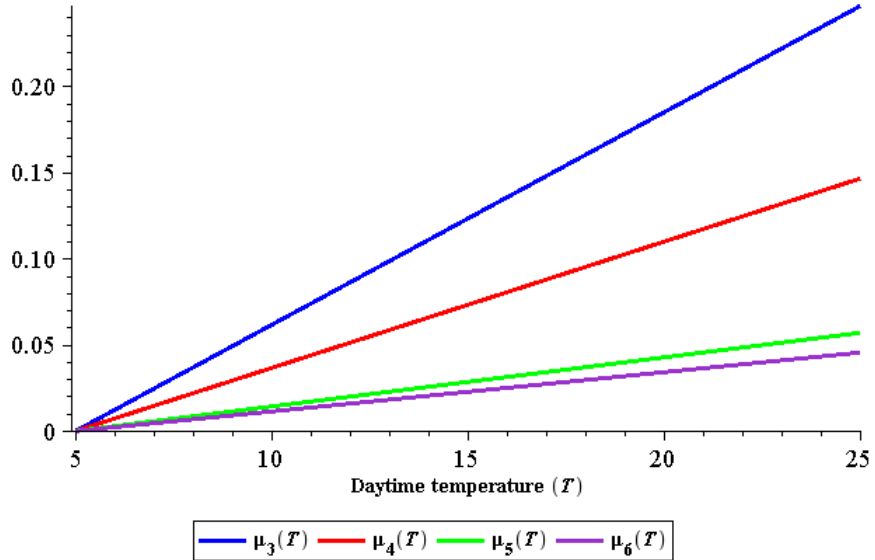


Figure 3.8: Linear transitional probability functions,  $\mu_i(T) = a_i(T - 5)$ ,  $i = 3, \dots, 6$ , using bootstrapped slope estimates as presented in Figure 3.7.

Year	# observations	$F$	$F_{\text{crit}}$	Conclusion
2001	7	2.57	8.43	Do not reject $H_0$
2003	6	1.48	10.6	Do not reject $H_0$
2004	7	1.97	8.43	Do not reject $H_0$
2005	5	0.45	16.0	Do not reject $H_0$
2006	11	1.19	5.71	Do not reject $H_0$
2007	20	3.80	4.56	Do not reject $H_0$
2008	18	3.75	4.69	Do not reject $H_0$
2009	17	9.03	5.26	Reject $H_0$

Table 3.8: Results of linear regression of observed on predicted emergence, with critical values taken from Zar (2010). Predicted model emergence is not significantly different from observed emergence in 2001 – 2008, and is significantly different in 2009.

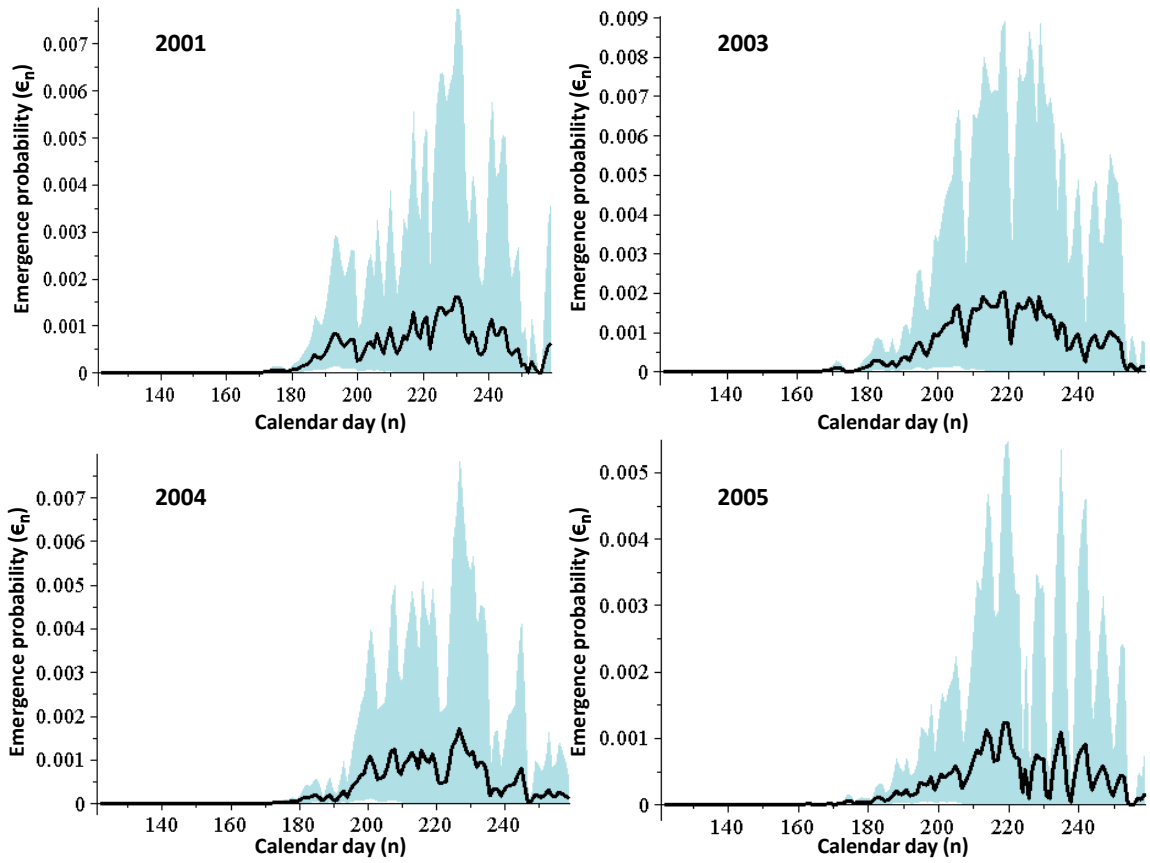


Figure 3.9: Adult emergence probability distributions  $\epsilon_n$  (black curves) predicted from the variable transition probability model, with associated error (3.27) shaded in blue. Temperature regimes used as input are those from 2001, 2003 – 2005.

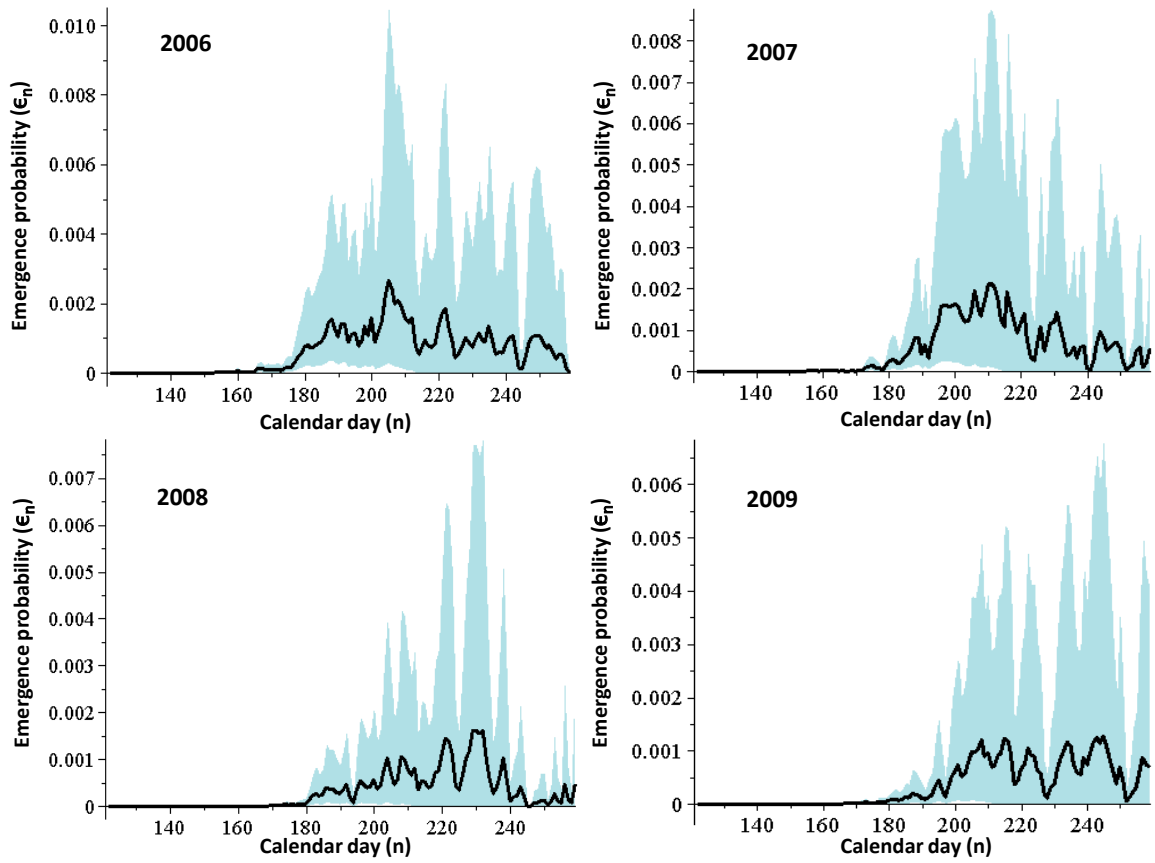


Figure 3.10: Adult emergence probability distributions  $\epsilon_n$  (black curves) predicted from the variable transition probability model, with associated error (3.27) shaded in blue. Temperature regimes used as input are those from 2006 – 2009.

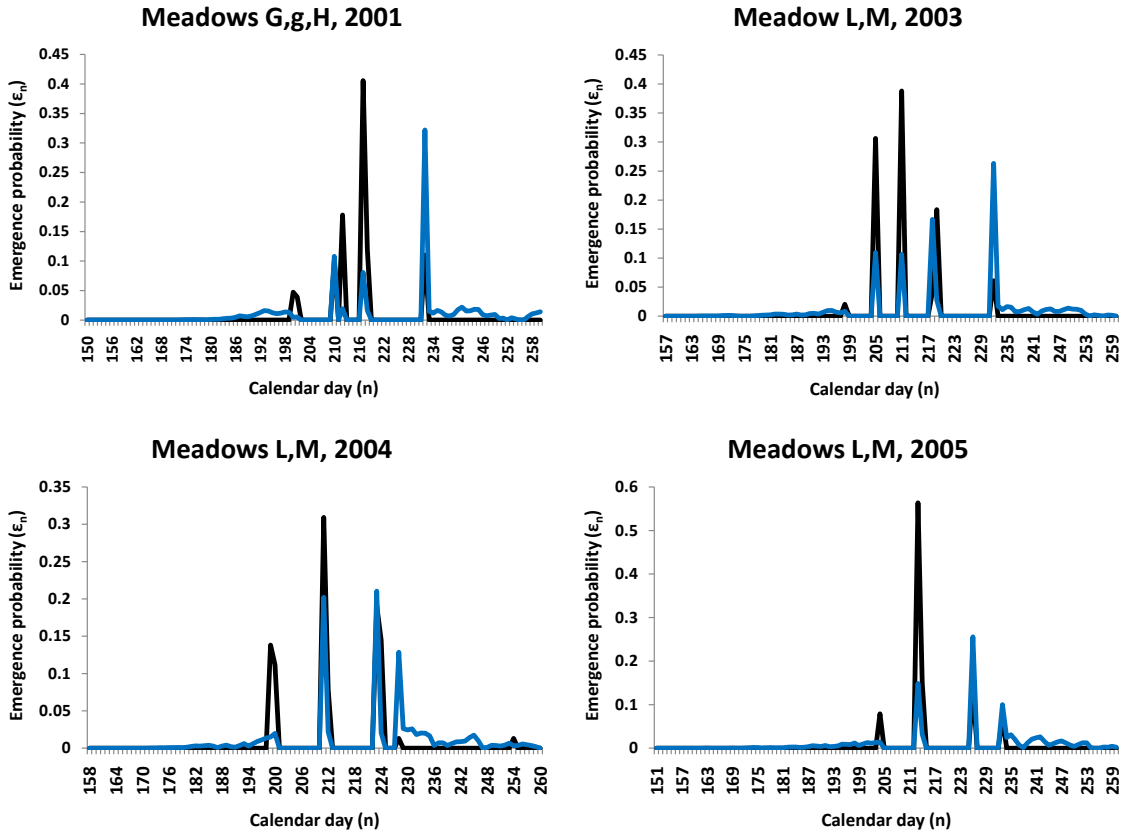


Figure 3.11: Observed versus predicted emergence probability distributions in 2001, 2003-2005. Black curves denote observed emergence (generated from mark-recapture data) and blue curves denote predicted emergence (generated from variable transition probability model with appropriate year's temperature regime as input).

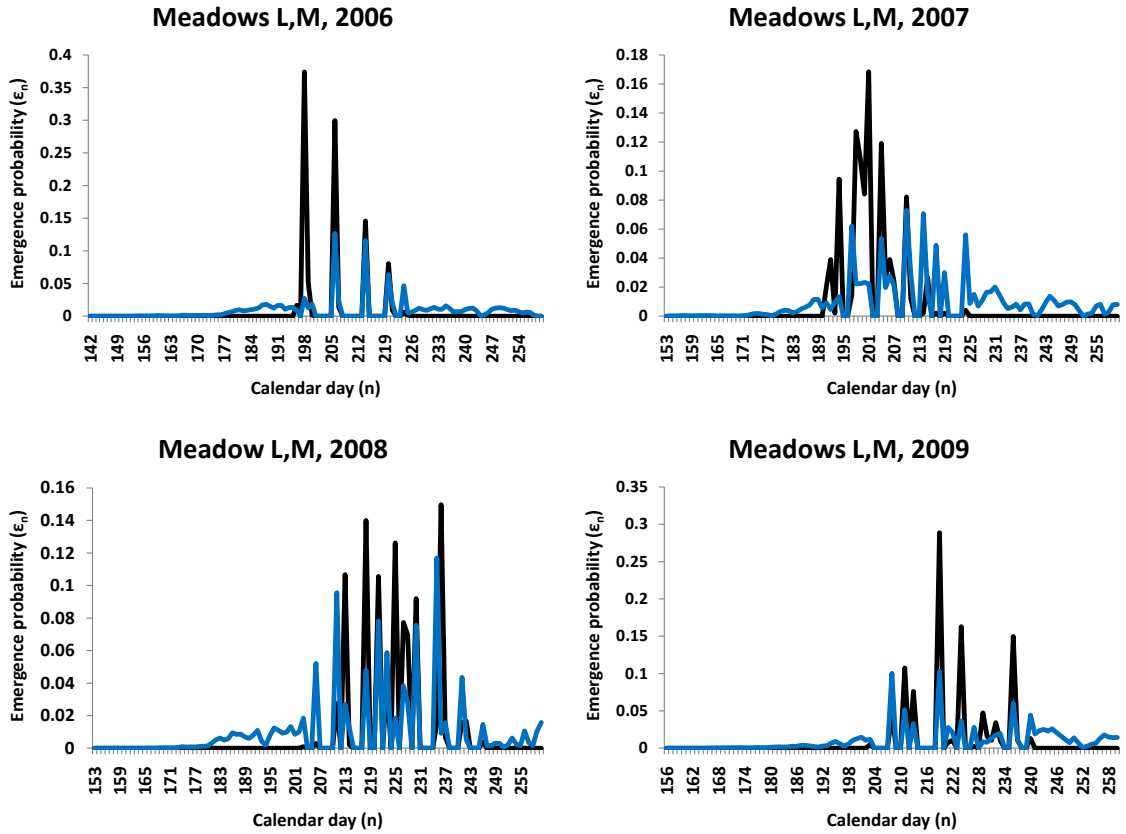


Figure 3.12: Observed versus predicted emergence probability distributions in 2006-2009. Black curves denote observed emergence (generated from mark-recapture data) and blue curves denote predicted emergence (generated from variable transition probability model with appropriate year's temperature regime as input).

## 3.7 Discussion

Both the constant and varying transition probability models exhibit biologically reasonable behaviour in their predictions of temperature-dependent adult emergence. The constant transition probability model indicates the utility of a simplified and analytically tractable model, demonstrating earlier emergence in the warmer treatment and similar emergence times in the cooler and ambient treatments. The varying transition probability model mostly captures the range and shape of the observed emergence distribution, though with some variability in the predicted values.

### 3.7.1 Constant-valued transition and mortality probabilities

In the constant probability model, individuals in the warmer treatment emerge earlier than those in the other treatments (Figure 3.6c), with a peak emergence 23 days before that of the ambient treatment and 25 days before that of the cooler treatment. This is expected from the experimental analysis of the previous chapter, which indicated a shorter fifth instar development time in the warmer treatment. Though experimental data was insufficient to determine differences between developmental times in other instars, this model suggests that a similar pattern holds at least in the fourth instar, where the maximum likelihood estimates for  $\mu_4$  (Figure 3.5) indicate a higher transitional probability in the warm treatment. The proximity of the emergence peaks in the ambient and cooler treatments is further supported by the statistical analysis of the previous chapter, which determined no significant differences between fifth instar development time in these treatments. However, overall mortality is higher in both the warmer and cooler treatments than in the ambient; from the previous statistical analysis, which links mortality to longer development time, one might expect mortality to be highest in the cooler treatment. An examination of the maximum likelihood estimates (Figure 3.5) offers a partial explanation. The estimated mortality probability for the third instar  $\hat{d}_3$  is ten times higher in the warmer treatment than the other two, but this is likely a product of the small third instar sample size which yielded the estimate. For  $\hat{d}_4$  and  $\hat{d}_5$ , the estimates are very consistent across the different treatments, lending credence to the idea that mortality probabilities do not depend directly on temperature (at least in the experimental thermal range), and higher mortality at low temperatures is attributable to longer development times. The sixth instar indicates a slightly higher mortality probability in the warmer treatment, which may be due to desiccation of pupae in the growth chambers. Such desiccation could have occurred if the chambers were insufficiently humid for the soil in which the pupae burrowed to retain moisture. Overall, the earlier emergence of the warmer treatment individuals using this model and parameterization method indicate the value of a simplified and analytically tractable model, should one desire to address general questions of “warming” or “cooling” on a population of *P. smintheus*. Such a model could be improved by a larger experimental sample size (especially in the third instar) and experimental data for transitional success and mortality in the first and second instars. Due to considerable difficulties in rearing this species in the laboratory (pers. comm., Matter), however, this model, as well its variable transitional probability analogue, may offer the best insight (when compared to pure experimental work) into the effects of temperature on *P. smintheus* development.

### 3.7.2 Variable transition probabilities

In the varying transitional probability model, the maximum likelihood method demonstrably fails to accurately estimate slopes ( $\hat{a}_i$ ) for transitional success functions (Figure 3.7). In all estimates but for the fourth instar, the mean of the bootstrapped estimates was larger than the original estimate. When the model fails to match the observed emergence distribution given the modified parameterization, the failing is a late predicted emergence (Figures 3.11 and 3.12, 2001 – 2003 and 2006 – 2007). In no year does the model predict substantial emergence prior to observed emergence. Since the transitional probabilities assume a linear relationship with temperature, the original model parameterization (having mostly smaller slopes) would predict later emergences and perform more poorly. Bootstrapping the data clearly indicates the importance of working with similar sample sizes at various temperatures, but the large variance in the estimates (Figure 3.7) may indicate a range for

parameter estimation, and the mean of the bootstrapped estimates, while a reasonable parameter estimate, is perhaps not the best. The estimates as used, however, demonstrate a strict decrease as instars increase (Figure 3.8), indicating that an individual in the third instar at a given temperature has a larger transitional probability than a member of its cohort in the sixth instar. This offers some evidence that the parameter estimates are at least biologically reasonable, as energy requirements are higher in later instars, normally prompting longer development times.

The estimates for  $a_i$  can further be influenced by the fixed value of  $T_0$ , the thermal lower bound for development, since this parameter was fixed prior to either maximum likelihood estimation or bootstrapping for  $a_i$ . The experimental data offers little insight into what such a parameter value might be, as the experimental temperature range was too high to prompt a cessation in development for any individual. A review of the literature prompted the fixed  $T_0 = 5$ , as it is seen in multiple butterfly species (Hill et al., 1999; Taylor, 1981) as an approximate lower developmental threshold for larvae. In fact, as estimated from the data for *P. smintheus*,  $\hat{a}_3$  and  $\hat{a}_6$  do not change significantly as  $T_0$  is varied from 3 – 6°C (that is, each estimate falls within all confidence intervals for estimates between 3 – 6°C), as reported in Table 3.6. The estimate  $\hat{a}_5$  does not change significantly as  $T_0$  is varied from 3 – 5°C, and  $\hat{a}_4$  does not change significantly as  $T_0$  is varied from 4 – 5°C. It can thus be concluded that the model demonstrates some robustness to a varying  $T_0$ .

The model is also robust to changes in start date, due to very low temperatures in the range of hatching dates used. Hatching in *P. smintheus* eggs is triggered by snowmelt, so sufficiently high temperatures were required prior to the calendar day on which the model simulations were to begin. Given that transitional probabilities were zero at temperatures lower than 5°C, the adult emergence distribution changed very little in shape or range given simulated hatching dates from April 15th to June 3rd (Figures D.1 and D.2), due to low temperatures within these time periods. Care must still be taken when fixing simulated hatch dates, however, as the constant daily mortality probability used in the model causes lower overall adult emergence in simulations where hatching occurred earlier (as individuals, trapped in first instar by low temperatures, fall prey to mortality).

A comparison of predicted versus observed emergence in *P. smintheus* adults gives some indication of the model’s validity. The Wilcoxon signed-rank test (Table 3.7) did not reject that observed and predicted emergence distributions were the same (excepting 2005, when an insufficient number of sampling days precluded the use of the test). A linear regression of observed on predicted emergence probabilities (Table 3.8), rejected the null hypothesis that the emergence probabilities corresponded in 2009 only. This rejection may have been due to model failure, but may also have been due to the large amount of variability in the data, which can cause Type I errors in linear regression analysis (Haefner, 2005).

By inspecting Figures 3.11 and 3.12, one may note, as mentioned earlier, that predicted emergence lagged behind observed emergence most especially in 2001, 2003, 2006, and 2007. In validating the model, however, one must also consider the validity of the data against which it is compared. In early years of the field experiment, sampling was intermittent, with periods of up to 13 days between samples in a meadow in 2001, 12 days in 2003, 10 days in 2004, and 11 days in 2005. In 2006 – 2009, sampling was more frequent, with at most 6, 4, 4, and 5 days between samples in a meadow, respectively. Large gaps between samples are sometimes attributable to bad weather (*P. smintheus*, like many butterflies, does not fly on non-sunny days) but other gaps may be due to sampling taking place in other meadows. While it was demonstrated that migration between meadows likely has a negligible impact on emergence probability (Table 3.4), mortality within a meadow might influence emergence probabilities should the period between sampling be sufficiently long. That is, a butterfly may emerge after one sampling day and die prior to the next sampling day; lifespans between 2 – 20 days have been documented in female *P. smintheus* adults (pers. comm., Matter). This might influence the shape of the observed emergence distributions, especially in 2001 – 2005 when sampling was less frequent. The difference between predicted and observed emergence in 2001 and 2003 (Figure 3.11), for instance, on the last sampling day (calendar day 232 in both years) may be in part explained by natural mortality in the observed system between sampling days.

In the years with more sampling days, however, such an explanation is less likely. In 2006 and 2007, the model by visual inspection predicts emergence later than that observed, in contrast to 2008, where the model temporally overlaps the observed emergence quite well. Both 2006 and 2007

were characterized by warm temperatures and early, brief emergence periods, having initial observed emergence on calendar days 196 and 191 and peak emergence on days 198 and 201, respectively. (It is worth noting however that the abrupt peak in 2006, immediately after sampling began, may indicate that initial emergence in that meadow was missed, having occurred prior to the start of the sampling period). In contrast, the cooler 2008 temperatures may have prompted the later and longer observed emergence period, having initial emergence on day 203 and peak emergence on day 236. That the model captured the emergence in 2008, but not 2006 and 2007 suggests that the model parameterization works best for cooler temperatures, and that it underestimates transitional success at higher temperatures. One may speculate that the linear form of the temperature-dependent transition probability function is generally unsuitable, though appropriate for cooler years. The linear form was chosen as the most appropriate based on the experimental data used for parameterization, given the narrowness of the experimental temperature range. A natural extension to this research would conduct the developmental experiments again at a wider range of temperatures, with a larger number of individuals. Such experimental work might give a better indication of the thermal lower threshold for development, as well as a potential upper threshold for development (a point at which heat stress prevents development and prompts mortality (Taylor, 1981)). Then a different functional form could better capture the temperature-dependent dynamics of the system, and better predict emergence in the warm years.

### 3.7.3 Implications for *P. smintheus*

Understanding the developmental behaviour of *P. smintheus* near the thresholds of its developmental temperature range is important when considering climate change, which may cause warming as well as increased variability in temperatures. If warm years prompt early and brief emergence periods, it may have a profound effect on population dynamics and community dynamics. The early emergence from faster larval development (as demonstrated both experimentally and through modelling) may confer both advantages and disadvantages to a population. Experimental results suggested that mortality is lower in faster developing larvae, so that more successfully reach adulthood. Growth experiments in *Procllossiana eunomia* indicate death rates in adults increase in time from first emergence, possibly caused by higher fitness in early emerging individuals or increasing competition for limited resources (Schtickzelle et al., 2002), though it is unknown whether such a pattern is present in *P. smintheus*. The present model also treats individuals as identical, so such individual effects would be difficult to capture. Emergence of adults may also influence reproductive success in *Paranassius clodius* and *P. smintheus* (Calabrese et al., 2008), an area which will be explored more fully in the next chapter.

Temperature-driven effects on adult emergence must also be studied at a community level. In the previous chapter, *P. smintheus* emergence synchrony with host plants, both at larval and adult stages, was indicated to be critical to population survival (Fred and Brommer, 2010; Matter et al., 2009). Warming temperatures may destabilise the synchrony of these interacting species or even force species out of a previously shared habitat. The effects of temperature on interacting species is thus an important subsequent step to this research.

Another area of interest for effects of temperature on *P. smintheus* development lies in adapting the model to consider protandry and sex-specific larval development. Protandry has been observed in *P. smintheus* adult populations, with earlier initial emergence of males than females (Calabrese et al., 2008). The current model framework permits protandrous species modelling, given sex-specific development data; separate parameterizations for male and female larvae would allow two distinct adult emergence distributions. Protandry is not considered in the present study as male and female *P. smintheus* are physically indistinguishable in their larval form. That is, while individuals surviving to adulthood may be sexed *posteriori*, no information can be determined from individuals dying prior to adulthood. While it is possible to genetically determine sex after death in larvae (Roland, pers. comm.), such analysis is beyond the scope of the present study.

Understanding temperature-driven effects on insect phenology is crucial to the understanding of how species will react to climate change. In this chapter, a model framework has been presented to predict developmental success and adult emergence in *P. smintheus*, but this represents only the

first steps in understanding how a changing climate may impact this alpine species.

# Bibliography

- Atkinson, D. (1994). Temperature and organism size –A biological law for ectotherms? *Advances in Ecological Research* 25, 1–58.
- Bentz, B. J., J. E. Logan, and G. D. Amman (1991). Temperature-dependent development of the mountain pine beetle (Coleoptera:Scolytidae) and simulation of its phenology. *The Canadian Entomologist* 123, 1083–1094.
- Berryman, A. A., B. Dennis, K. F. Raffa, and N. C. Stenseth (1985). Evolution of optimal group attack, with particular reference to bark beetles (Coleoptera: Scolytidae). *Ecology* 66(3), 898–903.
- Bocharov, P. P. and C. D’Apice (2004). *Queueing Theory*. Walter de Gruyter.
- Both, C., M. van Asch, R. B. Bijlsma, A. B. van den Burg, and M. E. Visser (2009). Climate change and unequal phenological changes across four trophic levels: Constraints or adaptations? *Journal of Animal Ecology* 78, 73–83.
- Calabrese, J. M. and W. F. Fagan (2004). Lost in time, lonely, and single: Reproductive asynchrony and the Allee effect. *The American Naturalist* 164(1), 25–37.
- Calabrese, J. M., L. Ries, S. F. Matter, D. M. Debinski, J. N. Auckland, J. Roland, and W. F. Fagan (2008). Reproductive asynchrony in natural butterfly populations and its consequences for female matelessness. *Journal of Animal Ecology* 77, 146–156.
- Coolen-Schrijner, P. and E. A. van Doorn (2006). Quasi-stationary distributions for a class of discrete-time Markov chains. *Methodology and Computing in Applied Probability* 8, 449–465.
- Elaydi, S. (2005). *An Introduction to Difference Equations* (3rd ed.). Undergraduate Texts in Mathematics. Springer.
- Environment Canada (2010). National climate data and information archive. [www.climate.weatheroffice.ec.gc.ca](http://www.climate.weatheroffice.ec.gc.ca), accessed May 2009 - January 2010.
- Feller, W. (1970). *An Introduction to Probability Theory and Its Application* (3rd revised ed.), Volume 1. John Wiley & Sons.
- Flajolet, P. and R. Sedgewick (2009). *Analytic Combinatorics*. Cambridge University Press.
- Fred, M. S. and J. E. Brommer (2010). Olfaction and vision in host plant location by *Parnassius apollo* larvae: Consequences for survival and dynamics. *Animal Behaviour* 79, 313–320.
- Haefner, J. W. (2005). *Modeling Biological Systems: Principles and Applications* (2nd ed.). Springer Science.
- Hill, J. K., C. D. Thomas, and B. Huntley (1999). Climate and habitat variability determine 20th century changes in a butterfly’s range margin. *Proceedings of the Royal Society of London* 266, 1197–1206.
- Hoye, T. T. and M. C. Forchhammer (2008). Phenology of high-arctic arthropods: Effects of climate on spatial, seasonal, and inter-annual variation. *Advances in Ecological Research* 40, 299–324.
- Iwasa, Y. and S. A. Levin (1995). The timing of life history events. *Journal of Theoretical Biology* 172, 33–42.
- Lactin, D. J., N. J. Holliday, D. L. Johnson, and R. Craigen (1995). Improved rate model of temperature-dependent development by arthropods. *Population Ecology* 24(1), 68–75.

- Larson, H. J. and B. O. Schubert (1979). *Probabilistic Models in Engineering Sciences: Random Variables and Stochastic Processes*, Volume 1. John Wiley & Sons.
- Lawler, G. F. (2006). *Introduction to Stochastic Processes* (2nd ed.). Chapman and Hall/CRC.
- Logan, J. A., D. J. Wollkind, S. C. Hoyt, and L. K. Tanigoshi (1976). Analytic model for description of temperature-dependent rate phenomena in arthropods. *Environmental Entomology* 5, 1133–1140.
- Matter, S. F., M. Ezzeddine, E. Duermit, J. Mashburn, R. Hamilton, T. Lucas, and J. Roland (2009). Interactions between habitat quality and connectivity affect immigration but not abundance or population growth of the butterfly *Parnassius smintheus*. *Oikos* 118, 1461–1470.
- Matter, S. F. and J. Roland (2002). An experimental examination of the effects of habitat quality on the dispersal and local abundance of the butterfly *Parnassius smintheus*. *Ecological Entomology* 27, 308–316.
- Matter, S. F., J. Roland, N. Keyghobadi, and K. Sabourin (2003). The effects of isolation, habitat area and resources on the abundance, density, and movement of the butterfly *Parnassius smintheus*. *American Midland Naturalist* 150, 26–36.
- Matter, S. F., J. Roland, A. Moilanen, and I. Hanski (2004). Migration and survival of *Parnassius smintheus*: Detecting effects of habitat for individual butterflies. *Ecological Applications* 14(5), 1526–1534.
- Nelson, R. (1995). *Probability, stochastic processes, and queueing theory: The mathematics of computer performance modelling*. Springer.
- Parnesan, C. (2006). Ecological and evolutionary responses to recent climate change. *Annual Review of Ecology, Evolution and Systematics* 37, 637–669.
- Roland, J., N. Keyghobadi, and S. Fownes (2000). Alpine *Parnassius* butterfly dispersal: Effects of landscape and population size. *Ecology* 81(6), 1642–1653.
- Roland, J. and S. F. Matter (2007). Encroaching forests decouple alpine butterfly population dynamics. *Proceedings of the National Academy of Sciences* 104(34), 13702–13704.
- Schoolfield, R. M., P. J. H. Sharpe, and C. E. Magnuson (1981). Non-linear regression of biological temperature-dependent rate models based on absolute reaction-rate theory. *Journal of Theoretical Biology*, 719–731.
- Schtickzelle, N., E. L. Boulengé, and M. Baguette (2002). Metapopulation dynamics of the bog fritillary butterfly: Demographic processes in a patchy population. *Oikos* 97, 349–360.
- Schweiger, O., J. Settele, O. Kudrna, S. Klotz, and I. Kühn (2008). Climate change can cause spatial mismatch of trophically interacting species. *Ecology* 89, 3472–3479.
- Sharpe, P. J. H., G. L. Curry, D. W. DeMichele, and C. L. Cole (1977). Distribution model of organism development times. *Journal of Theoretical Biology* 66, 21–38.
- Sharpe, P. J. H. and D. W. DeMichele (1977). Reaction-kinetics of poikilotherm development. *Journal of Theoretical Biology* 64, 649–670.
- Stinner, R. E., G. D. Butler, J. S. Bacheler, and C. Tuttle (1975). Simulation of temperature-dependent development in population dynamics models. *The Canadian Entomologist* 107, 1167–1174.
- Stinner, R. E., A. P. Gutierrez, and G. D. Butler (1974). An algorithm for temperature-dependent growth rate simulation. *The Canadian Entomologist* 106, 519–524.
- Stork, N. E., J. A. Coddington, R. K. Colwell, R. L. Chazdon, C. W. Dick, C. A. Peres, S. Sloan, and K. Willis (2009). Vulnerability and resilience of tropical forest species to land-use change. *Conservation Biology* 23(6), 1438–1447.
- Tanigoshi, L. K. and J. A. Logan (1979). Tetranychid development under variable temperature regimes. In J. G. Rodriguez (Ed.), *Recent advances in acarology*, Volume 1, pp. 165–175. Academic Press.
- Taylor, F. (1981). Ecology and evolution of physiological time in insects. *The American Naturalist* 117, 1–23.

- Taylor, J. R. (1997). *An Introduction to Error Analysis: The Study of Uncertainties in Physical Measurements* (2nd ed.). University Science Books.
- Thomson, L. J., S. Macfadyen, and A. A. Hoffmann (2010). Predicting the effects of climate change on natural enemies of agricultural pests. *Biological Control* 52, 296–306.
- Tornambè, A. (1995). *Discrete-Event System Theory: An Introduction*. World Scientific.
- Uvarov, B. P. (1931). Insects and climate. *Transactions of the Entomological Society of London* 79, 1–279.
- van der Have, T. M. and G. de Jong (1996). Adult size in ectotherms: Temperature effects on growth and differentiation. *Journal of Theoretical Biology* 183, 329–340.
- Visser, M. E. and C. Both (2005). Shifts in phenology due to global climate change: The need for a yardstick. *Proceedings of the Royal Society B* 272, 2561–2569.
- Wagner, T. L., H.-I. Wu, P. J. H. Sharpe, and R. N. Coulson (1984). Modelling distributions of insect development time: A literature review and application of the Weibull function. *FORUM: Annals of the Entomological Society of America* 77, 475–487.
- Worner, S. (1992). Performance of phenological models under variable temperature regimes: Consequences of the Kauffmann or rate summation effect. *Environmental Entomology* 21(4), 689–699.
- Yurk, B. P. and J. A. Powell (2009). Modelling the evolution of insect phenology. *Bulletin of Mathematical Biology* 71, 952–979.
- Zar, J. H. (2010). *Biostatistical Analysis* (5th ed.). Prentice Hall.

## Chapter 4

# A model for temperature-dependent reproductive success and egg production in *Parnassius smintheus*

### 4.1 Introduction

Temperature and other climatic variables may influence larval development in insects, which in turn impact the individuals later in life. Specifically, phenological changes in insect species stemming from larval development may impact resource availability for adults (Hoye and Forchhammer, 2008; Schweiger et al., 2008; Both et al., 2009; Thomson et al., 2010), predator avoidance (Thomson et al., 2010), and adult reproductive success (Iwasa and Levin, 1995; Calabrese and Fagan, 2004; Calabrese et al., 2008). It is this final point, adult reproductive success, which is considered in this chapter.

Multiple theoretical and empirical studies have been conducted which consider effects of low population density on persistence. Allee effects at low population densities may threaten a population, especially by way of mate-finding success (see Gascoigne et al., 2009). Links between component spatial mate-finding Allee effects and demographic Allee effects have been found (in insects) in gypsy moth *Lymantria dispar* (Tchesslavskaja et al., 2002; Tobin et al., 2009), and Glanville fritillary *Melitaea cinxia* (Kuussaari et al., 1998).

Mate-finding Allee effects are not restricted to the spatial domain, as some studies have considered temporal effects on population density. Calabrese and Fagan (2004) and Calabrese et al. (2008) considered models of adult reproductive success in reproductively asynchronous populations; that is, populations in which individual lifetimes do not completely overlap. Reproductive asynchrony is common in species where individual lifespan is less than the overall breeding period, as in univoltine butterflies, and Calabrese et al. (2008) correspondingly parameterized their model for *Parnassius smintheus* and *P. clodius*. Populations may also suffer from combined temporal asynchrony and low spatial density, the combination of which can exacerbate demographic Allee effects (Fagan et al., 2010). From a mathematical perspective, the standard deviation of an adult emergence function is

an approximate measure of temporal synchrony, as it determines the proximity of high emergence rate days to the mean emergence rate day. When the standard deviation in adult emergence is small, the bulk of adults emerge quickly over a short time period (synchronous emergence), while increasing the standard deviation increases the time period over which the bulk of adults emerge (asynchronous emergence).

Climate change increases the importance of understanding temperature effects on insect development (Parmesan, 2006). With this in mind, attempts have been made at predicting insect response to thermal change at the larval level (as discussed in Chapter 3), as well as the adult level. Yurk and Powell (2009) presented a theoretical model for multiple generations with temperature-dependent development and heritable phenological traits such as dependence of developmental time on temperature, so that variations in development time evolve in response to changing temperatures. Further, populations which do not evolve with changing temperatures risk changing their voltinism patterns (Logan and Powell, 2001).

Currently there exist models which present temporal Allee effects (Calabrese and Fagan, 2004; Calabrese et al., 2008; Fagan et al., 2010) and models which allow for evolutionary response to temperature changes through inheritance of phenological traits (Yurk and Powell, 2009). However, to my knowledge, no model frameworks presently exist which explicitly explore how a temperature increase affects the synchrony of a population's emergence, and how this temperature increase thus affects adult reproductive success. That is, no studies exist which examine the direct impact of temperature on total adult emergence and the timing of adult emergence, which in turn affect reproductive success. Such direct effects have not previously been studied due to the lack of models such as that presented in Chapter 3, which uses a seasonal temperature regime to predict an adult emergence distribution. Total emergence and standard deviation in adult emergence are controlled by larval survival and development time, which are in turn controlled by temperature-dependent parameters. Therefore, to construct a temperature-dependent adult reproductive success model requires the incorporation of the mechanistic temperature-dependent larval development model from the previous chapter.

The purpose of the present study is to understand how spring and early summer temperatures as experienced by *P. smintheus* larvae influence population persistence both within seasons and over multiple years. To this end, a model framework for reproductive success in adult *P. smintheus* is constructed, modified from Calabrese et al. (2008) in which the temperature-dependent emergence function of Chapter 3 may be used as input. A system of ordinary differential equations models the breeding period dynamics of male, unmated female, and mated female butterflies, as well as the eggs produced by the breeding females.

Two emergence functions are studied: a Gaussian function to isolate effects of varying total emergence and standard deviation, and a continuous-time analogue to the discrete numerical temperature-dependent emergence function considered in the previous chapter. The Gaussian emergence function is used because it has a closed form and the direct effects of varying its parameters (total emergence and standard deviation) independently may be studied. The parameters and input of the mechanistic temperature-dependent model may then be linked to the parameters in the Gaussian function: increasing temperature increases total emergence and standard deviation in the temperature-dependent emergence function, while increasing mortality probability decreases total emergence and increases standard deviation. Studying the independent effects of parameters in

the Gaussian function offers a clearer insight than studying the temperature-dependent function alone, as competing effects are observed in the temperature-dependent emergence function as the parameters of interest (total emergence and standard deviation) may not be varied independently. Using the temperature-dependent emergence function, effects of varying larval mortality, as well as temperatures experienced by larvae are considered.

Errors as propagated through the previous chapter's developmental model to adult emergence, as well as new errors accumulated in the larger reproductive model are considered. Such error analysis demonstrates how under the present parameterization the model contains too great an error for quantitative predictions of reproductive success. A qualitative example of multi-year egg production is instead presented, to demonstrate how temperature variation between years may prompt constantly fluctuating population dynamics in the system.

The model indicates that total adult emergence and emergence synchrony are crucial to reproductive success in a season, suggesting that temperature regimes as experienced by larvae are important contributors to population persistence. Further, yearly variations in these spring and summer temperature regimes may drive reproductive success in the system to produce the fluctuating population sizes as observed from year-to-year in the field for *P. smintheus*.

## 4.2 Model formulation and parameterization

A reproductive success model for *P. smintheus* is constructed based on Calabrese et al. (2008). Let  $M$ ,  $U$ ,  $R$ , and  $E$  be the number of adult males, unmated adult females, reproducing adult females, and eggs, respectively. A dynamical model is proposed which tracks these quantities over time throughout a single season, which is presented here as a system of non-linear coupled ordinary differential equations.

In the year  $\tau$ ,

$$\begin{aligned}
 \underbrace{\frac{dM_\tau}{dt}}_{\substack{\text{rate of change} \\ \text{in \# males}}} &= \underbrace{\theta_M E_{\tau-1}(t_f)\epsilon(t)}_{\text{emergence of males}} - \underbrace{\gamma_M M_\tau}_{\text{male mortality}} \\
 \underbrace{\frac{dU_\tau}{dt}}_{\substack{\text{rate of change} \\ \text{in \# unmated females}}} &= \underbrace{\theta_F E_{\tau-1}(t_f)\epsilon(t)}_{\text{emergence of unmated females}} - \underbrace{\gamma_F U_\tau}_{\text{unmated female mortality}} - \underbrace{cM_\tau U_\tau}_{\text{mating success}} \quad (4.1) \\
 \underbrace{\frac{dR_\tau}{dt}}_{\substack{\text{rate of change} \\ \text{in \# mated females}}} &= \underbrace{cM_\tau U_\tau}_{\text{mating success}} - \underbrace{\gamma_F R_\tau}_{\text{mated female mortality}} \\
 \underbrace{\frac{dE_\tau}{dt}}_{\substack{\text{rate of change} \\ \text{in \# eggs}}} &= \underbrace{\beta R_\tau}_{\text{egg production}}
 \end{aligned}$$

where  $\theta_M$  and  $\theta_F$  are proportions of eggs which are male and female,  $\gamma_M$  and  $\gamma_F$  are constant male and female per-day death rates,  $c$  is a constant per-day mating rate, and  $\beta$  is a fecundity rate

(average number of eggs produced per mated female per day). The adult emergence rate  $\epsilon(t)$  is continuous and integrates to give the total proportion of the population which successfully emerges in the season, so  $\int_t \epsilon(k)dk < 1$  unless no larval mortality occurs. Further,  $\epsilon(t) \geq 0$  for all  $t$ . An estimate for  $\beta$  is generated by taking the mean fecundity rate from unpublished experiments (pers. comm., Matter). The confidence interval for  $\beta$  as presented in Table 4.1 is calculated assuming a normal distribution for the fecundity rate. The initial number of eggs in year  $\tau$  is the number of eggs produced in year  $\tau - 1$ , or  $E_{\tau-1}(t_f)$ . Here  $t_f$  is the fixed season end date, where  $t_f = 260$  in Julian calendar days (September 16th or 17th). This was fixed as the end date as no butterflies were observed flying after this day. So the number of eggs at the end of the  $(\tau - 1)$ th year gives the number of eggs at the beginning of the  $\tau$ th year. The in-season population dynamics of the model thus produce a number of eggs which act as input to the male and unmated female populations in the next year. Over-winter mortality is presently ignored. This type of model, with continuous-time dynamics for part of the year (the emergence and breeding period, in this case) with repeated discrete changes (linking eggs produced in year  $\tau$  with the initial number of eggs in year  $\tau + 1$ ) has recently been classified as a *semi-discrete model* (Mailleret and Lemesle, 2009). Table 4.1 presents parameter estimates and confidence intervals where known for these parameters. The initial conditions for the above model are  $M_\tau(t_0) = U_\tau(t_0) = R_\tau(t_0) = E_\tau(t_0) = 0$ , where  $t_0$  is egg hatching date used to generate the temperature-dependent adult emergence function. In the simulations presented in this chapter,  $t_0$  is fixed at  $t_0 = 122$  in Julian calendar days (May 1st or 2nd). For notational simplicity the  $\tau$  subscript is hereafter omitted, except where required for clarity.

A brief consideration of the mathematical properties of the model assure existence and uniqueness of solutions, continuous dependence on initial conditions, and positive invariance in the positive state space (i. e., the region where  $M$ ,  $U$ ,  $R$  and  $E$  are all non-negative). As the non-autonomous system is continuous in time and continuously differentiable in state variables  $M$ ,  $U$ ,  $R$ , and  $E$ , the system has a unique solution in some time interval containing the initial time  $t_0$  (Perko, 2000). Further, the same continuity and differentiability conditions ensure that the unique solution depends continuously on  $t$  and (continuous) differentiability on  $M$ ,  $U$ ,  $R$ , and  $E$  (Anosov et al., 1997). Numerical simulations demonstrate that this time interval exceeds the breeding season length  $t_f - t_0$ . To consider positive invariance to the positive state space, the axes are considered as follows: when  $M = 0$ ,  $\frac{dM}{dt} = \theta_M E_\tau \epsilon(t) \geq 0$ ; when  $U = 0$ ,  $\frac{dU}{dt} = \theta_F E_\tau \epsilon(t) \geq 0$ ; when  $R = 0$ ,  $\frac{dR}{dt} = cMU \geq 0$  if  $M \geq 0$  and  $U \geq 0$ ; and finally, when  $E = 0$ ,  $\frac{dE}{dt} = \beta R \geq 0$  if  $R \geq 0$ . Therefore, supposing  $M, U, R, E \geq 0$ , no trajectory can escape the positive state space. The region thus is positively invariant, so no biologically unreasonable solutions (negative population sizes) may occur.

### 4.2.1 Emergence rate functions

The model equations are non-autonomous due to  $\epsilon(t)$ , which is a continuous adult emergence rate function. In this chapter, two functions will be presented as adult emergence rates: first, a simple Gaussian function

$$\epsilon(t) = \frac{A}{\sqrt{2\pi}\sigma} \exp\left(\frac{-(t-t_1)}{2\sigma^2}\right)$$

where  $A$  is the proportion of individuals which survive to adulthood,  $t_1$  is the mean, and  $\sigma^2$  is the variance. The second function is a continuous temperature-dependent emergence

Notation	Units	Estimate	95% CI	Biol. Interpretation	Source
$a_1$	$^{\circ}\text{C}^{-1}$	0.012341	(0.008303, 0.016379)	$a_1(T - 5)$ is the daily transitional success probability out of the first instar at temperature $T$ .	Chapter 3
$a_2$	$^{\circ}\text{C}^{-1}$	0.012341	(0.008303, 0.016379)	$a_2(T - 5)$ is the daily transitional success probability out of the second instar at temperature $T$ .	Chapter 3
$a_3$	$^{\circ}\text{C}^{-1}$	0.012341	(0.008303, 0.016379)	$a_3(T - 5)$ is the daily transitional success probability out of the third instar at temperature $T$ .	Chapter 3
$a_4$	$^{\circ}\text{C}^{-1}$	0.007337	(0.006270, 0.008404)	$a_4(T - 5)$ is the daily transitional success probability out of the fourth instar at temperature $T$ .	Chapter 3
$a_5$	$^{\circ}\text{C}^{-1}$	0.002837	(0.002314, 0.003361)	$a_5(T - 5)$ is the daily transitional success probability out of the fifth instar at temperature $T$ .	Chapter 3
$a_6$	$^{\circ}\text{C}^{-1}$	0.002273	(0.001934, 0.002613)	$a_6(T - 5)$ is the daily transitional success probability from pupation to adulthood at temperature $T$ .	Chapter 3
$d$	dimensionless	0.019807	(0.009127, 0.054254)	Daily probability of mortality.	Chapter 3
$\theta_M, \theta_F$	dimensionless	0.5	–	Proportion of eggs which are male and female, respectively.	(Calabrese et al., 2008)
$\gamma_M$	$(\text{day})^{-1}$	0.0714	–	Death rate for male adults.	–
$\gamma_F$	$(\text{day})^{-1}$	0.1	–	Death rate for female adults.	(Matter et al., 2009), (pers. comm., Matter)
$c$	$(\text{day})^{-1}$	0.061	–	Mating rate for adults.	(Calabrese et al., 2008)
$\beta$	$(\text{mated females} \cdot \text{day})^{-1}$	3.176	(2.317, 4.035)	Number of eggs produced per day per mated female.	(pers. comm., Matter)

Table 4.1: Summary of parameters for adult emergence model (3.9)-(3.12) and reproductive success model (4.1). Transitional success probability functions are expressed  $a_i(T - 5)$  due to prior fixing of  $T_0 = 5^{\circ}\text{C}$  as the lower temperature threshold for development.

rate analogous to the temperature-dependent adult emergence probability distribution derived in the previous chapter. Given that the previous discrete function is numerically generated as a set of daily emergence probabilities, the continuous analogue  $\epsilon(t)$  is produced by linear interpolation between successive days' emergence probabilities. Figure 4.1 shows two sample emergence functions, the first a Gaussian function and the second a temperature-dependent function.

The purpose of presenting two emergence functions is as follows: the Gaussian is simpler than the temperature-dependent function, and thus it is simpler to see how population dynamics and egg production are influenced by varying its parameters. The tractable and closed form of the function approximates the emergence shape of the more complicated temperature-dependent function, and furthermore, the parameters which influence egg production,  $A$  and  $\sigma$ , have analogous parameters which generate the temperature-dependent emergence function: daily temperature  $T_i$  and mortality probability  $d$ , respectively.

The parameter  $A$  of the Gaussian function gives the total emergence over all time (the proportion of individuals which successfully emerge),

$$A = \int_{-\infty}^{\infty} \epsilon(t) dt,$$

so increasing  $A$  increases the total emergence within a season. Total emergence proportion in the temperature-dependent function can be increased by several mechanisms: first, due to the linear dependence of transitional probability on temperature and fixed death probability, an increased daily temperature would increase emergence as individuals would move through the larval instars more quickly, having less opportunity to die. Second, decreasing the constant mortality probability would also increase emergence, as individuals would have a higher probability of surviving to adulthood. Thus, either an increase in temperature or a decrease in mortality probability in the temperature-dependent function should generate qualitatively similar dynamics to those generated by an increasing  $A$  in the Gaussian function. An increase to the slopes of the linear transitional probability functions ( $a_i, i = 1 \dots 6$ ) in the temperature-dependent case would also generate similar dynamics, though these are not considered here, as the slope estimates of the previous chapter have considerably smaller confidence intervals than the mortality probability, so there is a larger interval in which mortality can be varied to produce different dynamics that remain within the range of confidence.

The standard deviation  $\sigma$  is a measure of the width of the emergence distribution in the Gaussian function and also influences reproductive success. In the temperature-dependent function, standard deviation can be calculated by

$$\sqrt{\int_{t_i}^{t_f} k^2 \tilde{\epsilon}(k) dk - \left( \int_{t_i}^{t_f} k \tilde{\epsilon}(k) dk \right)^2},$$

where

$$\tilde{\epsilon}(k) = \frac{\epsilon(k)}{\int_{t_i}^{t_f} \epsilon(k) dk}$$

(since  $\int_{t_i}^{t_f} \epsilon(k) dk < 1$  in a system with larval mortality, so normalization is necessary to produce a probability distribution). Here  $t_i$  is the first day of non-zero emergence rate and  $t_f$  is the previously defined end of the season. An increase in the mortality probability  $d$  increases the standard deviation in the temperature-dependent  $\epsilon(t)$  for a range of  $d$ , as will be demonstrated in Section 4.3, so an

increase to  $d$  is analogous to an increase in  $\sigma$  in the Gaussian function. It should be noted that the relationship between  $d$  and standard deviation in  $\epsilon(t)$  is roughly parabolic, as will be later demonstrated, but for simplicity,  $d$  in the results is restricted to values in which a positive relationship between  $d$  and standard deviation exists.

The second benefit of the Gaussian emergence function, apart from its simplicity, is that the total emergence  $A$  and the width of the emergence  $\sigma$  can be varied independently to consider independent effects of each on egg production. The temperature-dependent emergence function is incapable of easily separating such effects. For instance, when the mortality probability  $d$  is decreased, the total emergence increases and the standard deviation decreases: these effects are simultaneous. The Gaussian emergence function is thus more useful for considering independent effects, but the use of the temperature-dependent function is more biologically realistic in the present study, as the current objective is to determine effects of temperature-forcing on seasonal dynamics in *P. smintheus*. Because the interest of the present study lies in the qualitative similarities in reproductive success effects which occur when parameters in each emergence function are varied, no attempt is made to fit the Gaussian function to the temperature-dependent function. The final section of the results will discuss a potential mechanism by which spring and summer temperatures force these population fluctuations.

#### 4.2.2 Error propagation

Error in the total number of eggs produced in a given year propagates through the model from the error in the individual parameters. This accumulated error, if large enough, can reduce the predictive value of the model for reproductive success. If enough error accumulates from the individual parameter uncertainty, the error in egg production in a given year may encompass the reproductive success threshold ( $\frac{E_{\tau+1}}{E_{\tau}} = 1$ ), which indicates the model may falsely indicate reproductive success or failure.

The method by which error is determined is similar to that presented in the previous chapter, where total error in adult emergence probabilities was calculated using the individual errors of the parameters in the temperature-dependent developmental model. In this case, the error is propagated still further, as the adult emergence model is used as input to predict a temperature-dependent number of eggs produced in a seasonal breeding period. For a given parameter  $x$ , the error contributed to  $E_{\tau+1}$  is  $\left(\frac{\partial E_{\tau+1}}{\partial x} \delta x\right)^2$  where  $\delta x$  is the error associated with the individual parameter  $x$ . The error contributions of all the individual parameters are summed in quadrature (Taylor, 1997), so that

$$\delta E_{\tau+1} = \sqrt{\sum_{i=1}^6 \left(\frac{\partial E_{\tau+1}}{\partial a_i} \delta a_i\right)^2 + \left(\frac{\partial E_{\tau+1}}{\partial d} \delta d\right)^2 + \left(\frac{\partial E_{\tau+1}}{\partial \beta} \delta \beta\right)^2}.$$

The errors associated with  $\theta_M$ ,  $\theta_F$ ,  $\gamma_M$ ,  $\gamma_F$ , and  $c$  are unknown (pers. comm., Calabrese) so they are neglected in this sum, though it should be noted that their absence makes the total error  $\delta E_{\tau+1}$  smaller.

Derivatives in error terms  $\frac{\partial E_{\tau+1}}{\partial x}$  are computed numerically using a forward difference scheme.

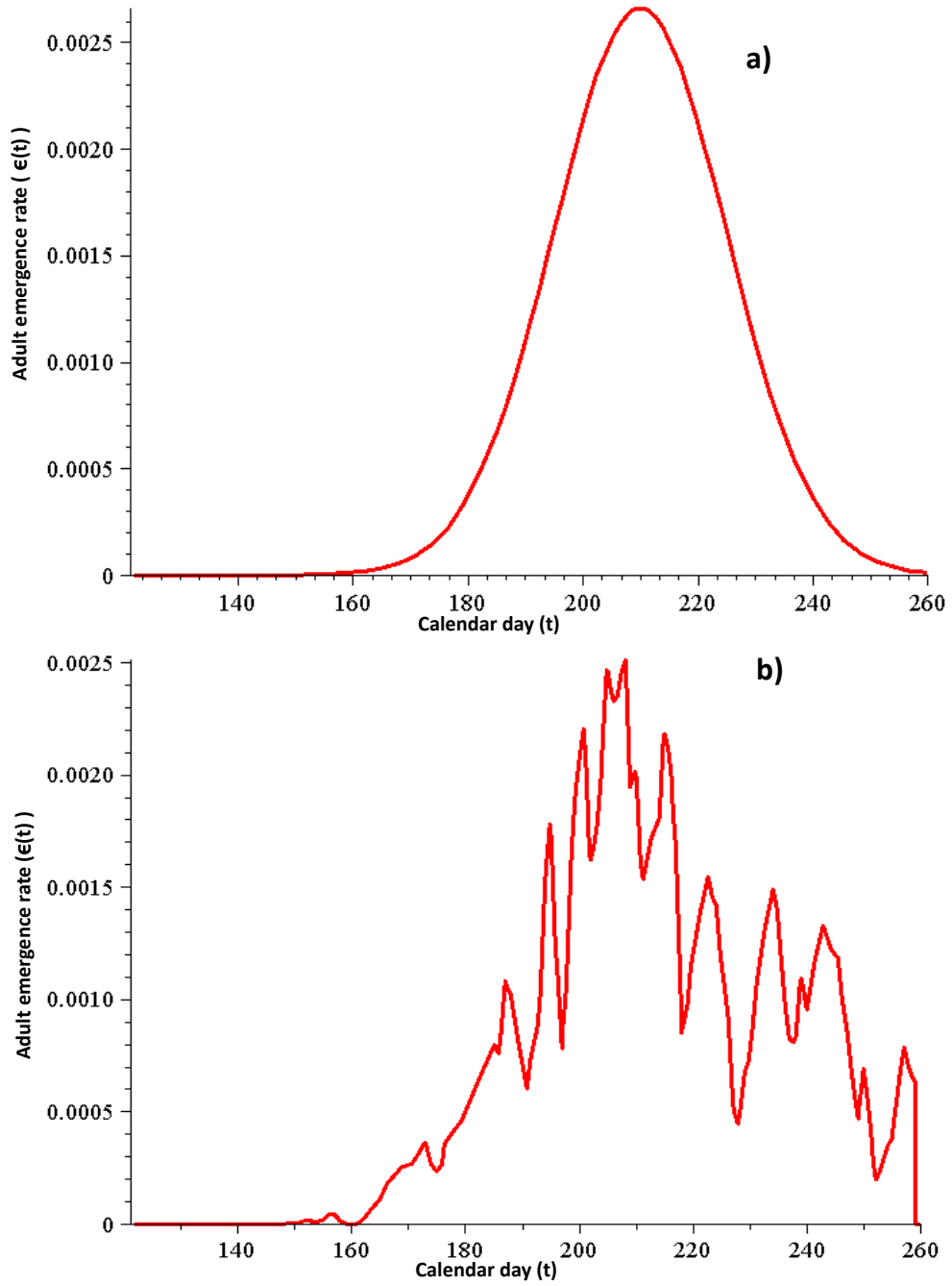


Figure 4.1: Sample adult emergence functions  $\epsilon(t)$ : a) Gaussian emergence function with  $A = 0.1$ ,  $\sigma = 15$ , and  $t_1 = 210$ . b) Temperature-dependent emergence function generated from 2009 temperature data, using parameter values in Table 4.1.

## 4.3 Results

In the following section, the effects on egg production of varying parameters in both the Gaussian emergence function and the temperature-dependent emergence function are presented. Egg production in year  $\tau$  is denoted by  $E_\tau$ , and reproductive success from year  $\tau$  to year  $\tau + 1$  is denoted by the ratio of eggs produced in these successive years,  $\frac{E_{\tau+1}}{E_\tau}$ . The year  $\tau$  is called reproductively successful if  $\frac{E_{\tau+1}}{E_\tau} > 1$ , so that more eggs are produced for the next year than existed at the beginning of the year. The number of eggs  $E_{\tau+1}$  is generated by numerically solving the equations in (4.1) and thus determining the number of eggs at the end of a season. As the initial number of eggs in a season  $E_\tau$  is unknown, the plots are generated to compare  $\frac{E_{\tau+1}}{E_\tau}$  against  $E_\tau$  with varying parameter values. Such plots graphically indicate the initial number of eggs  $E_\tau$  required to surpass the reproductive success ratio, if such reproductive success is indeed possible. They may also indicate the presence of an Allee effect at low initial numbers of eggs. Further, in the temperature-dependent case, the errors associated with each parameter are propagated through the model to determine which parameter generates the most error in  $E_{\tau+1}$ , and if within the given parameter ranges, any quantitative predictions concerning year-to-year population dynamics can be made. All numerical calculations were completed using the numerical solver *dsolve* in Maple12™ (Monagan et al., 2005). Associated figures were also completed using Maple12™.

### 4.3.1 Gaussian emergence function

Reproductive success ratios  $\frac{E_{\tau+1}}{E_\tau}$  in year  $\tau$  are calculated against initial number of eggs  $E_\tau$ , for varying  $A$  (Figure 4.2a) and  $\sigma$  (Figure 4.2b). For all fixed parameter values, reproductive success ratios increase at low egg numbers before levelling off at higher egg numbers (a demographic Allee effect). An increase in  $A$  increases the reproductive success ratio when other parameter values are fixed, and in the case of standard deviation  $\sigma$ , the reproductive success ratio decreases with increasing  $\sigma$ . For the values of both parameters, initial number of eggs  $E_\tau$  is important: in the varying  $A$  case,  $A = 0.07$  is large enough that the population crosses the reproductive success threshold, except where  $E_\tau$  is very small. In the varying  $\sigma$  case, the initial  $E_\tau$  required for the population to cross the reproductive success threshold increases with increasing  $\sigma$ : for  $\sigma = 25$  days, approximately  $E_\tau = 2400$  eggs are required to cross the threshold, while for  $\sigma = 35$  days, approximately  $E_\tau = 7000$  eggs are required. For  $\sigma = 45$  days, reproductive failure results independent of the initial number of eggs. The model therefore predicts that both low total emergence and high standard deviation in adult emergence may aggravate an Allee effect, inducing reproductive failure at higher initial numbers of eggs.

### 4.3.2 Temperature-dependent emergence function

In the temperature-dependent case, the error associated with each parameter value (when known) is presented in Table 4.2, for each year of temperature data, given  $E_\tau = 10^4$ . These errors  $\left(\frac{\partial E_{\tau+1}}{\partial x} \delta x\right)^2$  are presented as they contribute to the error in the total eggs produced in a given year, to indicate the magnitude of the contribution with respect to other parameters. In each year, similar patterns occur as to the magnitude of the errors associated with each parameter. Within each year, the errors contributed by  $a_1$ ,  $a_2$  and  $a_3$  are very similar in magnitude, while the error contributed by  $a_4$  is the smallest. The error contributed by  $a_5$  is the largest of that contributed by the  $a_i$  parameters, and

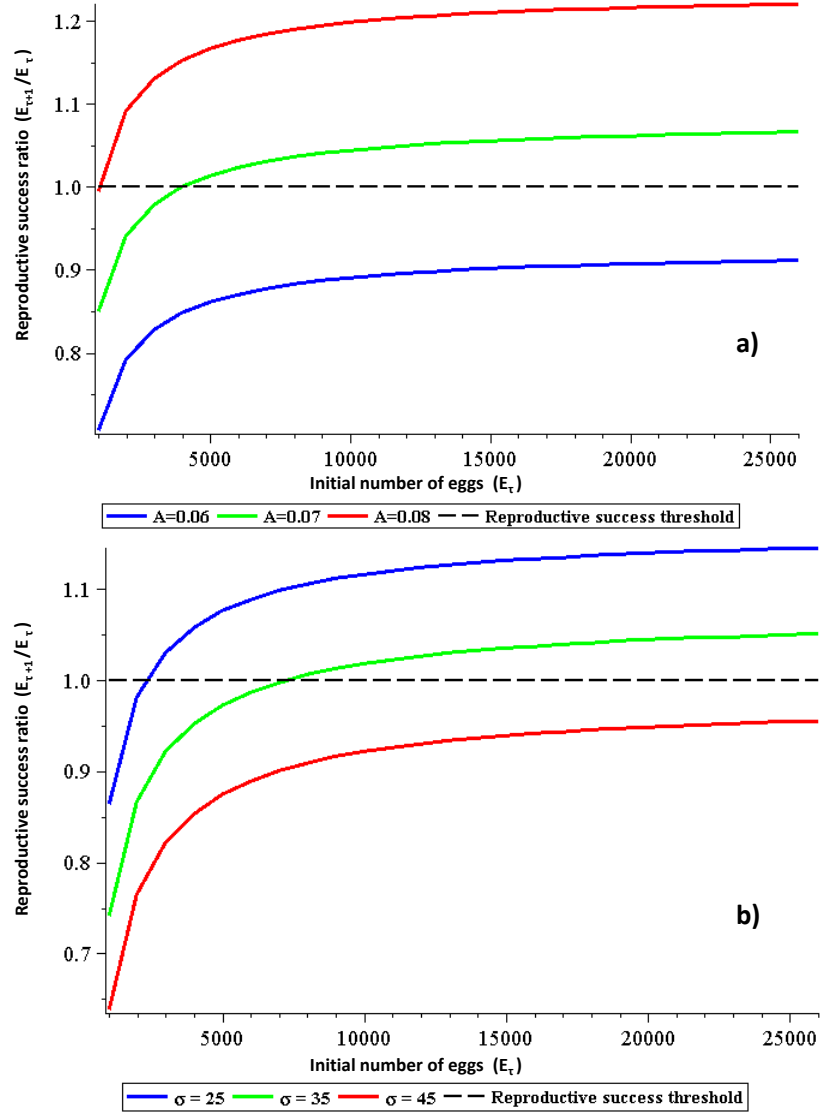


Figure 4.2: Reproductive success ratios in year  $\tau$  with respect to initial number of eggs, using a Gaussian emergence function. The reproductive success threshold is denoted by the dashed line. a) Varying the total emergence  $A$  in the Gaussian emergence function demonstrates an increase in reproductive success with increasing  $A$ . Sample reproductive success curves represent guaranteed reproductive failure (blue curve), reproductive success at a given threshold  $E_\tau$  (green curve), and guaranteed reproductive success at all but very low initial numbers of eggs (red curve), given  $A = 0.06, 0.07,$  and  $0.08$ , respectively. Other parameter values are fixed at  $t_1 = 210$  and  $\sigma = 20$ . b) Varying standard deviation  $\sigma$  in the Gaussian emergence function demonstrates a decrease in reproductive success with increasing  $\sigma$ . Sample reproductive success curves represent guaranteed reproductive failure (red curve), reproductive success at a given threshold  $E_\tau$  (green curve), and guaranteed reproductive success except at very low initial egg numbers (blue curve). Other parameter values are fixed at  $t_1 = 210$  and  $A = 0.08$ .

$a_6$  falls between  $a_{1,2,3}$  and  $a_5$ . The error contributed by  $d$  is at least a full order of magnitude larger than any other contribution, and the error contributed by  $\beta$  is the second largest at a full order of magnitude higher than that contributed by  $a_5$ .

These results suggest that given the present magnitude of error in the system, no quantitative predictions can be made from year-to-year, as the error range in the number of eggs includes the reproductive success ratio in all years except 2005 (Figure 4.3). That is, if the model predicts an increase in population size, a decrease in population size is within the bounds of the error on the parameter values, and *vice versa*. Further, the error  $\delta E_{\tau+1} > E_{\tau+1}$  in all years, suggesting that the error is considerable enough that biologically unreasonable results may occur (where  $E_{\tau+1} < 0$  within the error bounds).

$\left(\frac{\partial E_{\tau+1}}{\partial x} \delta x\right)^2$	2001	2003	2004	2005
$a_1$	$3.014 \times 10^5$	$3.595 \times 10^5$	$2.779 \times 10^5$	$2.040 \times 10^5$
$a_2$	$3.013 \times 10^5$	$3.596 \times 10^5$	$2.779 \times 10^5$	$2.042 \times 10^5$
$a_3$	$3.015 \times 10^5$	$3.594 \times 10^5$	$2.778 \times 10^5$	$2.040 \times 10^5$
$a_4$	$1.256 \times 10^5$	$1.606 \times 10^5$	$1.147 \times 10^5$	$8.043 \times 10^4$
$a_5$	$5.368 \times 10^5$	$8.059 \times 10^5$	$4.745 \times 10^5$	$3.052 \times 10^5$
$a_6$	$4.109 \times 10^5$	$6.383 \times 10^5$	$3.605 \times 10^5$	$2.282 \times 10^5$
$d$	<b><math>5.122 \times 10^7</math></b>	<b><math>1.080 \times 10^8</math></b>	<b><math>4.089 \times 10^7</math></b>	<b><math>2.348 \times 10^7</math></b>
$\beta$	<b><math>3.769 \times 10^6</math></b>	<b><math>7.852 \times 10^6</math></b>	<b><math>4.089 \times 10^6</math></b>	<b><math>1.525 \times 10^6</math></b>
$E_{\tau+1}$	7051	10419	6354	4660
$\delta E_{\tau+1}$	7547	10889	6750	5122
$\left(\frac{\partial E_{\tau+1}}{\partial x} \delta x\right)^2$	2006	2007	2008	2009
$a_1$	$5.354 \times 10^5$	$4.416 \times 10^5$	$2.710 \times 10^5$	$2.593 \times 10^5$
$a_2$	$5.357 \times 10^5$	$4.415 \times 10^5$	$2.711 \times 10^5$	$2.591 \times 10^5$
$a_3$	$5.354 \times 10^5$	$4.414 \times 10^5$	$2.709 \times 10^5$	$2.590 \times 10^5$
$a_4$	$2.350 \times 10^5$	$1.922 \times 10^5$	$1.090 \times 10^5$	$1.070 \times 10^5$
$a_5$	$1.135 \times 10^6$	$8.925 \times 10^5$	$4.315 \times 10^5$	$4.474 \times 10^5$
$a_6$	$8.926 \times 10^5$	$6.941 \times 10^5$	$3.252 \times 10^5$	$3.409 \times 10^5$
$d$	<b><math>1.211 \times 10^8</math></b>	<b><math>8.621 \times 10^7</math></b>	<b><math>3.381 \times 10^7</math></b>	<b><math>4.264 \times 10^7</math></b>
$\beta$	<b><math>1.042 \times 10^7</math></b>	<b><math>7.078 \times 10^6</math></b>	<b><math>2.477 \times 10^6</math></b>	<b><math>2.950 \times 10^6</math></b>
$E_{\tau+1}$	11996	9909	5819	6254
$\delta E_{\tau+1}$	11635	9818	6161	6875

Table 4.2: Error in total number of eggs produced in year  $\tau$ ,  $\delta E_{\tau+1}$ , as contributed by each parameter, for  $\tau = 2001, 2003, \dots, 2009$ , given initial number of eggs  $E_\tau = 10^4$ . Parameter values  $x$  and associated error  $\delta x$  are as presented in Table 4.1. Larval mortality probability  $d$  and fecundity rate  $\beta$  contribute the most error each year to the total error, denoted in bold in the table.

Next, the positive relationships between daytime temperature experienced by larvae ( $T_n$ ) and total adult emergence ( $\int_t \epsilon(t)$ ) and standard deviations are demonstrated. For the following simulations, 2009 temperature data was used, though similar patterns hold for all years.

In the simulations presented in Figure 4.4, daily temperatures are varied within a  $6^\circ\text{C}$  range of the actual 2009 daytime temperatures, up to  $3^\circ\text{C}$  above the daily temperature to  $3^\circ\text{C}$  below the daily temperature. Emergence functions are presented for the observed 2009 temperatures, as well as the two extremes, in Figure 4.4a, while in Figure 4.4b, the positive relationship between temperature and total emergence is demonstrated. The effect of temperature on standard deviation is also positive, however (Figure 4.5a).

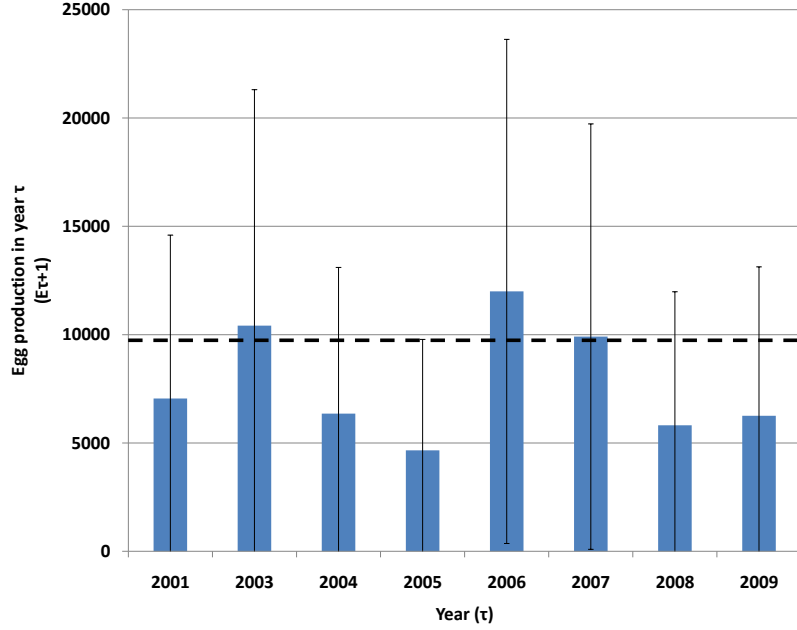


Figure 4.3: Predicted number of eggs  $E_{\tau+1}$  (wide bars) each year given initial  $E_{\tau} = 10^4$ , with associated error  $\delta E_{\tau+1}$  denoted by bars. Error values are taken from Table 4.2. Parameter values used are as presented in Table 4.1. The reproductive success threshold is denoted by the dashed line.

Increased temperatures, as previously discussed in Chapter 3, prompt earlier peak emergence and higher overall survivorship. Similar dynamics to those in Figure 4.2a are thus expected, if the increasing standard deviation does not negate the effects of higher total emergence. In the Gaussian case, increasing total emergence and increasing standard deviation have opposite effects, but in the temperature-dependent case, the temperature effects are stronger, as Figure 4.7a demonstrates a positive relationship between temperature and reproductive success. An increase in temperature also decreases the initial number of eggs necessary for reproductive success. In 2009, the model predicts that the population will decrease in size (blue curve, Figure 4.7a), but an increase per day of  $2.0^{\circ}\text{C}$  would allow the population to surpass the reproductive success threshold at all but small initial egg numbers (red curve, Figure 4.7a).

Next, the negative relationship between larval mortality probability ( $d$ ) and total adult emergence, as well as the positive relationship between  $d$  and standard deviation are demonstrated. In the following simulations, the daily mortality probability  $d$  is varied from its estimated value of  $d = 0.01981$  between 0.009127 and 0.05425 (the lower and upper bounds of its confidence interval). Figure 4.6a presents adult emergence functions using the estimated  $d = 0.01981$  (green curve) as well as  $d = 0.009127$  and 0.05425, (red and blue curves, respectively). Figure 4.6b demonstrates the negative relationship between  $d$  and total emergence.

Further, for small values of  $d$ , the standard deviation of  $\epsilon(t)$  increases with  $d$  (Figure 4.5b). Higher values which demonstrate the opposite relationship are not considered in subsequent simulations because in this region, total adult emergence is negligible (Figure 4.6b).

The negative relationship of  $d$  with total emergence  $\int \epsilon(t)dt$  (Figure 4.6b) and the positive relationship of  $d$  with the emergence function's standard deviation (Figure 4.5b) lead to two conclusions.

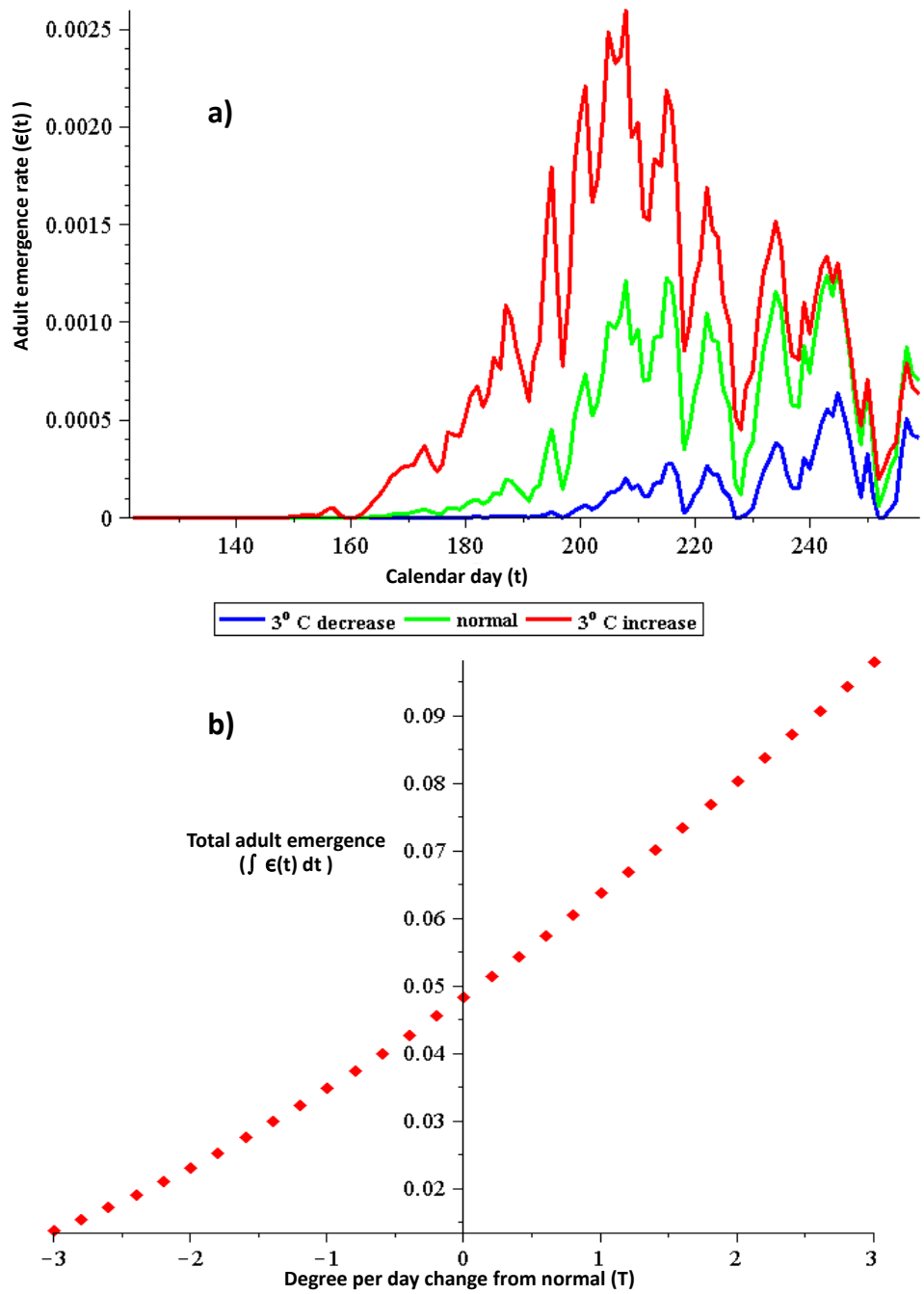


Figure 4.4: Effects of daily temperature change (experienced by larvae) on overall adult emergence, using parameter values presented in Table 4.1. a) Adult emergence function  $\epsilon(t)$  (green curve) changes when 2009 daily temperature values are decreased and increased by  $3^\circ\text{C}$  (blue and red curves, respectively). b) The positive relationship between temperature and total adult emergence.

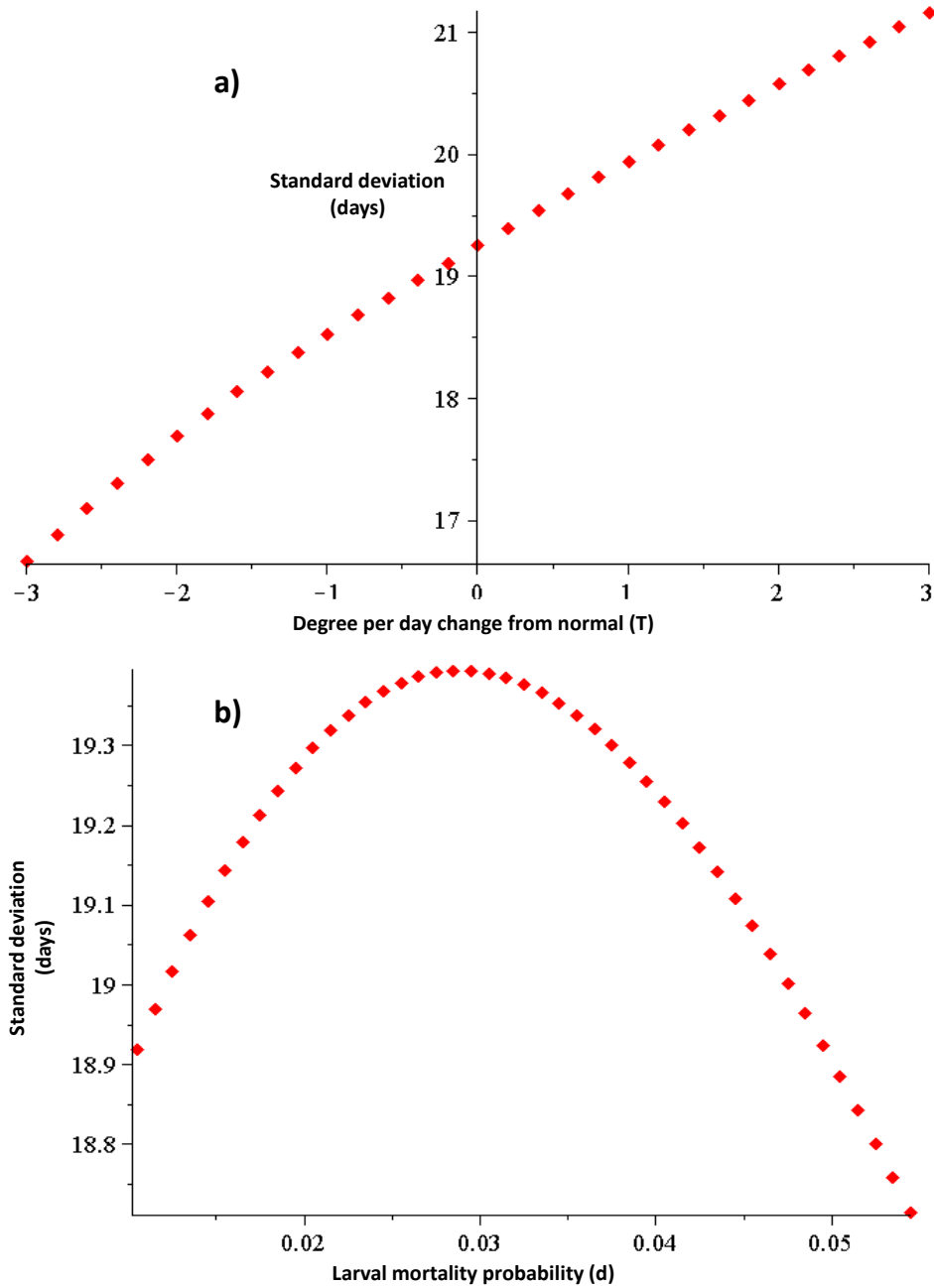


Figure 4.5: Effects on standard deviation of temperature-dependent emergence function, due to varying parameter  $d$  and varying input  $T$ . a) Positive relationship of temperature and standard deviation of emergence function. b) Within 95% confidence interval for  $d$ , a roughly quadratic relationship with standard deviation is observed.

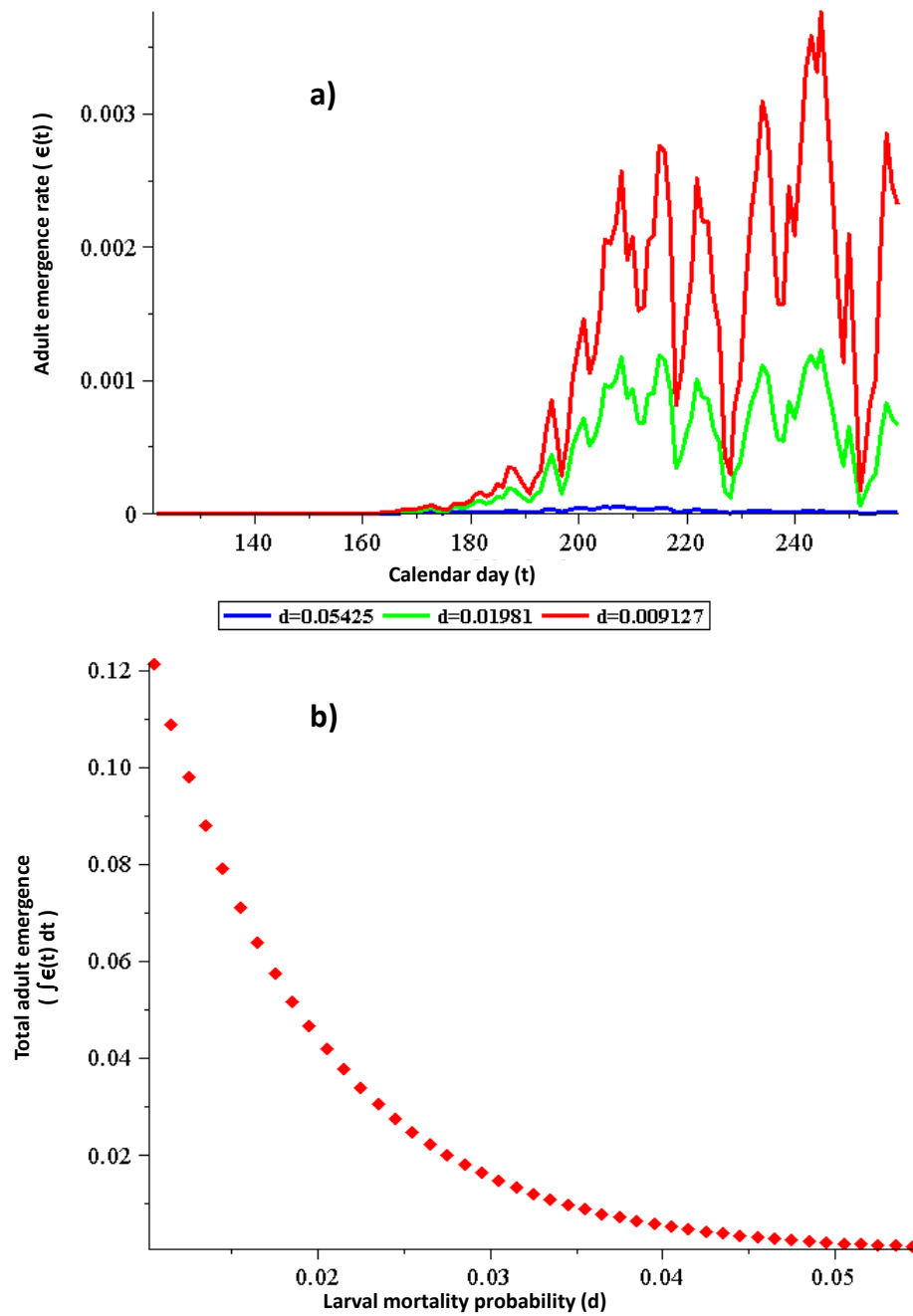


Figure 4.6: Effects of varying larval mortality probability  $d$  on overall adult emergence, using parameter values presented in Table 4.1. a) Adult emergence function  $\epsilon(t)$  (green curve) changes when mortality probabilities are decreased and increased to the extrema of the estimate's 95% confidence interval (red and blue curves, respectively). b) The negative relationship between larval mortality and total adult emergence.

Decreasing  $d$  will have a similar effect on reproductive success as increasing  $A$  or decreasing  $\sigma$  in the Gaussian emergence function model. Figure 4.7b supports these conclusions, as decreasing  $d$  increases the reproductive success ratio: similar qualitative effects were seen in increasing  $A$  (Figure 4.2a) and decreasing  $\sigma$  (Figure 4.2b). Decreasing temperature and increasing larval mortality also aggravates the predicted demographic Allee effect.

### 4.3.3 Effects of temperature on multi-year population dynamics

Population size in *P. smintheus* has fluctuated considerably in the last ten years of mark-recapture field experiments (pers. comm., Roland). Figure 4.8 illustrates the apparent instability in the population size. Examining the predicted effects of temperature on adult reproductive success (Figure 4.7a), the model indicates that the fluctuations in population size are driven by yearly climatic variations, so that the population has no stable non-zero equilibrium size but instead is forced above or below the reproductive success threshold by environmental conditions as experienced by larvae. Figure 4.9 illustrates how year-to-year dynamics might play out in a temperature-forced system. The “cooler” year temperature regime is taken from 2009 temperature data, and the “warmer” regime shifts the mean daytime temperatures from 2009 up by 2°C. In Year 1, an initial number of eggs  $E_1 = 10^4$  is used, and supposing a cooler year, reproductive failure occurs, with a reproductive success ratio of  $\frac{E_2}{E_1} = 0.71$ . That is, only 71% of the initial number of eggs are produced in the breeding season, which, neglecting overwinter mortality, gives  $E_2 = 7100$  at the beginning of Year 2, since

$$E_2 = E_1 \left( \frac{E_2}{E_1} \right) = 10000(0.71) = 7100.$$

Supposing another cool year, reproductive failure again occurs, with  $\frac{E_3}{E_2} = 0.70$ . Note that even assuming an identical temperature regime, the lower initial number of eggs in Year 2 results in a lower reproductive success ratio than in Year 1, indicating the importance of initial population size to reproductive success. The initial number of eggs in Year 3 is therefore  $E_3 = 4970$ . Supposing a warm year, reproductive success occurs, with  $\frac{E_4}{E_3} = 1.18$ , giving the initial number of eggs in Year 4 to be  $E_4 = 5865$ , denoted by the star in Figure 4.9.

Using this simple example of year-to-year population dynamics, the egg population size in a three year period generated in Figure 4.9 is qualitatively similar to the observed population size in adults for 2001 – 2004 as shown in Figure 4.8: a decrease, a decrease, and an increase in population size. This simple example demonstrates how yearly temperature variability could cause fluctuating population sizes similar to those observed for *P. smintheus* in the field.

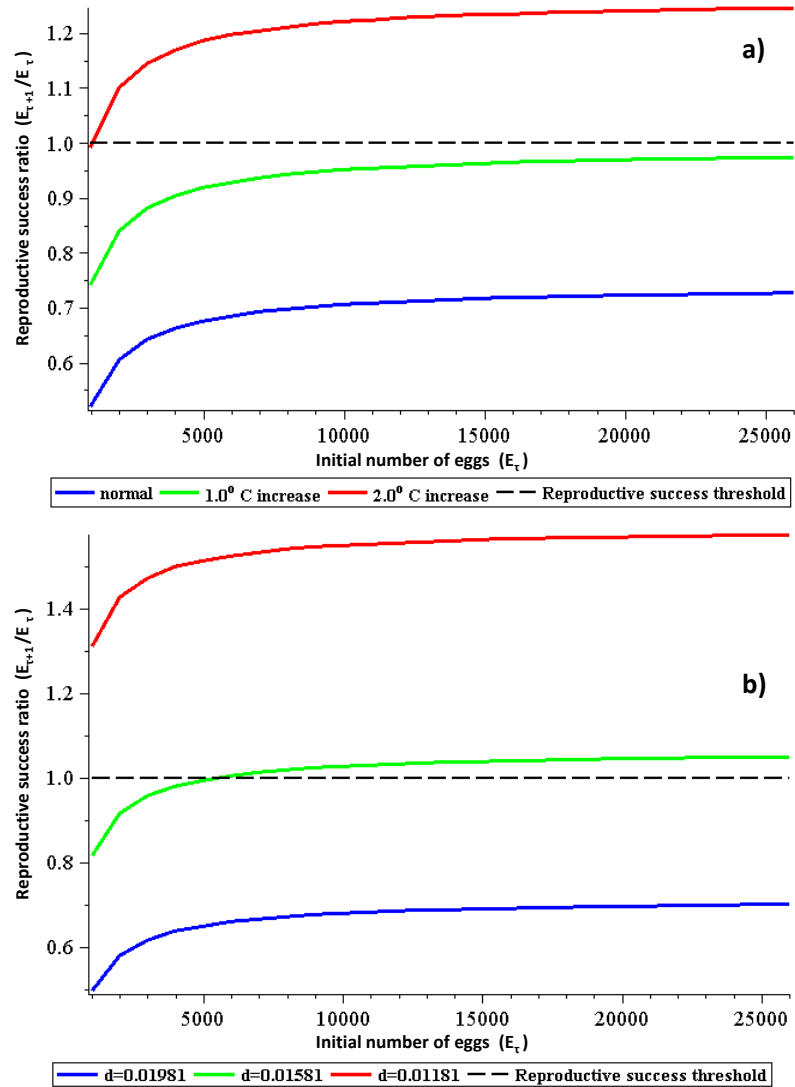


Figure 4.7: Reproductive success ratios in year  $\tau$  with respect to the initial number of eggs, using a temperature-dependent emergence function with 2009 temperature data as input. The reproductive success threshold is denoted by the dashed line. a) Increasing daily temperature input to the temperature-dependent emergence function demonstrates an increase in reproductive success. The reproductive success model predicts reproductive failure in 2009 with the observed temperature regime (blue curve), reproductive failure with a 1.0°C degree increase in daily temperature (green curve), and reproductive success at all but very low initial egg numbers with a 2.0°C degree increase in daily temperature (red curve). b) Decreasing larval mortality probability  $d$  increases reproductive success. The reproductive success model predicts reproductive failure in 2009 with maximum likelihood estimate  $\hat{d} = 0.01981$  (blue curve). Decreasing  $d = 0.01581$  allows reproductive success at a threshold  $E_\tau$  (green curve), and  $d = 0.01181$  allows guaranteed reproductive success at all but very low initial egg numbers (red curve).

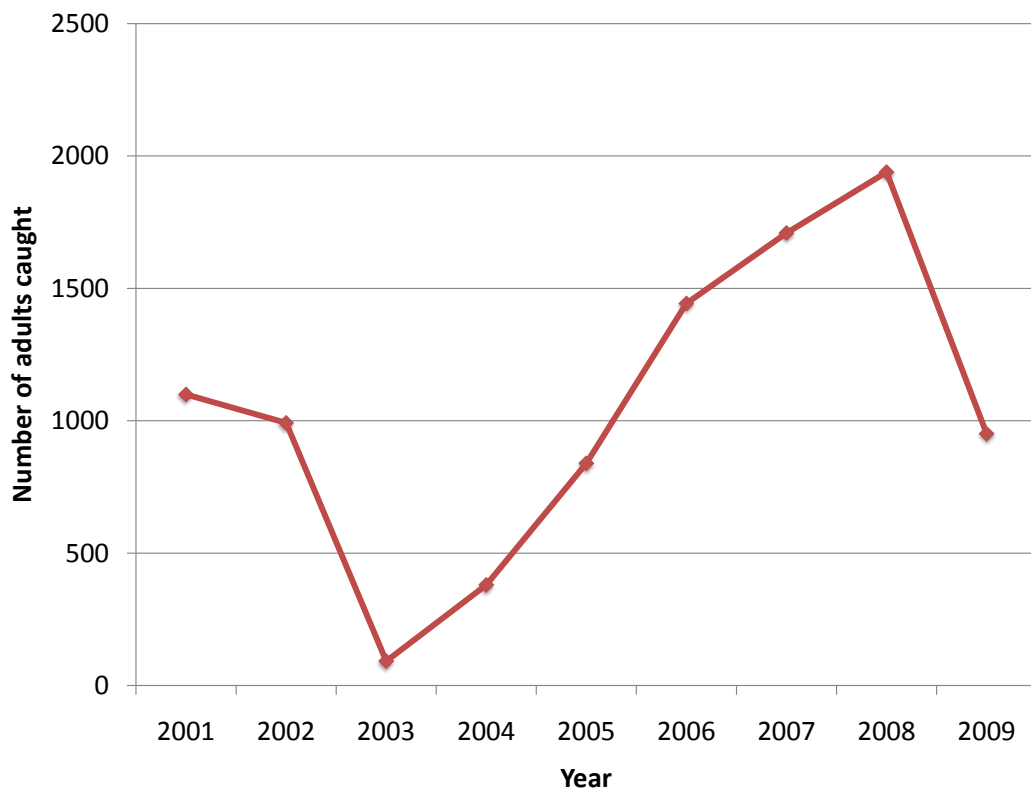


Figure 4.8: Fluctuations in captured adult population sizes from 2001 – 2009, taken from mark-recapture data for new adult captures. The time series exhibits a large amount of variability over a ten year period.

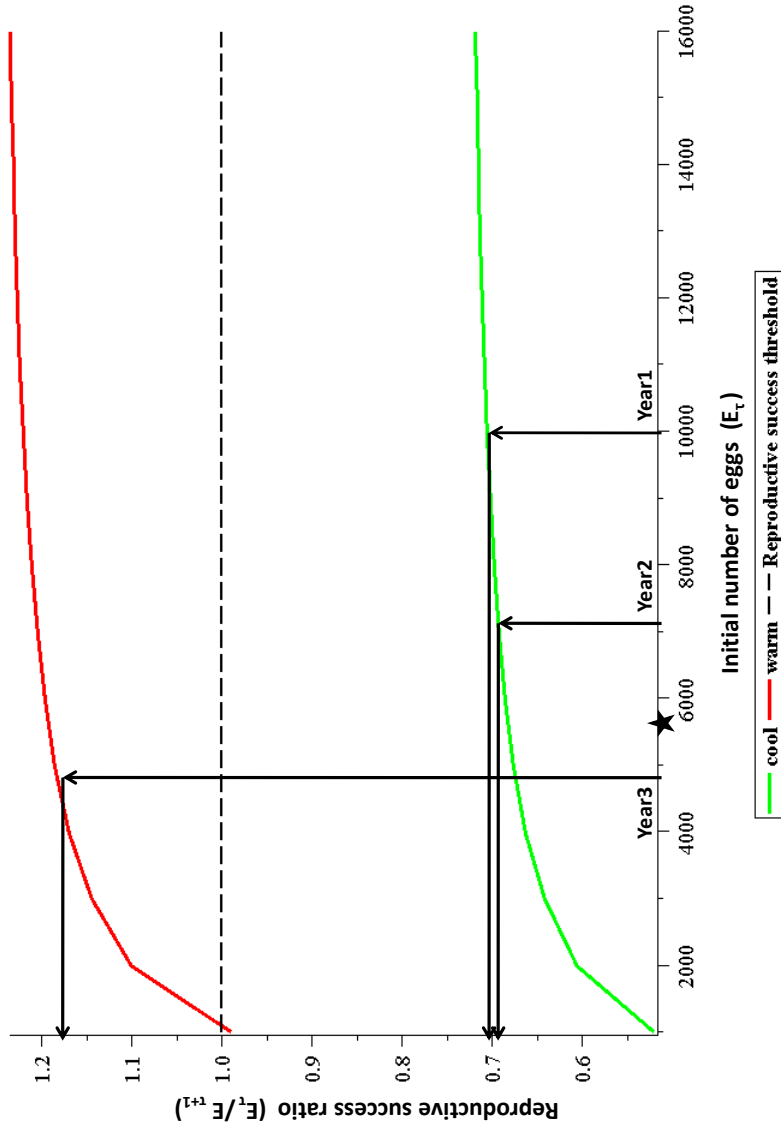


Figure 4.9: Simulated change in population size over a three year period where temperature-forcing drives reproductive success. Potential overwinter mortality is neglected. An initial number of eggs in Year 1,  $E_1 = 10^4$  produces 0.71 times its initial number, given a “cooler” year (green curve). The population of eggs in Year 2 correspondingly decreases to  $E_2 = 7100$ . Another cool year prompts 0.70 times the initial number of eggs to give  $E_3 = 4970$  for Year 3. If Year 3 is “warmer” (red curve), the reproductive success threshold (denoted by the dashed line) is surpassed and 1.18 times the initial number of eggs is produced, giving  $E_4 = 5865$  for the start of Year 4, denoted by the star.

## 4.4 Discussion

Reproductive success in adult *P. smintheus* butterflies is considered where adult emergence is controlled by two different functions, an analytic Gaussian function and a numerically computed temperature-dependent function. Simulations using each emergence function give qualitatively similar behaviours. Reproductive success, measured by  $\frac{E_{\tau+1}}{E_{\tau}}$ , increases when total emergence increases (controlled directly by  $A$  for the Gaussian case and by an increase in temperature or a decrease in larval mortality for the temperature-dependent case). Reproductive success decreases when standard deviation in the emergence function increases (controlled directly by  $\sigma$  in the Gaussian case and by increased larval mortality in the temperature-dependent case). Further, an analysis of the error contribution by each parameter in the temperature-dependent model leads to the conclusion that in its present state, the model is not suitable for quantitative predictions using 2001 – 2009 mark-recapture data for validation, as the reproductive success threshold falls within the bounds of the error in all years except 2005. Further experimental work is likely necessary to decrease the confidence intervals on the component parameters of the model. Finally, a potential mechanism for observed fluctuations in adult population size is proposed: yearly variability between spring and summer temperatures may influence changes in egg production, where warmer years force egg production over the reproductive success threshold and colder years fail to do so.

### 4.4.1 Comparing results of emergence functions

Both the Gaussian and temperature-dependent emergence functions yield qualitatively similar results when used as input in the reproductive success model. The Gaussian model is useful for independently considering the effects of varying total emergence and standard deviation, as it is difficult to decouple these parameters in the temperature dependent case. This is important in the case of increasing temperatures: while increasing temperatures increase overall emergence in the temperature-dependent emergence function (Figure 4.4b), they also increase the standard deviation (Figure 4.5a). The Gaussian model shows opposing effects of increasing total emergence and increasing standard deviation, as reproductive success increases with total emergence and decreases with standard deviation. While these opposing effects may not be easily separated in the temperature-dependent case, one may conclude that the effects of total emergence are stronger, as a positive relationship between temperature and reproductive success is observed in the temperature-dependent model (Figure 4.7a). Still, the effect of standard deviation is lost in the temperature-dependent model but captured in the Gaussian model.

From a biological standpoint, a decreasing standard deviation means a briefer period of highly synchronized emergence among individuals in a population (Calabrese and Fagan, 2004). Iwasa and Levin (1995) and Post et al. (2001) proposed that asynchrony (higher standard deviations in emergence) increases in cases of environmental perturbation, though their results are not specific to insects. Further, Yurk and Powell (2009) suggested that developmental synchrony is temperature-dependent and that insects lose synchrony outside a narrow range of temperatures. Thus it may be reasonable to expect greater asynchrony in populations faced with warming temperatures, so an increasing standard deviation in adult emergence at higher temperatures in the present model may be biologically realistic. This argument, however, is sensitive to the functional form of temperature-dependent larval development. While Yurk and Powell (2009) suggested a narrow range of tem-

peratures at which emergence synchrony occurs, the assumed linear, increasing relationship of temperature with larval transition success suggests that standard deviation in adult emergence will increase strictly with temperature. That is, there is no cooler temperature regime, according to this model, where synchronous emergence will shift towards asynchronous emergence. The increasing relationship of temperature and standard deviation is illustrated in a 6°C range in Figure 4.5a.

The effects of decreasing larval mortality on reproductive success are unsurprising, as decreasing  $d$  is analogous to an increase in total emergence and a decrease in standard deviation.

Simple emergence functions such as stretched Beta distributions (Calabrese and Fagan, 2004) and Gamma distributions (Calabrese et al., 2008) have previously been used in reproductive success models. These were not chosen for biological reasons, unlike the temperature-dependent emergence function as used in the present study. Ultimately, however, it is reassuring that both the simple Gaussian and more complex temperature-dependent emergence functions demonstrate qualitatively similar dynamics when considering reproductive success.

#### 4.4.2 Toward quantitative predictions

The larval mortality parameter  $d$  is the most problematic to the reproductive success model as it contributes the most error to the model output (egg production in a given year). Table 4.2 presents the contributions of each parameter to  $\delta E_{\tau+1}$ , and the error associated with  $d$  is at least a full order of magnitude larger than that of any other parameter. Furthermore, the reproductive success model suggests that larval mortality may be overestimated in the current model, as in only 2003 and 2006 does the model presently predict increases in population size from year-to-year (Table 4.2) while the mark-recapture data suggests population size increases in 2003 through 2007 (Figure 4.8). Such unexpected decreases in the model predictions could also be due to an underestimated fecundity rate  $\beta$ , which has the second highest contribution to error in egg production. However, as previously discussed, error in predicted egg production is so high that in all years except for 2005, the reproductive success threshold lies within the error range (Figure 4.3), so that predictions of population increase or decrease are meaningless. It is evident that quantitative prediction requires further experimental work to narrow the confidence intervals on the parameter values.

The current model presents what may be a valid framework for studying multi-year temperature-forced reproductive success in *P. smintheus*, if error in the system can be controlled. The reproductive success model allows iteration from year-to-year by the presence of some initial number of eggs  $E_{\tau}$ , taken in the present study directly from the previous year's production  $E_{\tau-1}$ . A quantitative model for reproductive success would also require a better understanding of overwinter survival of *P. smintheus* eggs, which may also be regulated by temperature and precipitation (pers. comm., Roland). Currently overwinter mortality is neglected, an obvious simplification which impedes quantitative prediction of population dynamics. However, this offers still further evidence that  $d$  may be overestimated or  $\beta$  may be underestimated: in all years but 2003 and 2006, the model predicts decreases in population size, and these predictions would only be exaggerated by further overwinter mortality. Further discussion of overwinter mortality is presented in the next section.

One result of the experimental work conducted in Chapter 2 found no significant effect on larval body size by temperatures under which larvae developed. This result greatly simplifies the biological constraints on the present model, as no disadvantages are conferred by faster development and earlier emergence times. Small body size in some insects is associated with lower adult mating success and

lower fecundity (Atkinson, 1994), so if an effect of temperature on body size had been apparent, a non-autonomous mating rate  $c(t)$  or a non-autonomous fecundity rate  $\beta(t)$  might have been more appropriate than the constant parameters used in the present model. Further discussion of the analysis of the non-autonomous reproductive success model, as well as a discussion of direct and indirect effects of temperature on fecundity are presented in the next section.

Working toward a quantitative understanding of *P. smintheus* population dynamics is particularly important due to the predicted demographic Allee effect at low initial egg numbers (Figures 4.2 and 4.7). Such an Allee effect could potentially be disastrous for *P. smintheus* population persistence, as severe population crashes have been observed in the past (Figure 4.8). The model presented in this chapter demonstrates this Allee effect from a mechanistic, biologically-motivated model, such as the models presented in Veit and Lewis (1996); McCarthy (1997); Drake (2004); Molnár et al. (2008); Jerde et al. (2009); Wittmann et al. (2010). These models all identify decreased reproductive success at low population densities, similarly to the present model. Only Wittmann et al. (2010), however, identified temperature explicitly as a potential driver of reproductive success, which suggests there remains much to explore by way of modelling temperature-dependent reproductive success and the potential for Allee effects.

#### 4.4.3 Model extensions and future directions

The reproductive success model as presented in this chapter is a simple model in most respects, with constant adult mortality rates, coupling rate, and fecundity rate. Calabrese et al. (2008) presented multiple functional forms for coupling rate in *P. smintheus*, finding that inverse male density fit better to data than a constant rate, so a similar analysis to that presented here with a more complicated coupling function is a viable area for further research. Fecundity may also be more complicated than a constant rate would indicate. In fact, temperature influences fecundity in *P. smintheus* as egg production by mated females is partially dependent on resources available to larvae (Matter et al., 2006). Effects of temperature on larval food source *Sedum lanceolatum* were briefly considered in the previous two chapters, and adult fecundity represents another imperfectly understood area on how thermally-affected food sources may indirectly influence population dynamics. Temperature may also influence fecundity directly: increased temperatures have been linked to increased fecundity rates in butterflies *Pararge aegeria* (Gibbs et al., 2010) and *Bicyclus anynana* (Steigenga and Fischer, 2007). At present, direct effects of temperature on *P. smintheus* fecundity are unknown.

Should a more complicated temperature-dependent fecundity function be introduced into the model, it also introduces another non-autonomous element to the system. In the present model, only emergence rates depend on time, but if fecundity rate was modelled as temperature-dependent, it would also be implicitly time-dependent (i.e., the function could be constructed numerically from a temperature time series in a similar manner to the emergence function). If so, the temporal dependence of the emergence function could influence the adult dynamics via additional mechanisms. For instance, at present, an increase in temperature influences the reproductive success model through increasing total emergence and decreasing synchrony. However, increased temperatures in the larval developmental model also lead to earlier emergence, an effect which is irrelevant in the adult reproductive model because there is no explicit time-dependence outside the emergence function itself. That is, if emergence shifts in time, it does not currently influence reproductive success. If fecundity were to be modelled as time-dependent, however, then these shifts in emergence time would begin

to influence adult mating dynamics.

As mentioned previously, overwinter mortality is at present neglected in the model, a simplification which makes quantitative predictions about population dynamics difficult. A high correlation exists between the Pacific Decadal Oscillation (PDO) and the winter temperatures and precipitation levels of the Rocky Mountain foothills in Alberta where *P. smytheus* is found (pers. comm., Roland). Current research for *P. smytheus* suggests that climate is an important factor in overwinter egg survival, with higher mortality in colder, snowier winters (associated with negative PDO) and in warmer, drier winters (associated with positive PDO). Further research is necessary to determine the magnitude of influence of spring and summer temperatures (affecting larval growth and adult reproductive success) compared to winter temperatures (affecting egg survival) on the persistence of the population.

In this chapter, a model framework is presented for determining influences of temperature (as experienced by larvae) on adult reproductive success in *P. smytheus*. Effects of temperature within a season are considered using a reproductive success model, in which the parameters of the adult emergence function are varied to determine effects on egg production. Though currently no quantitative conclusions may be drawn for population dynamics or egg production, a potential mechanism is presented by which temperature forcing may drive observed yearly fluctuations in the population size. The model proposed in this chapter allows the qualitative study of both single season reproductive success and multi-year reproductive success in *P. smytheus* under changing climatic conditions.

# Bibliography

- Anosov, D. V., V. I. Arnold, S. K. Arenson, I. U. Bronshtein, V. Z. Grines, and Y. S. Il'yashenko (1997). *Ordinary Differential Equations and Smooth Dynamical Systems*. Springer.
- Atkinson, D. (1994). Temperature and organism size –A biological law for ectotherms? *Advances in Ecological Research* 25, 1–58.
- Both, C., M. van Asch, R. B. Bijlsma, A. B. van den Burg, and M. E. Visser (2009). Climate change and unequal phenological changes across four trophic levels: Constraints or adaptations? *Journal of Animal Ecology* 78, 73–83.
- Calabrese, J. M. and W. F. Fagan (2004). Lost in time, lonely, and single: Reproductive asynchrony and the Allee effect. *The American Naturalist* 164(1), 25–37.
- Calabrese, J. M., L. Ries, S. F. Matter, D. M. Debinski, J. N. Auckland, J. Roland, and W. F. Fagan (2008). Reproductive asynchrony in natural butterfly populations and its consequences for female matelessness. *Journal of Animal Ecology* 77, 146–156.
- Drake, J. M. (2004). Allee effects and the risk of biological invasion. *Risk Analysis* 24(4), 795–802.
- Fagan, W. F., C. Cosner, E. A. Larsen, and J. M. Calabrese (2010). How mating behaviour can modulate Allee effects arising from isolation in both space and time. *The American Naturalist* 175(3), 362–373.
- Gascoigne, J., L. Berec, S. Gregory, and F. Courchamp (2009). Dangerously few liaisons: A review of mate-finding Allee effects. *Population Ecology* 51, 355–372.
- Gibbs, M., H. V. Dyck, and B. Karlsson (2010). Reproductive plasticity, ovarian dynamics and maternal effects in response to temperature and flight in *Pararge aegeria*. *Journal of Insect Physiology* 56(9), 1275–1283.
- Hoye, T. T. and M. C. Forchhammer (2008). Phenology of high-arctic arthropods: Effects of climate on spatial, seasonal, and inter-annual variation. *Advances in Ecological Research* 40, 299–324.
- Iwasa, Y. and S. A. Levin (1995). The timing of life history events. *Journal of Theoretical Biology* 172, 33–42.
- Jerde, C. L., C. J. Bampfyld, and M. A. Lewis (2009). Chance establishment for sexual, semelparous species: Overcoming the Allee effect. *The American Naturalist* 173(6), 734–746.
- Kuussaari, M., I. Saccheri, M. Camara, and I. Hanski (1998). Allee effect and population dynamics in the Glanville fritillary butterfly. *Oikos* 82, 384–392.
- Logan, J. and J. Powell (2001). Ghost forests, global warming, and the mountain pine beetle (Coleoptera: Scolytidae). *American Entomologist* 47, 160–173.
- Mailleret, L. and V. Lemesle (2009). A note on semi-discrete modelling in the life sciences. *Philosophical Transactions of the Royal Society A* 367, 4779–4799.
- Matter, S. F., M. Ezzeddine, E. Duermit, J. Mashburn, R. Hamilton, T. Lucas, and J. Roland (2009). Interactions between habitat quality and connectivity affect immigration but not abundance or population growth of the butterfly *Parnassius smintheus*. *Oikos* 118, 1461–1470.
- Matter, S. F., A. Wick, M. Gaydos, M. Frantz, and J. Roland (2006). Egg viability and larval contribution to fecundity of *Parnassius smintheus* Doubleday (Papilionidae). *Journal of the Lepidopterists' Society* 60(4), 101–102.

- McCarthy, M. A. (1997). The Allee effect, finding mates and theoretical models. *Ecological Modelling* 103, 99–102.
- Molnár, P. K., A. E. Derocher, M. A. Lewis, and M. K. Taylor (2008). Modelling the mating system of polar bears: A mechanistic approach to the Allee effect. *Proceedings of the Royal Society B* 275, 217–226.
- Monagan, M. B., K. O. Geddes, K. M. Heal, G. Labahn, S. M. Vorkoetter, J. McCarron, and P. DeMarco (2005). *Maple 10 Programming Guide*. Waterloo ON, Canada: Maplesoft.
- Parmesan, C. (2006). Ecological and evolutionary responses to recent climate change. *Annual Review of Ecology, Evolution and Systematics* 37, 637–669.
- Perko, L. (2000). *Differential Equations and Dynamical Systems* (3rd ed.). Texts in Applied Mathematics 7. Springer.
- Post, E., S. A. Levin, Y. Iwasa, and N. C. Stenseth (2001). Reproductive asynchrony increases with environmental disturbance. *Evolution* 55, 830–834.
- Schweiger, O., J. Settele, O. Kudrna, S. Klotz, and I. Kühn (2008). Climate change can cause spatial mismatch of trophically interacting species. *Ecology* 89, 3472–3479.
- Steigenga, M. J. and K. Fischer (2007). Ovarian dynamics, egg size, and egg number in relation to temperature and mating status in a butterfly. *Entomologia Experimentalis et Applicata* 125, 195–203.
- Taylor, J. R. (1997). *An Introduction to Error Analysis: The Study of Uncertainties in Physical Measurements* (2nd ed.). University Science Books.
- Tcheslavskaja, K., C. C. Brewster, and A. A. Sharov (2002). Mating success of gypsy moth (Lepidoptera: Lymantriidae) females in Southern Wisconsin. *Great Lakes Entomologist* 35(1), 1–7.
- Thomson, L. J., S. Macfadyen, and A. A. Hoffmann (2010). Predicting the effects of climate change on natural enemies of agricultural pests. *Biological Control* 52, 296–306.
- Tobin, P. C., C. Robinet, D. M. Johnson, S. L. Whitmire, O. N. Bjornstad, and A. M. Liebhold (2009). The role of Allee effects in gypsy moth, *Lymantria dispar* (L.) invasions. *Population Ecology* 51, 373–384.
- Veit, R. R. and M. A. Lewis (1996). Dispersal, population growth, and the Allee effect: Dynamics of the house finch invasion of Eastern North America. *The American Naturalist* 148(2), 255–274.
- Wittmann, M. J., M. A. Lewis, J. D. Young, and N. D. Yan (2010). Temperature-dependent Allee effects in a stage-structured model for *Bythotrephes* establishment. *Submitted to Biological Invasions*.
- Yurk, B. P. and J. A. Powell (2009). Modelling the evolution of insect phenology. *Bulletin of Mathematical Biology* 71, 952–979.

## Chapter 5

# General discussion and conclusions

In the course of this study, the following questions regarding climatic impacts on the alpine butterfly *Parnassius smintheus* were addressed. Firstly, does temperature influence development time and final larval body weight in *P. smintheus* larvae? Secondly, do such thermal effects influence adult emergence, and can a mechanistic model be constructed that directly predicts such effects? Thirdly and finally, do temperatures experienced by larvae impact adult reproductive success through adult emergence, and can a reproductive success model framework be constructed which incorporates the previous mechanistic adult emergence model?

The first question was addressed experimentally in Chapter 2. *P. smintheus* larvae were collected from the field site at Jumpingpound and Lusk Ridges Kananaskis, Alberta, and placed in growth chambers to mature. Three growth chambers were used, with three distinct temperature treatments denoted “cooler”, “ambient”, and “warmer”. The ambient temperature regime was constructed by averaging daytime and night time temperatures recorded over a ten year period from a nearby weather station at Nakiska Ridgetop. The warmer and cooler regimes were constructed by shifting the ambient regime daily temperatures up and down, respectively, by 2°C. Larvae were fed their primary host plant, *Sedum lanceolatum*, in abundant quantities, to avoid food influencing growth rates. Instar transition, mortality, and weight were recorded daily for analysis.

To address the primary research questions of the chapter, Kruskal-Wallis Rank Sum Tests were conducted on the fifth instar developmental times, pupal weights, and maximum weights in the three temperature treatments. In fifth instar developmental times, the Kruskal-Wallis Rank Sum Test indicated significant differences between the treatments, so Dunn’s test, a non-parametric multiple comparison test was applied to isolate the differences between treatments. A significant difference between fifth instar development times was detected in the warmer and ambient treatments, and in the warmer and cooler treatments. No significant difference in fifth instar development times was detected between the ambient and cooler treatment. With respect to body weight at pupation and maximum body weight, the Kruskal-Wallis Rank Sum Test detected no significant difference between the treatments.

Temperature significantly decreased developmental times in the warmer treatment with respect to the ambient and cooler treatment, but the decrease in ambient developmental times with respect to the cooler treatment was non-significant. One proposed explanation for these results was that individuals with longer developmental times in the cooler treatment had a higher probability of mortality prior to pupation. Even supposing that mortality is independent of temperature, a

constant daily probability of death would imply individuals with longer development times have a higher probability of dying before pupation. As only individuals which survived to pupation were considered in the analysis, the longer development times arrested by death would be neglected. This argument is supported by a higher variance in the ambient treatment's developmental times and the higher mortality in the lower temperature treatment. That is, low variance suggests that longer developmental times have been excluded, and higher mortality suggests that these slower-developing larvae died prior to pupation.

The lack of significance in body weight between the temperature treatments is interesting from an ecological perspective. Current ecological theory posits the temperature-size rule, where individuals mature faster at higher temperatures at the expense of body size (Atkinson, 1994). No evidence for *P. smintheus* was seen to support this theory, and in fact, mean weights (both pupal and maximum) were observed to increase, albeit non-significantly, as temperatures increased. Replication of the experiment is required to determine if *P. smintheus* is an exception to the temperature-size rule. However, from a modelling perspective, the lack of temperature-dependent body size in *P. smintheus* simplifies the mathematical analysis. Body size in insects is associated with individual fitness, influencing traits such as reproductive success and fecundity, and lifespan (Atkinson, 1994). If temperature influenced body size, then temperature experienced by larvae would also impact mating success rates, fecundity rates, and mortality rates in adults. This would lead to more complicated functions, likely exhibiting explicit time dependence, governing these rates, which would result in a more complex, non-autonomous reproductive success model.

The second question, considering how temperature effects on larval development and adult emergence may be modelled, was addressed in Chapter 3. Motivated by the variable temperature data collected in Chapter 2, a Bernoulli process model was constructed that considers effects of temperature non-cumulatively, owing to the memoryless nature of the Bernoulli process. An individual's transitional success on a given day was modelled as a function of temperature on that given day, so the temperature experienced by the individual on previous days was irrelevant to the current transitional success or failure. This model framework allowed a broad use of the data of Chapter 2, where transitional success or failure could be grouped with daytime temperature without regard to previous temperatures in the experimental thermal regime.

Two Bernoulli process models were considered: the first was a simple model with constant temperature-dependent transitional and mortality probabilities, dependent only on temperature treatment. That is, distinct transitional and mortality probabilities for each instar were estimated for each of the cooler, ambient, and warmer treatments. Parameter estimates were generated using maximum likelihood estimates. The advantages of the simple model included the existence of closed form solutions for larval instar probability distributions. Distributions were derived for the probability of an individual's being present in a given instar in a given time step, and from there, an adult emergence probability distribution (dependent on transitional and mortality probabilities) was derived.

When parameterized for the different temperature treatments, the effects of temperature on adult emergence were evident. Emergence in the warmer treatment was considerably earlier than in the ambient and cooler treatments, which were very similar (comparable to the experimental results of Chapter 2). Survivorship to adulthood was highest in the ambient model predictions, as the cooler treatment saw higher larval mortality probabilities and the warmer treatment saw high

pupal mortalities (possibly due to desiccation). The simple model produced results analogous to those observed in Chapter 2, and demonstrates its utility for qualitative predictions of effects of “warming” and “cooling” temperatures on adult emergence in *P. smintheus*.

The second model considered in Chapter 3 was a variable transition probability model, where transitional success in a given instar was modelled as having a positive, linear relationship with temperature. The slopes of the transitional success functions for each instar were estimated using maximum likelihood on the transitional success data of Chapter 2. When the entire data set was used for maximum likelihood estimation, slope estimates were underestimated, especially in the fifth and sixth instar. The mean estimated slopes from 1000 trials on bootstrapped data (sampling the same number of individuals in the cooler treatment as in the ambient and warmer) were instead used as the parameter estimates. A potential reason for the disparity was that the original dataset had a much larger sample size of individuals in the cooler treatment, which the estimation process weighted too heavily (decreasing the slope in a linear relationship). It was therefore concluded that the mean of estimates on bootstrapped data gave more appropriate estimates for use in simulation.

The parameterized variable transition probability model was then validated against observed emergence distributions constructed from eight years of mark-recapture data. Model input for these comparisons were temperature regimes for the appropriate years, taken from weather data recorded at Nakiska Ridgeway. A Wilcoxon signed-rank test and a linear regression of observed on predicted emergence were applied to determine whether the predicted and observed emergence distributions were statistically distinguishable. The Wilcoxon signed-rank test failed to distinguish between the distributions for all years except 2005, where an insufficient number of sampling days precluded the use of the test. The linear regression of observed on predicted emergence failed to reject the linear relationship when the two distributions were regressed in all years except 2009, when it rejected the model’s validity. These tests presented some evidence towards the predictive capabilities of the model. However, the smallness of the sample size compared in several of the years may call into question the acceptance of the null hypothesis, or non-rejection of model validity. Early years of mark recapture had low numbers of sampling days, such as 2005, which prevented the Wilcoxon signed-rank test analysis. Later years of mark recapture data had more sampling days, which lends more credence to the non-rejection of model validity. A field season in which a meadow were sampled daily (or as weather permits) would be exceptionally useful to model validation.

This study did present evidence, however, that temperature-dependent adult emergence can be predicted using a memoryless process which does not consider cumulative effects of temperature. Further, a very simple temperature-transition probability relationship was considered, and more data to parameterize more complicated and biologically-motivated functional forms might improve the current model. Linear transition functions, while biologically reasonable within a temperature range, do not consider heat stress and such adverse effects that occur at high temperatures.

The final research question, considering the effects of temperature-mediated *P. smintheus* adult emergence on reproductive success, was presented in Chapter 4. The model derived in Chapter 3 was therefore incorporated into a larger model framework for reproductive success in Chapter 4. A system of ordinary differential equations was constructed to model changes in population size within a season for adult males, unmated females, reproducing females, and eggs. Two adult emergence functions were used to provide input to the male and unmated female equations: a Gaussian function and the continuous-time analogue of the temperature-dependent adult emergence distribution

derived in Chapter 3. The Gaussian function was used because, unlike the numerically calculated temperature-dependent function, it had a closed form through which parameters controlling total adult emergence and variance in adult emergence could be varied directly and independently. That is, the Gaussian function was studied to ensure that varying parameters in the temperature-dependent function (temperature, juvenile mortality) which affected total emergence and emergence variance had similar qualitative effects to varying said parameters in the simpler Gaussian function. Further, the Gaussian parameters could be varied independently, allowing the study of component effects of varying each one, unlike the temperature-dependent model, where the parameters could not easily be considered independently. Parameters in the reproductive success model were taken from the literature (Calabrese et al., 2008; Matter et al., 2009), or estimated from experimental data (pers. comm., Matter).

Increasing total emergence in the Gaussian adult emergence function unsurprisingly increased adult reproductive success, though an Allee effect was observed for small initial population sizes (the initial number of eggs in a year). Increasing the variance in the Gaussian emergence function decreased reproductive success, as would be expected when a population exhibits a higher degree of asynchrony in emergence (Calabrese and Fagan, 2004). Again, the model predicted an Allee effect at low initial population sizes.

Using the temperature-dependent emergence function, increasing daytime temperature as experienced by larvae both increased total emergence and increased the variance of the emergence function. These two effects might then be competitive, but reproductive success was predicted to increase with temperature, suggesting that the increased survivorship to adulthood was sufficiently high to offset the increased asynchrony in the emergence. A decrease in larval mortality probability both increased total adult emergence and decreased variance in emergence, leading unsurprisingly to increased reproductive success. The reproductive success model with the temperature-dependent emergence distribution, like the Gaussian case, predicts an Allee effect at low initial population sizes.

The accumulated error in the reproductive success model was also considered, as error was introduced through the adult emergence model parameters, as well as through the reproductive success model parameters. It was concluded that the model, with its present parameterization, could not be used for quantitative predictions of reproductive success because accumulated error almost always overlapped the reproductive success threshold. That is, within the error bounds on the model prediction, both reproductive success and failure within a year were possible. It was concluded that quantitative predictions of reproductive success and resultant population dynamics could not be made without further experimental work, so that additional data could narrow the present confidence intervals on the parameters. Despite the lack of quantitative predictions, however, a mechanism was proposed for observed yearly fluctuations in population size. The model predicted that yearly variations in temperature force egg production in *P. smintheus* above the reproductive success threshold in warmer years and below the threshold in cooler years, driving fluctuation in population size.

In this study, advances were made in understanding the effects of temperature on the phenology of the alpine butterfly *P. smintheus*. Using a combination of experimental and modelling approaches, the effect of increasing temperatures was demonstrated to decrease larval developmental times, prompt earlier and higher adult emergence, and increase adult reproductive success. Though the larval development model assumed a simplistic relationship between temperature and transitional

success, the present study suggests that *P. smintheus* is not presently near its thermal developmental upper bound, where population persistence would be impossible. In fact, the reproductive success model suggests that cooler years are in fact highly detrimental to population persistence, as low temperatures decrease reproductive success ratios and aggravate Allee effects at low population densities. This is again, however, potentially a product of the chosen monotonically increasing relationship of temperature and transitional success in the larval development model. Further experimental work, with both a larger sample size, and a wider range of temperatures under study, is needed to construct a more biologically realistic transitional success probability function, which accurately models larval development near developmental thresholds. Furthermore, a more complete understanding of overwinter survival of eggs is necessary to construct quantitatively useful models of temperature-driven population dynamics over multiple years. Nonetheless, this work still presents the important first steps in understanding the impacts of climate change on the phenology and population dynamics of *P. smintheus*.

# Bibliography

- Atkinson, D. (1994). Temperature and organism size –A biological law for ectotherms? *Advances in Ecological Research* 25, 1–58.
- Calabrese, J. M. and W. F. Fagan (2004). Lost in time, lonely, and single: Reproductive asynchrony and the Allee effect. *The American Naturalist* 164(1), 25–37.
- Calabrese, J. M., L. Ries, S. F. Matter, D. M. Debinski, J. N. Auckland, J. Roland, and W. F. Fagan (2008). Reproductive asynchrony in natural butterfly populations and its consequences for female matelessness. *Journal of Animal Ecology* 77, 146–156.
- Matter, S. F., M. Ezzeddine, E. Duermit, J. Mashburn, R. Hamilton, T. Lucas, and J. Roland (2009). Interactions between habitat quality and connectivity affect immigration but not abundance or population growth of the butterfly *Parnassius smintheus*. *Oikos* 118, 1461–1470.

## Appendix A

# Dunn's test calculation

Dunn's test is a non-parametric analogue of a Tukey-type multiple comparison test to determine where significant differences occur between multiple treatments, when sample sizes are not equal. The method of determining statistical significance is taken from ?. Data is ranked from least to greatest, with equal data sharing a mean rank. The sum of the ranks for the data corresponding to each treatment is divided by the number of data points to obtain the mean rank  $\bar{R}_j$  for each treatment  $j$ . The standard error for data containing tied ranks is

$$SE = \sqrt{\left(\frac{N(N+1)}{12} - \frac{\sum T}{12(N-1)}\right) \left(\frac{1}{n_b} + \frac{1}{n_a}\right)}$$

where  $N$  is the total number of data points,  $n_a$  and  $n_b$  are the number of data points in the two treatments under comparison, and

$$\sum T = \sum_{i=1}^m (t_i^3 - t_i)$$

where  $m$  is the total number of groups having equal rank and  $t_i$  is the number of data points in the  $i$ th group of equal rank. Then the test statistic is

$$Q = \frac{\bar{R}_b - \bar{R}_a}{SE}.$$

The test is used here to determine the significance of differences in fifth instar developmental time in the temperature treatments. The null hypothesis ( $H_0$ ) states that the fifth instar development time is the same in the two temperature treatments under consideration, while the alternative hypothesis states that development time is different. The critical value of this test for 95% confidence is taken from ?. If the observed value of  $Q$  is greater than the critical value  $Q_{0.05,3}$ , then the developmental times in the two treatments are significantly different. The results are summarized in Table A.1.

Comparison ( $b$ vs $a$ )	Difference ( $\bar{R}_b - \bar{R}_a$ )	Standard Error	$Q_{\text{obs}}$	$Q_{0.05,3}$ (crit)	Conclusion
ambient vs +2	15.39	5.835	2.638*	2.394	Reject $H_0$
-2 vs ambient	0.24	5.075	0.047	2.394	Do not reject $H_0$
-2 vs +2	15.63	4.353	3.591*	2.394	Reject $H_0$

Table A.1: Results of Dunn's test for significance of differences between fifth instar developmental times in the temperature treatments, with critical values taken from Zar (2010).

## Appendix B

# Probability distribution for developmental time to adulthood

A sample calculation of (3.5) for  $r = 4$  is verified here. The following equality must be demonstrated:

$$\sum_{k=3}^{\infty} \mu_1 \mu_2 \mu_3 \sum_{m_1=0}^{k-3} (1 - \mu_1)^{k-3-m_1} \sum_{m_2=0}^{m_1} (1 - \mu_2)^{m_2} (1 - \mu_3)^{m_1-m_2} = 1.$$

Beginning with the rightmost sum,

$$\begin{aligned} \sum_{m_2=0}^{m_1} (1 - \mu_2)^{m_2} (1 - \mu_3)^{m_1-m_2} &= (1 - \mu_3)^{m_1} \sum_{m_2=0}^{m_1} \left( \frac{1 - \mu_2}{1 - \mu_3} \right)^{m_2} \\ &= (1 - \mu_3)^{m_1} \left( \frac{1 - \left( \frac{1 - \mu_2}{1 - \mu_3} \right)^{m_1+1}}{1 - \left( \frac{1 - \mu_2}{1 - \mu_3} \right)} \right). \end{aligned}$$

Now the next sum to the left gives

$$\begin{aligned} &\sum_{m_1=0}^{k-3} (1 - \mu_1)^{k-3-m_1} (1 - \mu_3)^{m_1} \left( \frac{1 - \left( \frac{1 - \mu_2}{1 - \mu_3} \right)^{m_1+1}}{1 - \left( \frac{1 - \mu_2}{1 - \mu_3} \right)} \right) \\ &= \frac{(1 - \mu_1)^{k-3}}{1 - \left( \frac{1 - \mu_2}{1 - \mu_3} \right)} \sum_{m_1=0}^{k-3} \left( \frac{1 - \mu_3}{1 - \mu_1} \right)^{m_1} \left( 1 - \left( \frac{1 - \mu_2}{1 - \mu_3} \right)^{m_1+1} \right) \\ &= \frac{(1 - \mu_1)^{k-3}}{1 - \left( \frac{1 - \mu_2}{1 - \mu_3} \right)} \sum_{m_1=0}^{k-3} \left( \frac{1 - \mu_3}{1 - \mu_1} \right)^{m_1} - \frac{(1 - \mu_1)^{k-3} \left( \frac{1 - \mu_2}{1 - \mu_3} \right)}{1 - \left( \frac{1 - \mu_2}{1 - \mu_3} \right)} \sum_{m_1=0}^{k-3} \left( \frac{1 - \mu_2}{1 - \mu_1} \right)^{m_1} \\ &= \frac{(1 - \mu_1)^{k-3}}{1 - \left( \frac{1 - \mu_2}{1 - \mu_3} \right)} \left( \frac{1 - \left( \frac{1 - \mu_3}{1 - \mu_1} \right)^{k-2}}{1 - \left( \frac{1 - \mu_3}{1 - \mu_1} \right)} \right) - \frac{(1 - \mu_1)^{k-3} \left( \frac{1 - \mu_2}{1 - \mu_3} \right)}{1 - \left( \frac{1 - \mu_2}{1 - \mu_3} \right)} \left( \frac{1 - \left( \frac{1 - \mu_2}{1 - \mu_1} \right)^{k-2}}{1 - \left( \frac{1 - \mu_2}{1 - \mu_1} \right)} \right). \end{aligned}$$

Recalling the variant on the infinite geometric sum formula

$$\sum_{k=p}^{\infty} x^k = \frac{x^p}{1 - x}, \quad |x| < 1,$$

the final sum thus has the form

$$\begin{aligned}
& \sum_{k=3}^{\infty} \mu_1 \mu_2 \mu_3 \left[ \frac{(1-\mu_1)^{k-3}}{1-\left(\frac{1-\mu_2}{1-\mu_3}\right)} \left( \frac{1-\left(\frac{1-\mu_3}{1-\mu_1}\right)^{k-2}}{1-\left(\frac{1-\mu_3}{1-\mu_1}\right)} \right) - \frac{(1-\mu_1)^{k-3} \left(\frac{1-\mu_2}{1-\mu_3}\right)}{1-\left(\frac{1-\mu_2}{1-\mu_3}\right)} \left( \frac{1-\left(\frac{1-\mu_2}{1-\mu_1}\right)^{k-2}}{1-\left(\frac{1-\mu_2}{1-\mu_1}\right)} \right) \right] \\
&= \frac{\mu_2 \mu_3}{\left[1-\left(\frac{1-\mu_2}{1-\mu_3}\right)\right] \left[1-\left(\frac{1-\mu_3}{1-\mu_1}\right)\right]} - \frac{\mu_1 \mu_2}{\left[1-\left(\frac{1-\mu_2}{1-\mu_3}\right)\right] \left[1-\left(\frac{1-\mu_3}{1-\mu_1}\right)\right]} \left(\frac{1-\mu_3}{1-\mu_1}\right) \\
&- \frac{\mu_2 \mu_3}{\left[1-\left(\frac{1-\mu_2}{1-\mu_3}\right)\right] \left[1-\left(\frac{1-\mu_2}{1-\mu_1}\right)\right]} \left(\frac{1-\mu_2}{1-\mu_3}\right) + \frac{\mu_1 \mu_3}{\left[1-\left(\frac{1-\mu_2}{1-\mu_3}\right)\right] \left[1-\left(\frac{1-\mu_2}{1-\mu_1}\right)\right]} \left(\frac{1-\mu_2}{1-\mu_3}\right) \left(\frac{1-\mu_2}{1-\mu_1}\right) \\
&= 1
\end{aligned}$$

after some algebraic manipulation.

## Appendix C

# Verification of model solutions

It can be shown that for the system of difference equations

$$\begin{aligned}
 p_{n+1}^1 &= [(1 - \mu_1)(1 - d_1)] p_n^1 \\
 p_{n+1}^2 &= [(1 - \mu_2)(1 - d_2)] p_n^2 + [\mu_1(1 - d_2)] p_n^1 \\
 &\vdots \\
 p_{n+1}^i &= [(1 - \mu_i)(1 - d_i)] p_n^i + [\mu_{i-1}(1 - d_i)] p_n^{i-1} \\
 &\vdots \\
 p_{n+1}^r &= p_n^r + \mu_{r-1} p_n^{r-1},
 \end{aligned}$$

having initial conditions  $p_0^1 = 1, p_0^j = 0, j = 2 \dots, r$ , the set of solutions

$$\begin{aligned}
 p_n^1 &= ((1 - \mu_1)(1 - d_1))^n \\
 p_n^i &= \prod_{k=2}^i [\mu_{k-1}(1 - d_k)] \sum_{j=1}^i \left\{ \frac{[(1 - \mu_j)(1 - d_j)]^n}{\prod_{\substack{k \neq j \\ 1 \leq k \leq i}} [(1 - \mu_j)(1 - d_j) - (1 - \mu_k)(1 - d_k)]} \right\} \\
 p_n^r &= \frac{1}{1 - d_1} \prod_{k=1}^{r-1} [\mu_k(1 - d_k)] \left( \sum_{j=1}^{r-1} \left\{ \frac{[(1 - \mu_j)(1 - d_j)]^n}{(-\mu_j - d_j + \mu_j d_j) \prod_{\substack{k \neq j \\ 1 \leq k \leq r-1}} [(1 - \mu_j)(1 - d_j) - (1 - \mu_k)(1 - d_k)]} \right\} + \right. \\
 &\quad \left. + \frac{(-1)^{r-1}}{\prod_{k=1}^{r-1} (-\mu_k - d_k + \mu_k d_k)} \right)
 \end{aligned}$$

holds where  $i = 2, \dots, r - 1$ .

The solution to the first instar equation holds since

$$\begin{aligned}
 (1 - \mu_1)(1 - d_1)p_n^1 &= (1 - \mu_1)(1 - d_1)(1 - \mu_1)^n(1 - d_1)^n \\
 &= (1 - \mu_1)^{n+1}(1 - d_1)^{n+1} \\
 &= p_{n+1}^1.
 \end{aligned}$$

A proof by induction demonstrates the validity of the intermediate instar solution. The solution

to the second instar equation holds since

$$p_n^2 = \mu_1(1-d_2) \left( \frac{(1-\mu_1)^n(1-d_1)^n}{(1-\mu_1)(1-d_1) - (1-\mu_2)(1-d_2)} + \frac{(1-\mu_2)^n(1-d_2)^n}{(1-\mu_2)(1-d_2) - (1-\mu_1)(1-d_1)} \right)$$

and

$$\begin{aligned} (1-\mu_2)(1-d_2)p_n^2 &= (1-\mu_2)(1-d_2) \left( \frac{\mu_1(1-d_2)(1-\mu_1)^n(1-d_1)^n}{(1-\mu_1)(1-d_1) - (1-\mu_2)(1-d_2)} \right. \\ &\quad \left. + \frac{\mu_1(1-d_2)(1-\mu_2)^n(1-d_2)^n}{(1-\mu_2)(1-d_2) - (1-\mu_1)(1-d_1)} \right) + \mu_1(1-d_2)(1-\mu_1)^n(1-d_1)^n \\ &= \frac{\mu_1(1-\mu_2)(1-d_2)^2(1-\mu_1)^n(1-d_1)^n - \mu_1(1-\mu_2)^{n+1}(1-d_2)^{n+2}}{(1-\mu_1)(1-d_1) - (1-\mu_2)(1-d_2)} \\ &\quad + \frac{\mu_1(1-d_2)(1-\mu_1)^{n+1}(1-d_1)^{n+1} - \mu_1(1-d_2)^2(1-\mu_2)(1-\mu_1)^n(1-d_1)^n}{(1-\mu_1)(1-d_1) - (1-\mu_2)(1-d_2)} \\ &= \mu_1(1-d_2) \left( \frac{(1-\mu_1)^{n+1}(1-d_1)^{n+1} - (1-\mu_2)^{n+1}(1-d_2)^{n+1}}{(1-\mu_1)(1-d_1) - (1-\mu_2)(1-d_2)} \right) \\ &= \mu_1(1-d_2) \left( \frac{(1-\mu_1)^{n+1}(1-d_1)^{n+1}}{(1-\mu_1)(1-d_1) - (1-\mu_2)(1-d_2)} + \frac{(1-\mu_2)^{n+1}(1-d_2)^{n+1}}{(1-\mu_2)(1-d_2) - (1-\mu_1)(1-d_1)} \right) \\ &= p_{n+1}^2. \end{aligned}$$

To complete the basis of the proof, we show that the third instar equation holds. From the intermediate solution equation for  $i = 3$ ,

$$\begin{aligned} p_n^3 &= \mu_1\mu_2(1-d_2)(1-d_3) \left( \frac{(1-\mu_1)^n(1-d_1)^n}{[(1-\mu_1)(1-d_1) - (1-\mu_2)(1-d_2)][(1-\mu_1)(1-d_1) - (1-\mu_3)(1-d_3)]} \right. \\ &\quad + \frac{(1-\mu_2)^n(1-d_2)^n}{[(1-\mu_2)(1-d_2) - (1-\mu_1)(1-d_1)][(1-\mu_2)(1-d_2) - (1-\mu_3)(1-d_3)]} \\ &\quad \left. + \frac{(1-\mu_3)^n(1-d_3)^n}{[(1-\mu_3)(1-d_3) - (1-\mu_1)(1-d_1)][(1-\mu_3)(1-d_3) - (1-\mu_2)(1-d_2)]} \right) \end{aligned}$$

we can see

$$\begin{aligned} &(1-\mu_3)(1-d_3)p_n^3 \\ &= \mu_1\mu_2(1-d_2)(1-d_3)^2(1-\mu_3) \left( \frac{(1-\mu_1)^n(1-d_1)^n}{[(1-\mu_1)(1-d_1) - (1-\mu_2)(1-d_2)][(1-\mu_1)(1-d_1) - (1-\mu_3)(1-d_3)]} \right. \\ &\quad + \frac{(1-\mu_2)^n(1-d_2)^n}{[(1-\mu_2)(1-d_2) - (1-\mu_1)(1-d_1)][(1-\mu_2)(1-d_2) - (1-\mu_3)(1-d_3)]} \\ &\quad \left. + \frac{(1-\mu_3)^n(1-d_3)^n}{[(1-\mu_3)(1-d_3) - (1-\mu_1)(1-d_1)][(1-\mu_3)(1-d_3) - (1-\mu_2)(1-d_2)]} \right) \\ &\quad + \mu_1\mu_2(1-d_2)(1-d_3) \left( \frac{(1-\mu_1)^n(1-d_1)^n}{(1-\mu_1)(1-d_1) - (1-\mu_2)(1-d_2)} + \frac{(1-\mu_2)^n(1-d_2)^n}{(1-\mu_2)(1-d_2) - (1-\mu_1)(1-d_1)} \right) \\ &= \alpha \left( (1-\mu_3)^{n+1}(1-d_3)^{n+1}(1-\mu_1)(1-d_1) - (1-\mu_3)^{n+1}(1-d_3)^{n+1}(1-\mu_2)(1-d_2) \right. \\ &\quad + (1-\mu_1)^{n+1}(1-d_1)^{n+1}(1-\mu_2)(1-d_2) - (1-\mu_1)^{n+1}(1-d_1)^{n+1}(1-\mu_3)(1-d_3) \\ &\quad \left. - (1-\mu_2)^{n+1}(1-d_2)^{n+1}(1-\mu_1)(1-d_1) + (1-\mu_2)^{n+1}(1-d_2)^{n+1}(1-\mu_3)(1-d_3) \right) \end{aligned}$$

where

$$\alpha = \frac{\mu_1\mu_2(1-d_2)(1-d_3)}{[(1-\mu_1)(1-d_1) - (1-\mu_2)(1-d_2)][(1-\mu_1)(1-d_1) - (1-\mu_3)(1-d_3)][(1-\mu_2)(1-d_2) - (1-\mu_3)(1-d_3)]}.$$

So

$$\begin{aligned} &(1-\mu_3)(1-d_3)p_n^3 \\ &= \mu_1\mu_2(1-d_2)(1-d_3) \left( \frac{(1-\mu_1)^{n+1}(1-d_1)^{n+1}}{[(1-\mu_1)(1-d_1) - (1-\mu_2)(1-d_2)][(1-\mu_1)(1-d_1) - (1-\mu_3)(1-d_3)]} \right. \\ &\quad + \frac{(1-\mu_2)^{n+1}(1-d_2)^{n+1}}{[(1-\mu_2)(1-d_2) - (1-\mu_1)(1-d_1)][(1-\mu_2)(1-d_2) - (1-\mu_3)(1-d_3)]} \\ &\quad + \frac{(1-\mu_3)^{n+1}(1-d_3)^{n+1}}{[(1-\mu_3)(1-d_3) - (1-\mu_1)(1-d_1)][(1-\mu_3)(1-d_3) - (1-\mu_2)(1-d_2)]} \left. \right) \\ &= p_{n+1}^3. \end{aligned}$$

This establishes the basis of the proof for the validity of the intermediate instar solution. Suppose now that the equation

$$p_{n+1}^i = (1 - \mu_i)(1 - d_i)p_n^i + \mu_{i-1}(1 - d_i)p_n^{i-1}$$

holds for  $p_n^i$  and  $p_n^{i-1}$  where these are intermediate instar solutions given above. Now it must be shown that

$$p_{n+1}^{i+1} = (1 - \mu_{i+1})(1 - d_{i+1})p_n^{i+1} + \mu_i(1 - d_{i+1})p_n^i$$

holds for  $p_n^{i+1}$  and  $p_n^i$ , where  $2 \leq i \leq r - 1$ . This differs from the standard induction proof where  $i \in \mathbb{N}$ , as the intermediate instar equation only holds only between  $i = 2$  and  $i = r - 1$  (the cases where  $i = 1$  and  $i = r$  have different solutions). Substituting these solutions into the model equation,

$$\begin{aligned} & (1 - \mu_{i+1})(1 - d_{i+1})p_n^{i+1} \\ = & (1 - \mu_{i+1})(1 - d_{i+1}) \prod_{k=2}^{i+1} [\mu_{k-1}(1 - d_k)] \sum_{j=1}^{i+1} \left\{ \frac{(1 - \mu_j)^n (1 - d_j)^n}{\prod_{\substack{k \neq j \\ 1 \leq k \leq i+1}} [(1 - \mu_j)(1 - d_j) - (1 - \mu_k)(1 - d_k)]} \right\} \\ + & \mu_i(1 - d_{i+1}) \prod_{k=2}^i [\mu_{k-1}(1 - d_k)] \sum_{j=1}^i \left\{ \frac{(1 - \mu_j)^n (1 - d_j)^n}{\prod_{\substack{k \neq j \\ 1 \leq k \leq i}} [(1 - \mu_j)(1 - d_j) - (1 - \mu_k)(1 - d_k)]} \right\} \\ = & \prod_{k=2}^{i+1} \mu_{k-1}(1 - d_k) \left( \sum_{j=1}^{i+1} \left\{ \frac{(1 - \mu_j)^n (1 - d_j)^n (1 - \mu_{i+1})(1 - d_{i+1})}{\prod_{\substack{k \neq j \\ 1 \leq k \leq i+1}} [(1 - \mu_j)(1 - d_j) - (1 - \mu_k)(1 - d_k)]} \right\} \right. \\ + & \left. \sum_{j=1}^i \left\{ \frac{(1 - \mu_j)^n (1 - d_j)^n [(1 - \mu_j)(1 - d_j) - (1 - \mu_{i+1})(1 - d_{i+1})]}{\prod_{\substack{k \neq j \\ 1 \leq k \leq i+1}} [(1 - \mu_j)(1 - d_j) - (1 - \mu_k)(1 - d_k)]} \right\} \right). \end{aligned}$$

Let  $\beta_{i,j} = \prod_{\substack{k \neq j \\ 1 \leq k \leq i}} [(1 - \mu_j)(1 - d_j) - (1 - \mu_k)(1 - d_k)]$  and then the calculation may be continued:

$$\begin{aligned} & (1 - \mu_{i+1})(1 - d_{i+1})p_n^{i+1} \\ = & \prod_{k=2}^{i+1} \mu_{k-1}(1 - d_k) \left( \sum_{j=1}^{i+1} \frac{1}{\beta_{i+1,j}} (1 - \mu_j)^n (1 - d_j)^n (1 - \mu_{i+1})(1 - d_{i+1}) \right. \\ - & \left. \sum_{j=1}^i \frac{1}{\beta_{i+1,j}} (1 - \mu_j)^n (1 - d_j)^n (1 - \mu_{i+1})(1 - d_{i+1}) + \sum_{j=1}^i \frac{1}{\beta_{i+1,j}} (1 - \mu_j)^{n+1} (1 - d_j)^{n+1} \right) \\ = & \prod_{k=2}^{i+1} \mu_{k-1}(1 - d_k) \left( \frac{1}{\beta_{i+1,i+1}} (1 - \mu_{i+1})^{n+1} (1 - d_{i+1})^{n+1} + \sum_{j=1}^i \frac{1}{\beta_{i+1,j}} (1 - \mu_j)^{n+1} (1 - d_j)^{n+1} \right) \\ = & \prod_{k=2}^{i+1} \mu_{k-1}(1 - d_k) \sum_{j=1}^{i+1} \frac{(1 - \mu_j)^{n+1} (1 - d_j)^{n+1}}{\prod_{\substack{k \neq j \\ 1 \leq k \leq i+1}} [(1 - \mu_j)(1 - d_j) - (1 - \mu_k)(1 - d_k)]} \\ = & p_{n+1}^{i+1} \end{aligned}$$

so the intermediate solution holds for all  $2 \leq i \leq r - 1$ .

Direct substitution demonstrates that the final instar  $p_n^r$  solution holds for

$$p_{n+1}^r = p_n^r + \mu_{r-1} p_n^{r-1}$$

where  $p_n^{r-1}$  is given by the intermediate instar solution where  $i = r - 1$ :

$$\begin{aligned} p_{n+1}^r &= \frac{1}{1-d_1} \prod_{k=1}^{r-1} [\mu_k(1-d_k)] \left( \sum_{j=1}^{r-1} \left\{ \frac{[(1-\mu_j)(1-d_j)]^n}{(-\mu_j-d_j+\mu_j d_j) \prod_{\substack{k \neq j \\ 1 \leq k \leq r-1}} [(1-\mu_j)(1-d_j) - (1-\mu_k)(1-d_k)]} \right\} \right) \\ &+ \frac{(-1)^{r-1}}{\prod_{k=1}^{r-1} (-\mu_k - d_k + \mu_k d_k)} + \mu_{r-1} \prod_{k=2}^{r-1} \mu_{k-1} (1-d_k) \\ &\cdot \sum_{j=1}^{r-1} \frac{(1-\mu_j)^n (1-d_j)^n}{\prod_{\substack{k \neq j \\ 1 \leq k \leq r-1}} [(1-\mu_j)(1-d_j) - (1-\mu_k)(1-d_k)]}. \end{aligned}$$

Recall that  $\beta_{i,j} = \prod_{\substack{k \neq j \\ 1 \leq k \leq i}} [(1-\mu_j)(1-d_j) - (1-\mu_k)(1-d_k)]$  and let

$$\gamma_{i,j} = \prod_{\substack{k \neq j \\ 1 \leq k \leq i}} (-\mu_k - d_k + \mu_k d_k).$$

Then

$$\begin{aligned} p_{n+1}^r &= \frac{1}{1-d_1} \prod_{k=1}^{r-1} \mu_k (1-d_k) \left( \sum_{j=1}^{r-1} \frac{\gamma_{r-1,j} (1-\mu_j)^n (1-d_j)^n}{\beta_{r-1,j} \prod_{k=1}^{r-1} (-\mu_k - d_k + \mu_k d_k)} + \frac{(-1)^{r-1}}{\prod_{k=1}^{r-1} (-\mu_k - d_k + \mu_k d_k)} \right) \\ &+ \sum_{k=1}^{r-1} \frac{(1-\mu_j)^n (1-d_j)^n \prod_{k=1}^{r-1} (-\mu_k - d_k + \mu_k d_k)}{\beta_{r-1,j} \prod_{k=1}^{r-1} (-\mu_k - d_k + \mu_k d_k)} \\ &= \frac{1}{1-d_1} \prod_{k=1}^{r-1} \mu_k (1-d_k) \left( \sum_{j=1}^{r-1} \left\{ \frac{(1-\mu_j)^n (1-d_j)^n \left( \gamma_{r-1,j} + \prod_{k=1}^{r-1} (-\mu_k - d_k + \mu_k d_k) \right)}{\beta_{r-1,j} \prod_{k=1}^{r-1} (-\mu_k - d_k + \mu_k d_k)} \right\} \right) \\ &+ \frac{(-1)^{r-1}}{\prod_{k=1}^{r-1} (-\mu_k - d_k + \mu_k d_k)} \end{aligned}$$

where

$$\begin{aligned}
\gamma_{r-1,j} + \prod_{k=1}^{r-1} (-\mu_k - d_k + \mu_k d_k) &= \prod_{\substack{k \neq j \\ 1 \leq k \leq r-1}} (-\mu_k - d_k + \mu_k d_k) + \prod_{k=1}^{r-1} (-\mu_k - d_k + \mu_k d_k) \\
&= \prod_{\substack{k \neq j \\ 1 \leq k \leq r-1}} [(1 - \mu_k)(1 - d_k) - 1] + \prod_{k=1}^{r-1} [(1 - \mu_k)(1 - d_k) - 1] \\
&= (1 + (1 - \mu_j)(1 - d_j) - 1) \prod_{\substack{k \neq j \\ 1 \leq k \leq r-1}} [(1 - \mu_k)(1 - d_k) - 1] \\
&= (1 - \mu_j)(1 - d_j) \prod_{\substack{k \neq j \\ 1 \leq k \leq r-1}} [(1 - \mu_k)(1 - d_k) - 1]
\end{aligned}$$

so that

$$\begin{aligned}
p_{n+1}^r &= \frac{1}{1 - d_1} \prod_{k=1}^{r-1} \mu_k (1 - d_k) \left( \sum_{j=1}^{r-1} \left\{ \frac{(1 - \mu_j)^n (1 - d_j)^n (1 - \mu_j)(1 - d_j) \prod_{\substack{k \neq j \\ 1 \leq k \leq r-1}} [(1 - \mu_k)(1 - d_k) - 1]}{\beta_{r-1,j} \prod_{k=1}^{r-1} (-\mu_k - d_k + \mu_k d_k)} \right\} \right. \\
&\quad \left. + \frac{(-1)^{r-1}}{\prod_{k=1}^{r-1} (-\mu_k - d_k + \mu_k d_k)} \right) \\
&= \frac{1}{1 - d_1} \prod_{k=1}^{r-1} [\mu_k (1 - d_k)] \left( \sum_{j=1}^{r-1} \left\{ \frac{(1 - \mu_j)^{n+1} (1 - d_j)^{n+1}}{(-\mu_j - d_j + \mu_j d_j) \prod_{\substack{k \neq j \\ 1 \leq k \leq r-1}} [(1 - \mu_j)(1 - d_j) - (1 - \mu_k)(1 - d_k)]} \right\} \right. \\
&\quad \left. + \frac{(-1)^{r-1}}{\prod_{k=1}^{r-1} (-\mu_k - d_k + \mu_k d_k)} \right) \\
&= p_{n+1}^r.
\end{aligned}$$

Thus all solutions to the model equations hold.

## Appendix D

# Model robustness to varying start date

Figures D.1 and D.2 present graphical evidence that adult emergence predicted by the developmental model is fairly robust to changes in start date. The temperature time series used reflect the input of the model validation section.

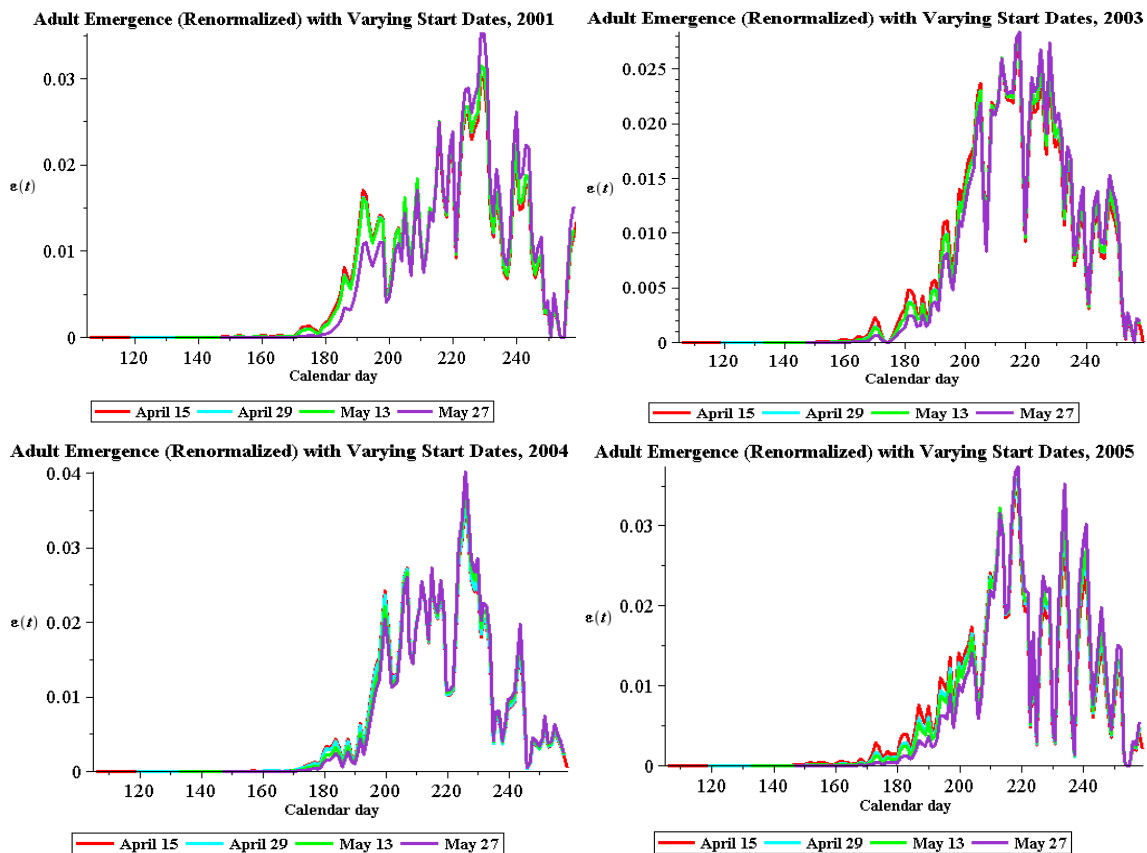


Figure D.1: Predicted adult emergence under varying start dates, 2001, 2003-2005.

The daily probabilities of adult emergence generated from the latest egg hatching, May 27th (purple curve in Figures D.1 and D.2) are regressed against the corresponding emergence probabilities given the earliest egg hatching, April 15th (red curve in Figures D.1 and D.2). The linear regression

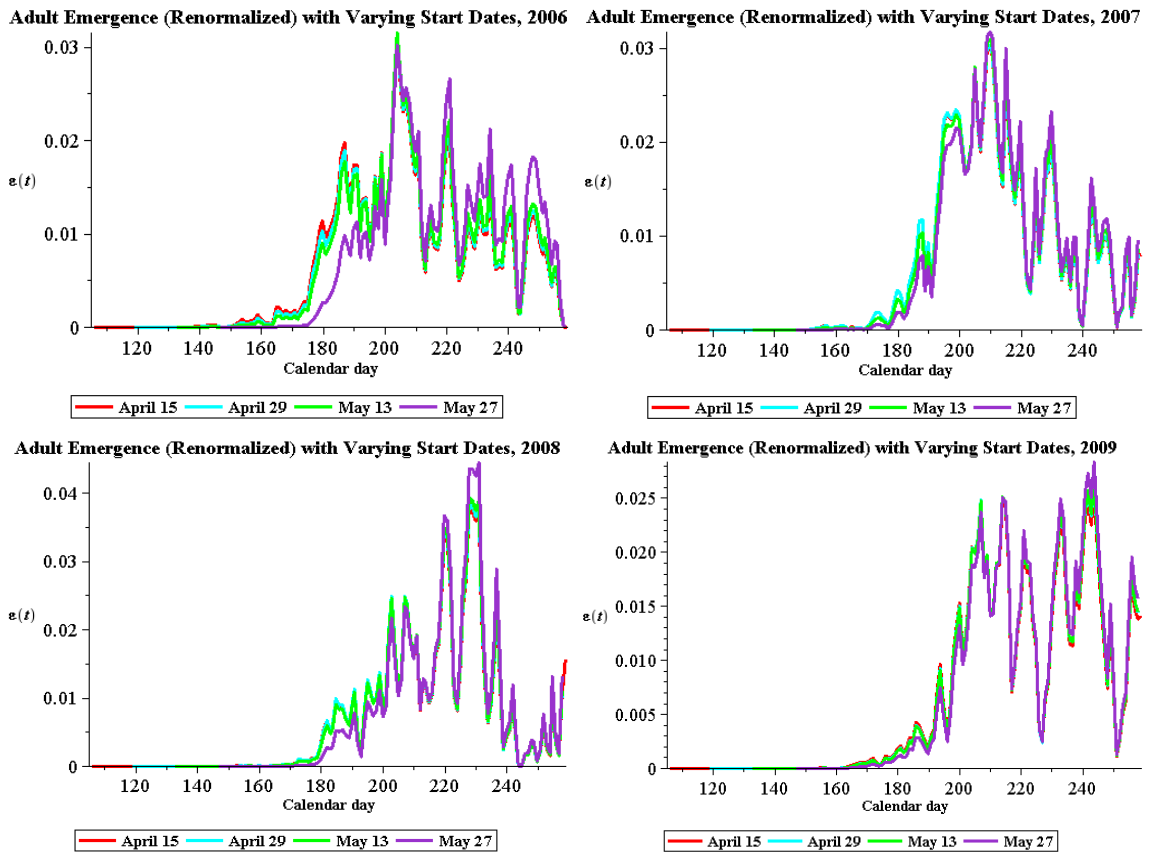


Figure D.2: Predicted adult emergence under varying start dates, 2006-2009.

is carried out according to the method described in Section 3.5.2. When compared against a critical  $F$  value  $F_{\text{crit}} = 3.78$  (?), observed  $F$  statistics for 2001, and 2003 – 2009 are  $F_{2001} = 0.072$ ,  $F_{2003} = 0.021$ ,  $F_{2004} = 0.112$ ,  $F_{2005} = 0.043$ ,  $F_{2006} = 0.015$ ,  $F_{2007} = 0.032$ ,  $F_{2008} = 0.067$ ,  $F_{2009} = 0.111$ . From the linear regression analysis, one may conclude that there is no significant difference between the adult emergence in the earliest versus latest egg hatching.